An Application of Evolutionary Algorithms for WAG Optimisation in the Norne Field

by

© Erfan Mohagheghian

A Thesis submitted to the

School of Graduate Studies

In partial fulfillment of the requirements for the degree of

Master's of Engineering

In

Oil and Gas Engineering

Memorial University of Newfoundland

May 2016

St. John's Newfoundland and Labrador

ABSTRACT

Water-alternating-gas (WAG) is an enhanced oil recovery method combining the improved macroscopic sweep of water flooding with the improved microscopic displacement of gas injection. The optimal design of the WAG parameters is usually based on numerical reservoir simulation via trial and error, limited by the reservoir engineer's availability. Employing optimisation techniques can guide the simulation runs and reduce the number of function evaluations. In this study, robust evolutionary algorithms are utilized to optimise hydrocarbon WAG performance in the E-segment of the Norne field. The first objective function is selected to be the net present value (NPV) and two global semi-random search strategies, a genetic algorithm (GA) and particle swarm optimisation (PSO) are tested on different case studies with different numbers of controlling variables which are sampled from the set of water and gas injection rates, bottom-hole pressures of the oil production wells, cycle ratio, cycle time, the composition of the injected hydrocarbon gas (miscible/immiscible WAG) and the total WAG period. In progressive experiments, the number of decision-making variables is increased, increasing the problem complexity while potentially improving the efficacy of the WAG process. The second objective function is selected to be the incremental recovery factor (IRF) within a fixed total WAG simulation time and it is optimised using the same optimisation algorithms. The results from the two optimisation techniques are analyzed and their performance, convergence speed and the quality of the optimal solutions found by the algorithms in multiple trials are compared for each experiment. The distinctions between the optimal WAG parameters resulting from NPV and oil recovery optimisation are also examined.

This is the first known work optimising over this complete set of WAG variables. The first use of PSO to optimise a WAG project at the field scale is also illustrated. Compared to the reference cases, the best overall values of the objective functions found by GA and PSO were 13.8% and 14.2% higher, respectively, if NPV is optimised over all the above variables, and 14.2% and 16.2% higher, respectively, if IRF is optimised.

ACKNOWLEDGMENTS

I am grateful to my academic supervisors, Dr. Lesley A. James and Dr. Ronald D. Haynes for their guidance, support and encouragement throughout my studies. Without their help, this work would not be possible.

I wish to acknowledge Hibernia Management & Development Company (HMDC) and Natural Sciences and Engineering Research Council of Canada (NSERC) for their financial support and Schlumberger for providing the University with the reservoir simulation software package.

My thanks also go to Mr. Xiang Wang for his technical and scientific help.

I would like to express my sincerest appreciation to my parents for their continuous support and unconditional love.

Finally, I want to acknowledge all the people whom I did not mention here, but helped me make this project a reality.

Table of Contents

List of Figures

List of Tables

NOMENCLATURE

AI = Artificial Intelligence

ANN = Artificial Neural Network

B = formation volume factor [Rm^3/Sm^3]

BHP = Bottom Hole Pressure

BP-ANN = Back Propopagation ANN

C_1 = cognitive learning coefficient (PSO)

C_2 = social learning coefficient (PSO)

c_g = gas injection cost [USD/Sm^3]

$c_g^{'}$ = gas recycling cost [USD/Sm^3]

C_i = concentration (mass fraction) of component i [-]

c_o = oil price [USD/Sm^3]

cP = centi-Poise

c_w = water injection cost [USD/Sm^3]

$c_w^{'}$ = water recycling cost [USD/Sm^3]

D = depth [m]

D = dimension of the search space of optimisation techniques

DOE (DOX) = Design of Experiment

EnKF = Ensemble Kalman Filter

EOR = Enhanced Oil Recovery

EOS = Equation of State

$f(X)$ = optimisation objective function

g = gravitational constant [m/s^2]

$g(X)$ = inequality constraint in optimisation formulation

GA = Genetic Algorithm

GOR = Gas-Oil-Ratio

GP = Genetic Programming

GPS = Generalized Pattern Search

h = capillary rise [m]

HCPV = HydroCarbon Pore Volume

i = year nemuber in NPV formulation

IFT = Inter-Facial Tension

IPR = Inflow Performance Relationship

IRF = Incremental Recovery Factor

K = absolute permeability [m^2]

K_i = distribution constant for component i [-]

k_r = relative permeability [-]

K_{rg} = gas relative permeability

K_{rog} = oil relative permeability (in a two-phase gas-oil system)

K_{row} = oil relative permeability (in a two-phase oil-water system)

K_{rw} = water relative permeability

$l(X)$ = inequality constraint in optimisation formulation

mD = milliDarcy

MME = Minimum Miscibility Enrichment

MMP = Minimum Miscibility Pressure

MSL = Mean Sea Level

n = the total number of evaluation years in NPV formulation

N_g = exponent of gas relative permeability

N_{og} = exponent of oil relative permeability (in a two-phase gas-oil system)

N_{ow} = exponent of oil relative permeability (in a two-phase oil-water system)

NPV = Net Present Value

N_w = exponent of water relative permeability

N_{well} = number of production wells

$OIIP$ = Oil Initially In Place

OWC = Oil Water Contact

p = pressure [Pa]

P_b = bubble point pressure [Pa]

p_c = capillary pressure [Pa]

PDF = Probability Distribution Function

P_g = global best in PSO formulation

P_i = local best in PSO formulation

P_i = initial reservoir pressure [Pa]

PR = Peng-Robinson

PSO = Particle Swarm Optimisation

PV = Pore Volume

PVT = Pressure-Volume-Temperature

Q = total volume of the produced or injected fluid in NPV formulation

q_i = mass rate of injection (or production, if negative) of component i per unit volume of reservoir [$kg/m^3.s$]

q_o = oil production rate [Sm^3/day]

r = capillary radius [m]

r = interest rate in NPVformulation

r_1, r_2 = random parameters in PSO formulation

RBA = Rising Bubble apparatus

RSM = Response Surface Methodology

S = saturation [-]

SA = Simulated Annealing

STB = Stock Tank Barrel

T = absolute temperature [K]

T = total time [day]

t = time [s] or [day]

TVD = True Vertical Depth

VAPEX = VAPour EXtraction

V_i = velocity of particle i in PSO formulation

v_{ij} = the j^{th} component of velocity of particle i in PSO formulation

VIT = Vanishing Interfacial Tension

WAG = Water Alternating Gas

w = weight parameter in history matching error calculation

WTI = West Texas Intermediate

X = optimisation (design) vector

x_i = decison variable

X_i = position of particle i in PSO formulation

x_{ij} = the j^{th} component of position of particle i in PSO formulation

μ = viscosity [Pa.s]

ρ = density [kg/m^3]

ϕ = porosity [-]

σ = interfacial tension [Pa.m]

θ = contact angle

ω = inertia weight in PSO formulation

Subscripts

c	refers to critical saturation
g	refers to gas phase
i	refers to well *i*
n	refers to normalized saturation
o	refers to oil phase
w	refers to water phase

Superscripts

∘	refers to end point relative permeability
hist	refers to historic data
inj	refers to injection
prod	refers to production
sim	refers to simulation data
t	refers to iteration index in PSO formulation

Chapter 1: Introduction

1.1 Water Alternating Gas (WAG) Background

Primary recovery is the recovery of crude oil from the reservoir by the natural energy of the reservoir [1]. The natural driving mechanisms providing the energy for oil recovery can be summarized according to their power: water drive, gas cap drive, depletion drive, rock and fluid expansion drive and gravity drainage drive [2]. In reality, combinations of the above natural drive mechanisms are at play during primary recovery. When production has dropped due to diminished natural drive or reduction in the reservoir pressure, secondary recovery techniques are employed. Typically, secondary recovery involves the injection of water or gas into the reservoir to re-pressurize the reservoir and force the oil to flow towards the production wells [3].

In many cases, oil recovery efficiency during primary and secondary stages is low, which has led to the development of a variety of enhanced oil recovery (EOR) techniques to postpone the decline of the reserves [1]. EOR processes normally can be categorized into thermal, chemical, gas injection and microbial methods. Gas injection as an EOR process is widely used for increasing oil recovery by injecting various gases (for example, natural gas, enriched natural gas, carbon dioxide, nitrogen, or flue gas) into the oil reservoir [3]. A low mobility ratio between injected gas and displaced oil during the immiscible displacement process leads to an unstable zone on the front as well as early breakthrough and viscous fingering [4]. Water Alternating Gas (WAG) was first proposed as a method to increase sweep efficiency of gas injection processes,

where water is injected alternatively with the gas to control the mobility ratio and to stabilize the front.

In conventional water flooding, the capillary pressure between water and oil results in low pore scale recovery due to bypass and snap-off mechanisms, and hence leads to high residual oil saturation [5]. Microscopic displacement of the oil by gas is better than by water. On the other hand, macroscopic displacement of the oil by water is better than by gas [6]. WAG injection integrates the improved displacement efficiency of the gas injection with an improved macroscopic sweep by water flooding to enjoy the advantages of both processes. Some other advantages of WAG include possible gas-oil miscibility which may provide an additional recovery and may affect the fluid viscosity and density [6]. In addition, the reduction in residual oil saturation, because of the three phases and hysteresis effects, and the decrease in interfacial tension (IFT) are also mechanisms for additional oil recovery during immiscible WAG injection [7]. The lower IFT of gas-oil compared to water-oil allows the gas to displace oil from the small pore spaces which are not accessible by water alone. A schematic representation of a WAG process is illustrated in Fig. 1-1 reproduced from [8].

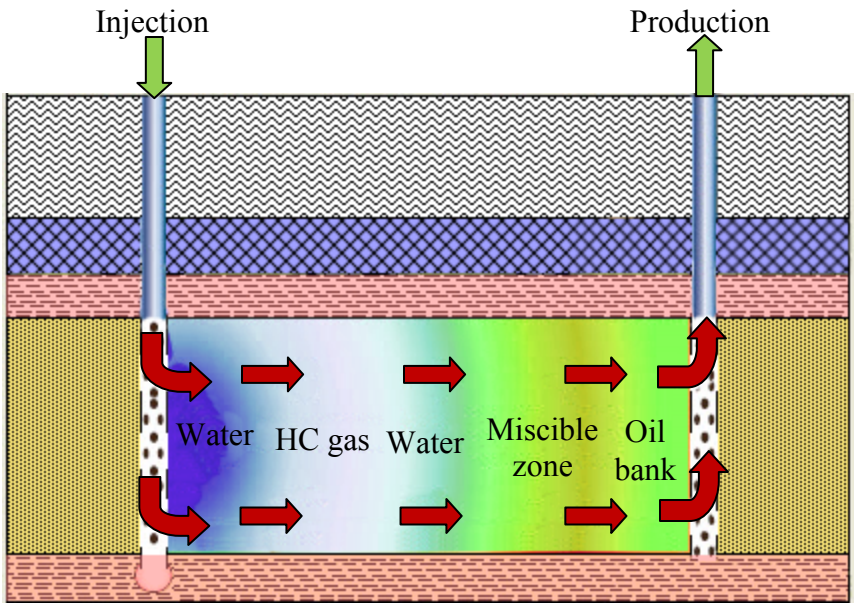

Fig. 1-1: Schematic representation of WAG injection [8]

1.2 Optimisation Background

Solving an optimisation problem is the act of finding the conditions which minimize or maximize a function under given circumstances. This general type of problem can be stated as follows [9]

$$\text{Find } X = \begin{Bmatrix} x_1 \\ x_2 \\ . \\ . \\ . \\ x_n \end{Bmatrix} \text{ which minimises } f(X),$$

subject to the constraints

$$g_j(X) \le 0, \quad j = 1,2,...,m$$
$$l_j(X) = 0, \quad j = 1,2,...,p \tag{1.1}$$

where X is an n-dimensional vector called the design vector, x_i's are the design or decision variables, $f(X)$ is the objective function and $g_j(X)$ and $l_j(X)$ are known as inequality and equality constraints, respectively. (Refer to the Nomenclature on page xv for a full description of the notations/variables.)

There are several ways to classify the optimisation problems. A simple categorization is based on the nature of the equations and variables involved [9].

If all the objective and constraint functions are linear functions of the decision variables, the problem is called a linear programming problem. If any of the above functions is nonlinear, the problem is known as a nonlinear programming problem. This is the most common type of optimisation problem and all other problems can be regarded as special cases of nonlinear programming problem. If at least one of the decision variables is allowed to take only integer values, the problem is classified as an integer programming problem [9]. These three categories of optimisation problems will be reviewed with more details in Chapter 2.

1.3 Introduction to the Norne Field

The Norne field dataset, including two case studies for the whole field and the E-segment, is hosted and supported by the Integrated Operations (IO) center at Norwegian University of Science and Technology (NTNU). The Norne field on the Norwegian Continental Shelf is

operated by Statoil, a partner of the IO center. The data has kindly been made available by Statoil and license partners. Memorial University of Newfoundland is one of the partner universities.

The Norne oil field was discovered in December 1991. The horst block is approximately 9 km x 3 km. It is located about 80 km north of the Heidrun field in the Norwegian Sea in about 380 m of water. The Norne main structure (Norne C, D and E-segments) containing 97% of the oil in place, and the North-East Segment (Norne G-segment) are the two separate oil compartments of the field [10]. Fig. 1-2 shows the field with all its segments.

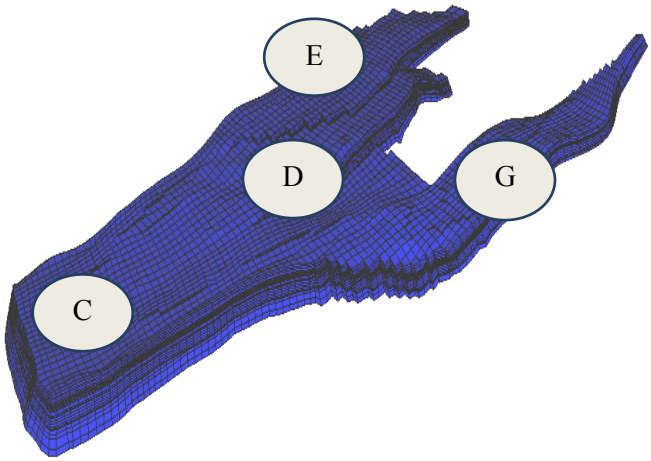

Fig. 1-2: The Norne field with all the segments

Garn, Ile, Tofte and Tilje are the four different formations of the reservoir from top to the bottom. Hydrocarbons in this reservoir are located in Lower to Middle Jurassic sandstones. The sandstones are buried at a depth of 2500 to 2700 m true vertical depth (TVD) and are affected by diagenetic processes. The initial reservoir pressure was approximately 273 bar in August 1996 and the reservoir temperature is 98.3°C. The porosity is in the range of 25-30% and permeability varies from 20 to 2500 mD.

The total hydrocarbon column is 135 m which contains 110 m of oil and 25 m of gas. Approximately 80% of the oil is located at Ile and Tofte formation and all the gas is in the Garn formation [11].

Development drilling began in August 1996 and oil production started on November 6th 1997. There have been 50 wells drilled in the field consisting of 33 producers (16 active wells, 2010), 10 water injectors (8 active wells, 2010) and 7 observation wells. Water injection is used as the main drive mechanism for oil production. Early in the production, gas injection was also used to produce oil, however it was stopped in 2005 and all the gas is exported now [12].

The Norne field was expected to produce for 20 to 24 years with abandonment in 2020. The revenues (undiscounted) of the field were expected to be $4.4 billion during its remaining life (starting from January 1st 2010) [12], however, Statoil has made an oil discovery in the Svale North prospect in the Norwegian Sea about 9 km northeast of Norne field and is pushing operation to 2030 [13].

1.4 Research Objectives

This study aims to optimise the production performance by choosing the best operational parameters for the WAG process on field scale. To do so, an optimisation methodology and framework is developed and different optimisation techniques and WAG operating parameters affecting oil production are investigated. The developed methodology and chosen optimisation techniques are applied to maximize the net present value (NPV) and oil recovery for the WAG performance in the E-segment of the Norne field. The variables which are optimised include water and gas injection rates, bottom hole pressures of the oil production wells, cycle ratio, cycle time, the injection gas composition (to consider the effect of miscibility) and the total WAG period. The results from different optimisation techniques will be analysed and compared.

1.5 Thesis Outline

The rest of the thesis consists of four chapters. Chapter 2 is a literature review of WAG, the optimisation techniques used in the oil and gas industry as well as a review of WAG optimisation specifically. Chapter 3 presents the methodology and framework for WAG optimisation for a field case. Chapter 4 demonstrates the results and discussion of the WAG performance optimisation. Finally, the conclusions are summarized and recommendations are proposed in Chapter 5.

Chapter 2: Literature Review

2.1 WAG Classification

WAG processes are usually classified based on miscibility; whether the displacing fluid is miscible or immiscible with the reservoir oil. Miscibility is a function of oil and gas compositions as well as reservoir pressure and temperature [14].

2.1.1 Immiscible WAG Injection

Immiscible WAG occurs when the injected gas and the oil form two separate phases and a capillary interface exists between them. Immiscible gas injection can be used for EOR. Although two separate phases remain upon immiscible gas injection, some mass transfer between the two phases occurs [15]. Some gas vaporization from the oil or condensation of gas into the oil or a combination of the two mechanisms can happen. According to the amount of mass exchange, the process can approach miscibility and lead to favorable changes in the fluid viscosity, fluid density and IFT [6, 16].

Immiscible displacement in WAG processes has been utilized to improve macroscopic sweep efficiency by improving the frontal stability as well as contacting un-swept regions [6], and to enhance the microscopic sweep efficiency by some mass transfer between oil and gas.

2.1.2 Miscible WAG Injection

Miscibility is defined as the property when substances mix in all proportions without the existence of any interface between the phases involved (i.e., zero equilibrium interfacial tension (IFT)) [17]. It should be noted that miscible displacement can be first contact miscible or multi-contact miscible. In a first contact miscible displacement, the injected gas and reservoir oil mix instantly to create a single phase at any ratio of gas and oil [14]. However, it is often not economical to inject a gas which is first contact miscible with the oil [18]. This is mainly because the high injection pressure or the level of enrichment required for miscibility is usually costly. In a multi-contact miscible displacement, mass transfer between the injection gas and the reservoir oil leads to miscibility between the two phases after a number of contacts within a mixing zone of the flood front [19]. Multi-contact miscibility can develop through a vaporizing process, a condensing process or a combination of the processes. In the vaporizing drive process, when a lean solvent is injected, the intermediate hydrocarbons are vaporized from the oil and enrich the composition at the solvent front progressively until the solvent is miscible with the reservoir fluid. In the condensing drive process, condensation of the intermediate hydrocarbons from the solvent into the oil is the mechanism for the development of multi-contact miscibility. In this process, miscibility is propagated through successive contacts at the rear of the transition zone [20].

The most important criterion for miscibility determination is the minimum miscibility pressure (MMP). MMP is defined as the lowest operating pressure at which the injected gas and the oil become miscible at reservoir temperature after dynamic multi-contact process is achieved [19]. It is worthwhile to note here that the MMP is a strong function of temperature and oil and gas

composition. Accurate determination of MMP is of a vital importance and should be taken into account for a precise estimation of the performance of WAG processes [21, 22]. Methods to predict MMP can be categorized into numerical and experimental methods. The most important experimental methods to determine MMP are slim tube displacement, the method of constructing pressure-composition (P-X) diagram, rising bubble apparatus (RBA), and the newly developed vanishing interfacial tension (VIT) technique [23].

The slim tube is designed to mimic a one dimensional reservoir and the length and packing materials of the tubing can be customized depending on the nature of analysis. The tubing is filled up with reservoir oil and the test gas is displaced up to 1.2 pore volumes. The test is conducted at four to six different pressures and oil recovery is recorded. The MMP is the pressure at which the break in the recovery curve occurs [24]. In RBA, a gas bubble moves upward in a visual high pressure cell filled with reservoir oil. The test is repeated at a series of pressures and the shape of the gas bubble is monitored. At or slightly above MMP, the gas-oil interface from the bottom of the bubble disappears [25]. In the P-X diagram, the phase boundaries (bubble point and dew point curves) of the reservoir fluid and injected gas mixture is experimentally derived relative to the mole percent of the gas, so two-phase and miscibility regions are distinguished [17]. In the VIT technique, the IFT of oil and gas are measured at pressures as high as the experimental accuracy allows and then the data are extrapolated to zero IFT [26].

Among the aforementioned experimental procedures, the slim tube method has been widely used, and is recognized as the well-accepted procedure to evaluate gas-oil miscibility. This

technique, however, provides neither a standard design nor a standard operating procedure and criterion for the measurement of miscibility [27]. Furthermore, this method is very time-consuming, i.e., it normally takes one month to complete one miscibility measurement, therefore, it is very expensive [23]. The P-X diagram is also time-consuming, expensive, and cumbersome as well as it needs a large amount of fluid [23]. The RBA, as a fast method for the determination of MMP, is entirely visual and qualitative in nature, and miscibility is inferred from visual observation. This technique suffers from some disadvantages, for instance subjective and arbitrary interpretations from visual observations and lack of quantitative data to support the results [23]. The VIT technique has some advantages over the other existing experimental models, however, it is still expensive, and time consuming and it is not performed in the presence of porous media, so does not accurately reflect the effect of dispersion and mass transfer on the developing miscibility process. Rao and Lee have claimed that the VIT technique is a rapid, reproducible and quantitative way of determining MMP, though this technique seems to produce slightly lower MMP, due to the zero-interfacial tension pressures. The MMP results using VIT are nonetheless in excellent agreement with other methods and correlations, with the exception of rising bubble technique which overpredicts MMP [28]. On the other hand, computational procedures for calculating MMP provide fast and cheap estimation.

In this study, the effect of miscibility will be examined in terms of the injection gas composition. The gas composition will be linked with immiscible/miscible WAG as an optimisation variable.

2.2 Factors Affecting the Success of a WAG Process

It is crucial to develop various WAG scenarios to determine the optimum operational parameters based on economics, such as net present value, overall project economics, and oil recovery [29]. The parameters which affect a WAG process are classified in several ways. The following parameters are often the most important ones: reservoir characteristics and heterogeneity, rock and fluid characteristics, injection pattern, WAG ratio, injection rates, bottom hole pressure and slug size [6, 30-34]. These parameters, in general, can be categorized into two main categories, namely reservoir parameters and operational parameters, as described below. The effect of these parameters on the success of a WAG process along with some examples in the literature are discussed further in sections 2.3 and 2.4.

2.2.1 Reservoir Parameter Definitions

Reservoir parameters can be divided into three categories including reservoir heterogeneity, petrophysical properties and fluid properties.

Reservoir heterogeneity: One of the most important factors affecting the water/gas displacement process is reservoir heterogeneity and stratification [32, 35]. In fact, the efficiency of recovering oil from the reservoir is influenced by how well the layers communicate with each other [36]. The existence of barriers to fluid flow such as lenses, unconformities, faults and lateral facies variation bring about some difficulties for effective communication. One of the most important reasons of the failure of most EOR projects is reservoir heterogeneity [37].

Reservoirs with higher vertical permeability are affected by cross-flow vertical to the bulk flow direction [38]. Cross-flow may enhance the vertical sweep, however, the gravity segregation and decreased flood velocity in the reservoir, in general, reduce oil recovery. As gas flows preferentially to the top section of thick, high permeability zone, injected water may flow preferentially to the lower section of the zone. Injection and sweep patterns in the flood are controlled by reservoir heterogeneity [29]. Bunge and Radke [39] conducted 2D and 3D simulation studies on the effect of crossflow between sublayers of a dolomite reservoir during alternate injection of CO_2 and water and the results of the simulations demonstrated that the higher ratio of vertical to horizontal permeability adversely impact oil recovery in a WAG process. The most permeable layer has the greatest fluid contribution because of the cyclic nature of the WAG, however, as water is injected, it rapidly displaces the highly mobile gases and all the layers achieve an effective mobility almost equal to the initial value [40]. It is worth noting that in highly stratified reservoirs, the layers with higher permeability always respond first, which leads to an early breakthrough as well as poor sweep efficiency [29].

Random heterogeneity exists in both carbonate and sandstone reservoirs. The reservoir may be comprised of layers of diverse permeable zones separated by thin deposits of shale. The thin shale deposits, which separate the layers, assist the recovery process by impeding the injected fluid from crossing over to the most permeable layers, helping the injected fluid to successfully sweep each stratified layer, and as a result, enhance the sweep and recovery efficiency [37].

Petrophysical properties: Porosity, saturation, permeability and wettability are the most influencing petrophysical properties in the WAG process [36].

Porosity: the ratio of the pore volume to the bulk volume [41]. Reservoirs with higher porosity have higher potential to store fluids, and are mostly good candidates for a wide range of EOR projects. Effective porosity, which is formed by the interconnected pores in rock, is important in petroleum engineering.

Saturation: the fraction of the pore volume occupied by a given fluid [41]. In a reservoir, often there are three phases; oil, water, and gas. The saturation of each phase is in the range of 0 to 1 and by definition the phase saturations add up to 1.

Permeability: a measure of connectivity in the porous medium [41] and a higher value of permeability shows that the reservoir has high potential to pass on fluids through the pores. Permeability plays a key role in reservoir characterization and is a required reservoir property for reserve estimation, numerical reservoir simulation, injection and production calculations, reservoir engineering calculations, mapping reservoir quality, and drilling planning [42]. Absolute permeability is the permeability of a rock sample fully saturated with one fluid, while the permeability of one fluid at a specific saturation in the presence of other fluid(s) is called the effective permeability. The ratio of the effective permeability of one fluid to the absolute permeability gives the relative permeability of the fluid [43].

Wettability: the tendency of a fluid to adhere to or spread on a solid surface when another immiscible fluid is present [44]. In fact, wettability is responsible for the way that fluids are distributed in a porous medium. In the porous medium, the wetting phase occupies the smaller pores, while the bigger pores are filled up by non-wetting phase [41].

Wettability preference can be evaluated in terms of the contact angle when two immiscible fluids are present on a rock surface. In Fig. 1-2, the balanced interfacial forces between water, oil and rock are shown. The contact angle (θ) is measured through the water phase. If it is less than 90 degrees, the rock is said to be water wet; otherwise, the rock is known as an oil wet sample. A contact angle near 90 degrees is an indication of intermediate or neutral wettability [45].

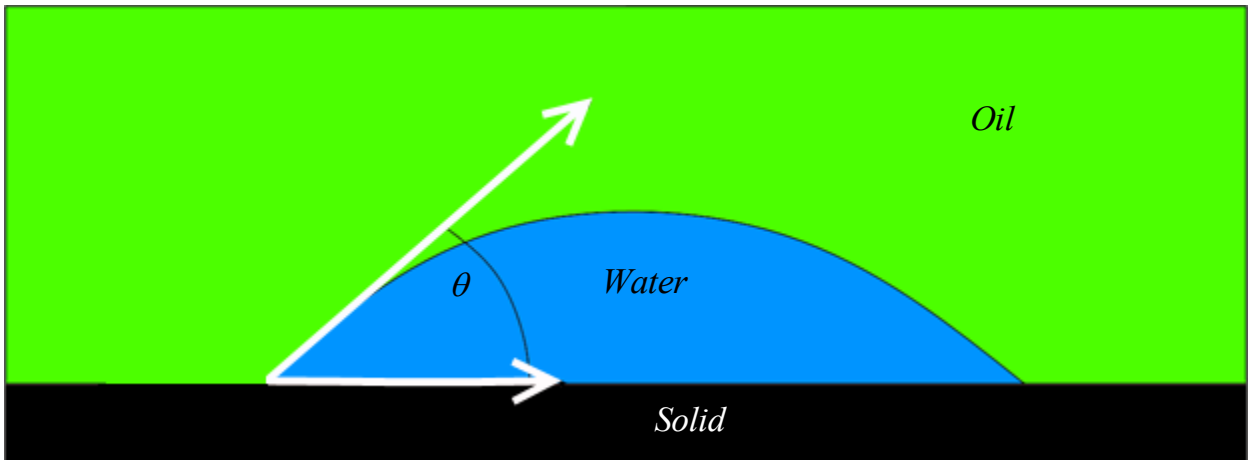

Fig. 2-1: Balanced interfacial forces between water, oil and rock in a water-wet system [45]

Wettability plays a significant role in the reservoir response to gas and water injection, for example, oil connectivity in oil-wet reservoirs improves the mass transfer between oil and gas during gas injection [46]. The optimum relative volumes of gas and water to be injected during a WAG process strongly depends on the wetting state of the rock [47].

Rock-fluid interactions such as wettability influence the displacement efficiency in the reservoir. In reservoir simulators all of these interactions are lumped into one parameter, namely relative permeability. Relative permeability is an important petrophysical parameter, as well as a critical input parameter, in the predictive simulation of miscible floods. It is a lumping parameter that

includes the effects of wetting characteristics, heterogeneity of reservoir fluids, reservoir rock and fluid saturation and describes the relative connectivity to a given fluid phase [48].

Fluid properties: Fluid properties can be divided into density, viscosity and interfacial tension.

Density*:* a physical property of crude oil which is a measure of heaviness of oil components and is a function of pressure, temperature and oil composition. It is usually expressed in terms of ˚API, which is the ratio of oil to water density at standard conditions and is called specific gravity. The lower the density of oil, the lower the residual oil saturation provided that everything else is the same in two reservoirs.

Viscosity: the viscosity of a fluid is defined as the internal resistance of the fluid to flow [43]. Viscosity is a fundamental physical property of crude oil, and plays an important role in reservoir evaluation, reservoir simulation, forecasting production, designing production facilities, and planning any enhanced oil recovery methods. Viscosity of crude oil is strongly dependent on temperature, pressure, solution gas oil ratio, and composition [49-51]. The lower the viscosity, the easier the fluid flows through the porous medium.

Interfacial tension: Interfacial tension (IFT) is defined as the energy required to create a unit surface area at the boundary of two immiscible phases. It is temperature dependent. It is also a measure of miscibility, and IFT becomes zero when the two phases become completely miscible [17]. The lower the IFT, the easier the fluids move together.

The microscopic and macroscopic displacement efficiencies determine the overall efficiency of an EOR process. The density and viscosity difference of the reservoir and injected fluids influence the macroscopic sweep, while microscopic displacement is affected by IFT and dynamic contact angles [40].

2.2.2 Operational Parameters

The most important operational parameters are injection pattern, WAG (cycle) ratio, slug size, cycle time and conformance control.

Injection Pattern: The well injection pattern and well spacing have a significant role in the sweep efficiency in a WAG process. Well spacing is a strong indicator of the average reservoir pressure (the greater the ratio of injectors to producers, the greater the average reservoir pressure) [52]. The five-spot injection pattern (a square of four injection wells placed at the corners with a producer well in the middle) seems to be the well-accepted onshore with a moderately close well spacing. In offshore operations, due to the high cost of drilling new wells, the wells are usually placed according to the geological factors and do not use fixed injection patterns [53] and well pairs are often used. Since many of the field applications are miscible operations, many wells give a good control of the field pressure, and consequently, the WAG injection performance improves [6].

Injection rate: Injection rates should be adjusted with regard to the fracture pressure, injectivity and formation flow capacity and the necessity of voidage balance [54]. Assigning suitable injection rates to each injector has a strong effect on the recovery and the success of the

WAG process. A reservoir-by-reservoir study is required to properly assign injection rates to the injection wells.

Bottom hole pressure: Bottom hole pressure at the producers should be adjusted with regard to the pipe flow conditions through the wellbore and the constraints involved in the surface facilities. This parameter has a direct effect on the production rate and miscibility through the reservoir [54]. Due to higher oil recovery from miscible WAG, it is preferred for the bottom hole pressures to be set at or higher than MMP if a sufficient drawdown can be applied in the reservoir. Therefore, the assignment of bottom hole pressures to each producer depends on the reservoir characteristics and production facilities and is a case-specific task. Normally, injection wells operate at fixed injection rates and producers are kept at fixed bottom hole pressures.

WAG (cycle) ratio: The WAG ratio is the ratio of injected water to gas and is expressed in terms of reservoir injection (volume of water per volume of gas injected at reservoir conditions) or in terms of duration or cycle ratio (the time over which injection takes place) [52]. For example, a WAG ratio of 0 refers to continuous gas injection and WAG ratio of 1 indicates that the same reservoir volumes of gas and water are injected during a cycle. Different WAG ratios create different structures of mixture zones and different displacement mechanisms [30]. The results of a previously published work [30] illustrate that injecting high rates of water (high WAG ratio) results in a more favorable mobility ratio. However, a lower WAG ratio diminishes the residual oil saturation as well as the velocity of the front, which increases the waterless production period. Therefore, the optimum WAG ratio for each WAG process should be carefully determined to improve the efficiency of WAG process. In field applications, a WAG

ratio of 1 is the most popular but it might vary up to 4 in some fields. A WAG ratio smaller than 1 has rarely been used [6].

Cycle time: Cycle time refers to the length of time of an injection cycle. It is actually the sum of the time for water injection (water half cycle) and the time for gas injection (gas half cycle) in a single injection cycle [52]. During the total economic WAG duration, varying the cycle time evidently varies the number of cycles and this might affect the ultimate recovery. The WAG (cycle) ratio determines what proportion of a cycle is allocated to water or gas injection. A cycle time of two or three months is reasonable in normal operations, however the scheduled cycle time may not be practical due to operational constraints or the limitations on gas export. Some authors believe that oil recovery is not very sensitive to the duration of cycles and the amount of the injected gas has a greater effect on oil production [55, 56].

Slug size: The slug size refers to the cumulative gas injected in a single cycle of gas injection. Normally, the slug volume is reported as a percentage of the hydrocarbon pore volume (%HCPV) [52]. Economic sensitivities should be conducted to find the optimum gas slug size. The optimum gas slug size for a given project mainly depends on economic factors such as crude oil price, gas cost, and the amount of the incremental recovery [57]. Total slugs of gas equal to about 20% to 50% HCPV have been used in diverse projects in the U.S.A [57]. It was also reported that the total slug sizes of the gas volume are normally in the range of 0.1 to 3 pore volumes (PV). When hybrid WAG injection is applied, the initial slug size can be up to 40% HCPV. In hybrid WAG, a large amount of gas is initially injected and then the operation is followed by normal WAG injection [6]. Slug size should be optimised independently of WAG

(cycle) ratio as large slug sizes may lead to channeling and small slug sizes might not be operationally feasible [58].

Conformance control: Conformance is a measure of the uniformity of the injected fluids (water or gas), as entering the pay zone. Ideally, injected fluids enter the formations only at pay zones, and spread out regularly across these zones to prevent early breakthrough. When a WAG process cannot successfully be applied to control sweep efficiency, other EOR techniques such as gel polymers, surfactant foams and conventional plugging methods can be used to enhance sweep efficiency of the injection process [52].

In the following diagram (Fig. 2-2), the influencing factors on WAG process have been categorized based on their controllability. As can be seen, altering reservoir heterogeneities and petrophysical properties is either impossible or too difficult, so they are categorized as uncontrollable parameters, while factors such as fluid properties and operational parameters can be changed and possibly optimised to increase the probability of the success of a WAG process. The above mentioned operational parameters, with the exception of injection pattern and conformance control, along with miscibility of the gas are investigated as part of the optimisation framework in this study.

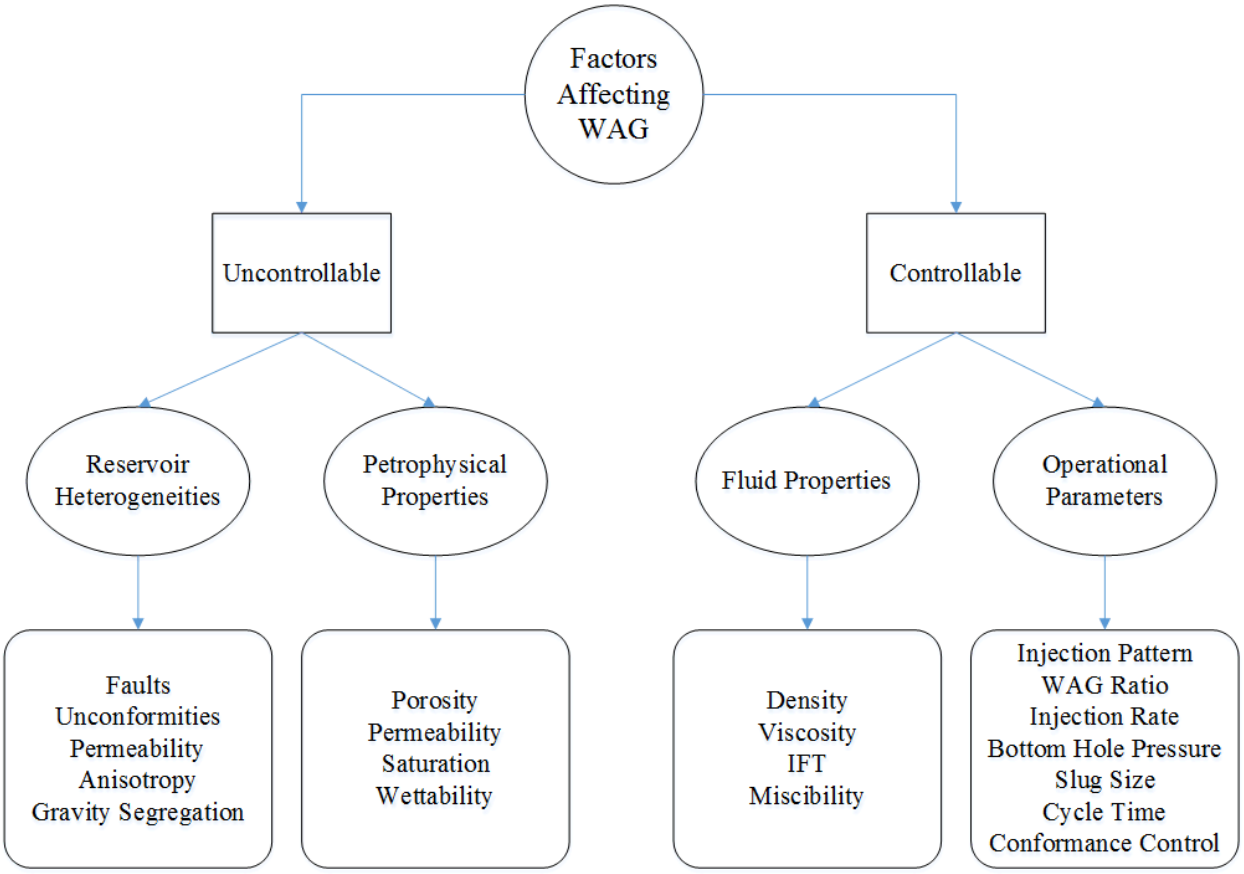

Fig. 2-2: Factors affecting WAG

2.3 WAG Review and Screening Criteria

The first reported WAG project was conducted in the North Pembina oil field in Alberta, Canada in 1957 by Christensen et al [6]. In 1958, Caudle and Dyes [59] proposed and carried out laboratory experiments of simultaneous water and gas injection on core plugs, and the results demonstrated an ultimate sweep efficiency of about 90% compared to 60% sweep efficiency of gas flooding alone. The WAG process has been conducted with success in most field trials. The majority of the fields subjected to WAG are located in Canada and the U.S., however, there are also some fields in the former USSR. Both miscible and immiscible injections have been applied, and many different types of gas including CO_2, N_2, and hydrocarbon gases have been used [6].

A comprehensive literature review of WAG field applications around the world was reported by Christensen et al. [6]. In their study, 59 field cases were reviewed, and it was found that most of WAG processes have been successful. Incremental recovery due to WAG processes are reported to be in the range of 5% to 10%, however, increased recovery has reached up to 20% in several fields, including Rangely Weber in Colorado, Dollarhide and Slaughter Estate in Texas, all of which implemented CO_2 miscible WAG [6]. Almost all of the WAG processes were applied as a tertiary recovery method, and only in newer applications in the North Sea has WAG been established earlier in the field life. For example, WAG was started at the Brage field early in its life after primary production [60]. Among the 59 reviewed projects, 47 were designed to be miscible and 10 were designed to be immiscible, while two have not been classified. As expected, the average incremental recovery from miscible WAG (9.7%) is reported to be higher than that of the immiscible case (6.4%) among the 59 investigated WAG applications [6].

Christensen et al. [6] classified the WAG field applications based on rock type, and the results showed that the high-permeability reservoirs are in the majority, however, the WAG process has been applied to rocks from very low-permeability chalk (Daqing, China) [61] up to high-permeability sandstone (Snorre, North Sea) [62]. Among these projects, thirty-three projects were carried out in reservoirs with sandstone as the main rock type, twelve fields were characterized as chiefly dolomite, five fields were mainly limestone, and six WAG field applications were in carbonate rock [6].

WAG performance was also compared in different fields according to the type of the injected gas. It was found that CO_2 improved oil recovery on an average of 10%, whereas nitrogen and

hydrocarbon gas had an improved oil recovery of 8%. The higher recovery by CO_2 may be attributed to the fact that most CO_2-WAG projects were miscible, whereas the hydrocarbon gas and N_2 WAG field tests are mostly immiscible. All the offshore WAG projects have used hydrocarbon gas since it is readily available from the production and is cheaper than CO_2 [6].

Fig. 2-3 to Fig. 2-6 show the distribution of WAG based on process type, rock type, location and injection gas for the 59 projects, respectively. As shown in these figures, 79% of the WAG projects are miscible indicating the popularity of miscible floods. WAG has been applied to a wide range of reservoir rock types from carbonate (10%) to sandstone (57%). Onshore reservoirs have utilized WAG about seven times more than offshore reservoirs (88% onshore compared to 12% offshore) and CO_2 has been used the most in WAG applications (47%), closely followed by hydrocarbon gas (42%).

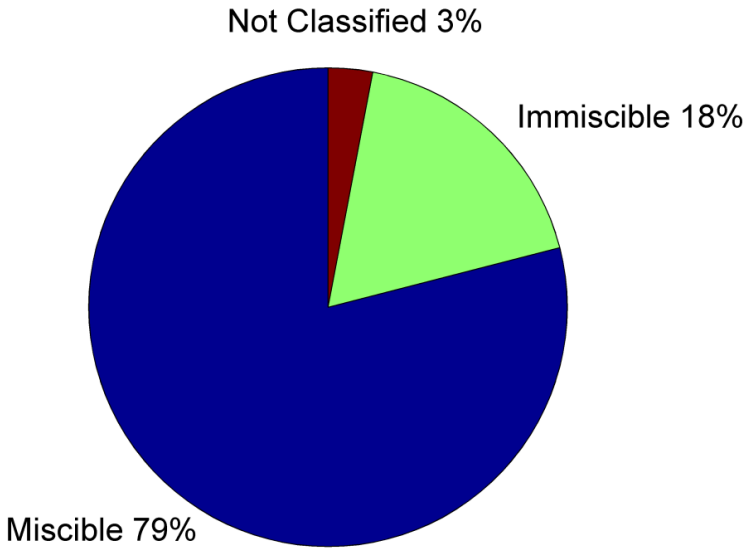

Fig. 2-3: WAG classification based on process type (totally 59 projects) [6]

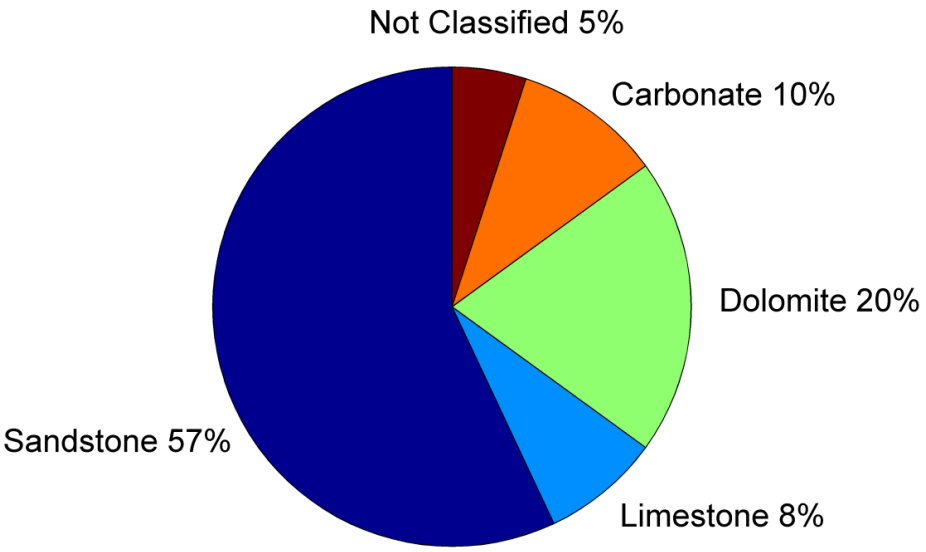

Fig. 2-4: WAG classification based on rock type (totally 59 projects) [6]

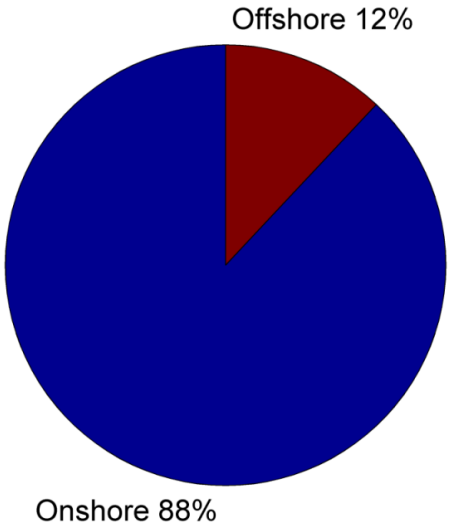

Fig. 2-5: WAG classification based on location (totally 59 projects) [6]

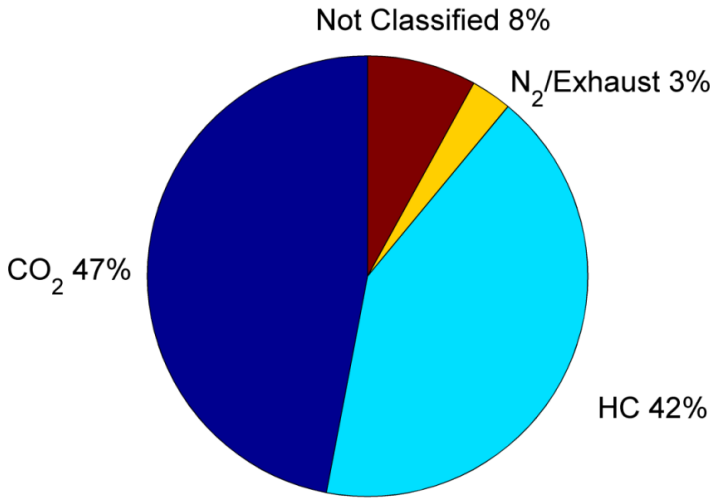

Fig. 2-6: WAG classification based on injection gas (totally 59 projects) [6]

In a more recent publication by Awan et al. [53], the results of 12 offshore WAG projects in the North Sea have been reported. 48% of EOR methods in the North Sea (nine out of 19) were WAG processes, 1/3 of which were miscible. Apart from the immiscible WAG in Ekofisk which was a failure because of hydrate formation in the pilot well, all other WAG projects in the North Sea have been successful.

In the North Sea, water flooding is the main recovery method after primary depletion due to its favorable mobility ratio, however, waterflooding alone cannot access the attic oil. Downdip WAG injection is the normal injection scheme of WAG which helps displace the attic oil by gas and the bottom oil by water through segregation of gas to the top and accumulation of water at the bottom. This leads to increase in oil recovery by contact of unswept zones in the reservoir [53]. In the following paragraphs, a few of WAG projects in the North Sea will be reviewed.

The most successful WAG is found in the Brent sandstone formation of Statfjord field [63]. Statfjord is a light-oil field with permeabilities in the range of 10 to 1000 mD in the lower Brent. Fluid laboratory tests had reported an MMP of about 414 bar which was far above the reservoir pressure at the start of the project (330 bar), so the process is supposed to have been immiscible although indications of swelling/vaporization and multi-contact miscibility were observed. At the time of full field WAG initiation, the recovery factor and water cut were approximately 56% and 70%, respectively. Horizontal WAG injectors were perforated deep in the formation to help gas displace as much oil as possible through its upward movement and the producers were sidetracked to hinder excessive gas or water production. Despite the success of this project, poor volumetric sweep of the gas due to its vertical migration were attributed to high permeability channels which resulted in low gas efficiency and considerable gas back production (up to 45% of the injected gas). The promising results of this project were the reduction in water cut (from 90% to 20% in some of the wells) and the increase in oil rate up to three times in many of the producers.

At Gullfaks [64, 65], Snorre [66] and Brage [67], the WAG ratio was planned to be 1:1. For other fields in the North Sea such as Statfjord, Brae South, Magnus, Thistle and Ekofisk, the WAG ratio was not reported. Christensen et al. [6] reports 1:1 as the optimum WAG ratio based on the WAG field experiences. Two or three months is the normal length of WAG cycle in most of the fields. A general trend is to decrease the length of gas cycle as gas breaks through [53]. For example, at Snorre, the initial cycle time was three months and then it was reduced to one month per well after the gas broke through [66]. Some authors believe that oil recovery does not depend on the length of the gas cycle and is mainly sensitive to the quantity of the gas injected

[55, 56]. The scheduled WAG cycle may not be executed in practice due to operational constraints and the restrictions on sales and export. In the North Sea, generally more gas is injected during summer and less during winter [53].

A miscible WAG pilot was conducted in Snorre field by Statoil [66]. The reservoir mainly consists of sandstone with permeabilities in the range of 200 to 2000 mD. The reservoir fluid is an undersaturated light oil with a saturation pressure between 90 and 130 bar and the initial reservoir pressure of 383 bar. The MMP has been estimated at 283 bar based on slim tube experiments and to ensure miscibility, the operating pressure in the WAG pilot has been kept above 300 bar for the first year of gas injection. Early gas breakthrough was reported in one of the wells which was attributed to high permeability layers. Other producers did not experience much gas-oil ratio (GOR) development and a small reduction in water cut development was also observed in the first year of WAG injection in the Snorre field. Gas was initially injected with a rate of 1.1×10^6 Sm^3/day with a cycle time of three months to maintain the voidage replacement and was reduced to 0.8×10^6 Sm^3/day after the early gas breakthrough.

An immiscible WAG injection started in the Fensfjord reservoir of the Brage field in 1994 [67]. The Fensfjord is a highly stratified reservoir with layers less than 5 m thick and permeabilities in the range of less than 1 mD to more than 200 mD with high permeability streaks and calcite layers. Cyclic gas and water injection started initially in two wells with a WAG ratio of 1:1 and cycle length of three months. The WAG injection was then expanded to six injection wells. The gas and water injection rates were 600,000 Sm^3/day and 3800 Sm^3/day, respectively [67]. Although it is recommended to start WAG as early as possible in some literature [53, 68], early

gas breakthrough occurred in the Brage field after three months and GOR increased from an initial value of 93 Sm^3/Sm^3 to 480 Sm^3/Sm^3 [60]. This was attributed to a high permeability streak which acted as a thief zone between the injector and the producer and resulted in WAG termination in 2000 [53].

The Gullfaks field [64, 65] is a large oil field in the Norwegian sector of the North Sea. The main reservoir is in the Brent group which is comprised of four formations with thicknesses from 15 m to 110 m mostly made of sandstone with a dense faulty pattern and permeabilities in the Darcy range except for some little areas which have permeabilities down to 10 mD. Immiscible WAG injection started when all the producers had a water cut exceeding 50%. A total volume of 5.6×10^6 Rm^3 or 1.5×10^9 Sm^3 gas and 1.59×10^7 Rm^3 water were injected in cycles of two-three months long from November 1987 to December 2000. The gas efficiency was pretty high in this field compared to the Statfjord, although it had less incremental oil recovery [53]. Gas back production was quite low (around 15% of the injected gas). No well went through significant increase in GOR and water cut development was also reduced in some of the wells. The vertical migration of injected gas and the formation of a secondary gas cap against the faults was observed. This resulted in a faster production of the attic oil [64].

Based on the literature reviewed above, it can be stated that WAG has been largely successful and resulted in incremental oil recovery by controlling gas mobility and integrating favorable volumetric sweep of water with microscopic sweep of gas. Before designing an experimental plan that is time consuming and costly, WAG screening criteria of simulations, pilot studies and field experiences need to be considered. For miscible and immiscible gas flooding, several

screening criteria have been suggested in literature [69-71], however little research exists specifically on WAG screening [72].

Manrique et al. [72] reported some of the main WAG screening criteria based on 56 projects in literature. More than half of successful WAG field projects have oil viscosities lower than 2 cP. Oil gravity is usually more than 30°API with an average of 45°API and a viscosity ratio of oil to gas in the range of 10 to 30. Water flooding is the preferred recovery method prior to WAG, however WAG has been applied in reservoirs produced by natural depletion or gas injection with success. Permeability is not a critical parameter and WAG field projects show high permeability contrast in the range of 50 mD up to 3 D, however most of the successful WAG projects have been applied in reservoirs with permeabilities less than 100 mD. The desirable net thickness is below 100 ft unless the reservoir presents high dip angles. The formation can be of any type and there are examples of successful WAG applications in sandstone, carbonate, dolomite and limestone. Temperature and depth of the reservoir are not critical parameters, however temperature is preferred to be between 100 and 200°F and depths of greater than 4000 ft are usually found in successful WAG applications.

Table 2-1 compares the above screening criteria against the Norne field characteristics, (NC stands for not critical). WAG was applied in the Norne field from 1998 to 2007 by Statoil and since 2007 there has been only sea water injection [73]. No information has been released on the WAG performance in the Norne field to the best of the author's knowledge. Nangacovie [12] conducted a black-oil simulation study on the E-segment of the Norne field and showed a

maximum recovery of 73% at a 1:3 simultaneous WAG (SWAG) ratio compared to 68% recovery from WAG injection technique.

Table 2-1: Suggested WAG criteria along with the Norne field characteristics

Fluid and reservoir characteristic	**Suggested WAG criterion**	**Norne characteristic**
Oil viscosity [cP]	< 2	0.58
Oil gravity [°API]	30-45	32.7
Preferred production method prior to WAG	Water flooding	Water flooding
Temperature [°F]	NC (100-200)	209
Depth [ft]	NC (> 4000)	8200-8860
Net thickness [ft]	< 100 unless dipping	440 (not highly dipping)
Average permeability [mD]	NC (< 100)	20-2500
Formation type	NC	Sandstone

As shown above, the Norne field approximately meets all the criteria except the net thickness. Reservoirs with higher net thickness are subject to increased gravity override which adversely impacts oil recovery and the success of WAG [58]. The notes on the suggested screening criteria do not necessarily mean that WAG cannot be performed in a reservoir which does not meet the mentioned criteria and conversely, if the above criteria exist in a reservoir, the success of the WAG would not be guaranteed in spite of its technical feasibility [72].

2.4 Operational Challenges

Some operational problems cannot be avoided during the production life of an oil field. Since the injection fluids must be changed repeatedly, WAG injection is more challenging than a pure gas or water flooding [6]. Gravity override and segregation and reduction in the sweep efficiency

farther from the injection well are usually observed in WAG projects. Moreover, since gas injection is usually applied after a secondary waterflood, high water saturation and the water shielding effect might shield the residual oil from the injected gas, especially in water-wet reservoirs [47].

Christensen et al. [6] summarized a number of routine operational problems reported in WAG applications. Some of the most severe operational problems are as follows

Early Breakthrough in Production Wells: Poor knowledge of the reservoir or an insufficient reservoir description can result in unexpected events such as early gas breakthrough. Channeling and overriding can cause early gas breakthrough in several fields. This might lead to shut in of the wells much earlier than scheduled, which is more critical in offshore projects due to the limited number of the wells [6].

Reduced Injectivity: Reduced injectivity leads to a more prompt pressure drop in the reservoir, which influences displacement and production. Three-phase flow and wellbore heating cause reduction in relative permeability which subsequently leads to reduced injectivity [6]. Reduced water injectivity after a gas slug sometimes occurs, however reduction in the injectivity of gas is not a major concern and gas injectivity after a water slug might even increase [74].

Corrosion: This problem exists in almost all WAG injection projects usually due to the fact that injection and production facilities are not originally designed for WAG injection. It must be

solved by means of high quality steels, pipe coating or changes in equipment. Only WAG projects using CO_2 as injection gas have reported severe corrosion problems [6].

Scale Formation: When CO_2 is the injected gas source, the formation of scales in WAG field trials usually happens, which might stress the pipeline and lead to failure [6].

Asphaltene Formation: Several fields have encountered problems due to asphaltene precipitation (East Vacuum in New Mexico, Wertz Tensleep in Wyoming and Mitsue in Alberta). East Vacuum and Wertz Tensleep applied miscible CO_2-WAG and the WAG in Mitsue was miscible hydrocarbon [75-77]. In fact, asphaltene precipitation during gas injection can cancel out the success of this method, and cause severe problems such as wettability alternation, formation damage, relative permeability reduction, and flow interruption in the reservoir as well as surface facilities [78-80]. In many cases, the asphaltene precipitation problem can be solved with solvent treatment at adequate intervals of the wells. In some cases wells have been shut in, however, in a majority of the cases reported production has not been severely influenced.

Hydrate Formation: Recently, a WAG pilot was postponed on Ekofisk (an immiscible hydrocarbon WAG project in the North Sea) due to plugging of the injector [81]. This was brought about by hydrate formation, due to low temperature in the injector. Another hydrate formation problem was reported by Wasson Denver (miscible CO_2-WAG in Texas). In this case, hydrate formation in wells resulted in freezing of the wellhead during the nights and periods of cold weather [82].

Most of these operational problems are a part of the daily routine for the operators and are usually handled successfully through close monitoring and good management [6].

The operational challenges and flow assurance is not part of the scope of this study and will not be investigated in the thesis.

2.5 Fundamental Equations of Fluid Flow in Porous Medium

In this section, the fundamental equations of three-phase flow through a porous medium are briefly reviewed. Darcy's law for a three-phase system of fluids is written as follows for each of the three phases [83]. We use the subscripts g, o and w to refer to the gas, oil and water phases, respectively.

$$v_g = -\frac{Kk_{rg}}{\mu_g}(\nabla p_g - \rho_g g \nabla D),$$
$$v_o = -\frac{Kk_{ro}}{\mu_o}(\nabla p_o - \rho_o g \nabla D),$$
$$v_w = -\frac{Kk_{rw}}{\mu_w}(\nabla p_w - \rho_w g \nabla D).$$

where

v = Darcy velocity [m/s]
K = absolute permeability [m^2]
k_r = relative permeability [-]
μ = viscosity [Pa.s]
p = pressure [Pa]
ρ = density [kg/m^3]
g = gravitational constant [m/s^2]
D = depth [m]

The conservation equation for each component is written as follows [83]

$$-\nabla.[C_{ig}\rho_g v_g + C_{io}\rho_o v_o + C_{iw}\rho_w v_w] + q_i = \frac{\partial}{\partial t}[\phi(C_{ig}\rho_g S_g + C_{io}\rho_o S_o + C_{iw}\rho_w S_w)].$$

where

$C_i =$ concentration (mass fraction) of component i [-]
$q_i =$ mass rate of injection (or production, if negative) of component i per unit volume of reservoir [kg/m^3.s]
$\phi =$ porosity [-]
$S =$ saturation [-]
$t =$ time [s]

Substitution of conservation equation into Darcy's law gives the following set of N differential equations for N components [83].

$$\nabla.[\frac{C_{ig}\rho_g K k_{rg}}{\mu_g}(\nabla p_g - \rho_g g \nabla D) + \frac{C_{io}\rho_o K k_{ro}}{\mu_o}(\nabla p_o - \rho_o g \nabla D) + \frac{C_{iw}\rho_w K k_{rw}}{\mu_w}(\nabla p_w - \rho_w g \nabla D)] + q_i$$
$$= \frac{\partial}{\partial t}[\phi(C_{ig}\rho_g S_g + C_{io}\rho_o S_o + C_{iw}\rho_w S_w)].$$

There are $3N$ dependent variables for the mass fractions in the three phases, three phase pressures, three densities, three viscosities, three saturations and three relative permeabilities. Therefore, there are totally $3N+15$ dependent variables, hence $3N+15$ independent relations are required in order to obtain a solution to the above system [83].

The saturations and mass fractions must add up to 1. Densities and viscosities are functions of phase pressures and compositions and relative permeabilities are functions of saturations [83]. There are two independent relationships for capillary pressures which are given below [43].

$$p_g - p_o = p_{c_{go}}(S_g, S_o) = \Delta\rho_{go} g h = \frac{2\sigma_{go}\cos\theta_{go}}{r},$$
$$p_o - p_w = p_{c_{ow}}(S_o, S_w) = \Delta\rho_{ow} g h = \frac{2\sigma_{ow}\cos\theta_{ow}}{r}.$$

where

$p_c =$ capillary pressure [Pa]
$h =$ capillary rise [m]
$\sigma =$ interfacial tension [Pa.m]
$\theta =$ contact angle
$r =$ capillary radius [m]

So there are already $N+15$ independent relations. Finally, there is a distribution constant for each component as a function of pressure, temperature and composition for each pair of phases which yields the $2N$ remaining required relations [83].

$$\frac{C_{ig}}{C_{io}} = K_{i_{go}}(T, p_g, p_o, C_{ig}, C_{io}),$$
$$\frac{C_{io}}{C_{iw}} = K_{i_{ow}}(T, p_o, p_w, C_{io}, C_{iw}).$$

where

$K_i =$ distribution constant for component i [-]
$T =$ absolute temperature [K]

2.6 Production Optimisation Techniques

In reservoir management, the objective is to find the optimal production and injection settings to minimize the residual oil saturation and displace the oil to the production wells by means of a displacing agent. The injected and produced fluids should be properly adjusted in order to

control the displacement process. The recovery factor can be improved by 3-25% through steady and monitored optimisation [84].

As the main goal of production optimisation, the optimisation approaches should be investigated to help the reservoir engineers make operational decisions to improve and enhance oil recovery while considering the operational and economic constraints.

Applications of optimisation techniques in the oil industry were initiated in the early 1940's and are still expanding. Optimisation techniques have been applied for well placement, history matching, drilling, facility design and operation, recovery processes, planning, etc. [85]. Linear, integer and nonlinear programming techniques have been widely used to optimise oil and gas production [86]. In the rest of this section, we briefly review the optimisation strategies which appear in the literature review of oil production and WAG optimisation.

2.6.1 Linear Programming Technique

The optimisation problem (equation (1.1)) is a linear one when both the objective function and the constraints are linear. Linear programming techniques have been in use in the oil and gas industry since the 1950's [87]. Linear programming is widely used in business and economics, for example to find the optimal distribution plan for the shipment of a product from several manufacturing plants to different places. It is also utilized to solve several types of engineering design problems, such as the design of frame structures [9]. There are mainly two kinds of techniques, i.e., the simplex algorithm and the interior point algorithm, which can be employed to solve a linear programming problem. The classical simplex algorithm was proposed and

developed by Dantzig [88]. A sequence of bases is generated in this method and the algorithm moves along the vertices of the feasible region to find the optimum solution. This indicates that the optimum found by this method is always an extreme point of the feasible region. Klee and Minty [89] mentioned that the simplex algorithm can be quite effective although it might require many iterations to converge in some cases.

The interior point algorithm or the polynomial-time algorithm was proposed by Karmarkar in 1984 [90]. It works based on continual centering through a projective scaling transformation. This algorithm always looks for the optimal solution in the interior of the feasible region and therefore, contrary to the simplex algorithm, the optimum found by this method is not an extreme point of the region. When the objective and/or constraint functions are not linear, a system of linear functions can be employed for finding the optimum.

2.6.2 Integer Programming Technique

When all the components of the unknown vector are discrete, the problem is an integer programming one. When only some of the components are discrete (such as coupled well control and placement optimisation), the problem is a mixed integer programming one. There does not exist a universal algorithm which can solve all the linear integer programming problems. The solution of such problems is usually time consuming or approximate. Two widely used solution algorithms are the cutting plane technique and the branch and bound method [91, 92].

In the cutting plane technique, an initial linear programming relaxation has to be established by assigning real values to each discrete component. After that, the constraints are added to a series

of linear programming relaxations of the linear integer problem until the optimal solution of a relaxation problem takes integer values [91]. On the other hand, the branch and bound method approach breaks an optimisation problem iteratively into multiple sub-problems to examine the set of feasible integer solutions. Instead of taking account of all the sub-problems, the method uses bounds on the optimal objective value of a sub-problem to avoid forming and solving other sub-problems [92].

2.6.3 Nonlinear Programming Technique

When either of the objective or constraint functions are nonlinear, the optimisation problem is a nonlinear one. Due to diverse structures of nonlinear programming problems, various techniques have been developed for different classes of the problems. The two main classes of nonlinear optimisation techniques are the derivative or gradient-based algorithms and the direct or derivative-free optimisation algorithms. Some commonly used algorithms are briefly presented below.

Derivative-based optimisation algorithms: In derivative-based optimisation algorithms, the steepest decent direction is looked for and the function extremes are usually found through analytical or numerical differentiation of the function. The numerical finite difference methods are based on Taylor series expansions. The steepest decent method, Newton's method, quasi-Newton method and sequential quadratic programming technique are examples of this type of optimisation algorithm. They are deterministic and converge quickly if the starting point is not too far from the true solution [93]. Derivative-based optimisation algorithms have also some disadvantages [94]. For example, the Newton-type methods might not be able to find the optimal

solution if the response surface is not smooth. Furthermore, the computation of the derivatives with finite difference approximations is expensive and time consuming.

Direct optimisation algorithms: The direct or derivative-free optimisation algorithms do not require the objective function derivatives required in gradient-based methods. This makes them suitable for situations when the derivatives of the function either do not exist or are too difficult or costly to compute. Currently, many direct optimisation algorithms are being used in the oil and gas industry.

Derivative-free optimisation approaches can be divided into deterministic (e.g., generalized pattern search) and stochastic (e.g., genetic algorithm) techniques. Stochastic approaches can be useful for dealing with rough functions with multiple local optima [95].

Extracting the gradient information requires in-depth knowledge of how the reservoir simulator works, hence may be challenging. Using "black box" optimisation algorithms, which deal only with inputs and outputs to the simulator, is a way to remove this requirement [96].

Recently, optimisation techniques based on evolutionary algorithms have attracted many researchers from various fields. Among these, genetic algorithms (GAs) have achieved more popularity and have been used extensively in petroleum engineering problems [97]. However, other evolutionary algorithms have emerged as very promising tools for optimisation problems in the oil industry. Some of the most important ones are particle swarm optimisation (PSO), ant colony optimisation and simulated annealing. In the following sections, we first introduce the

principles of GA and PSO and present some of their applications in the oil industry. Later on, the discussion focuses on the methods specifically used for WAG optimisation and the applications of optimisation algorithms for the purpose of WAG optimisation are reviewed.

Fig. 2-7 shows a classification of the optimisation techniques with a few examples for each and summarizes the above notes. Linear, integer and nonlinear programming are the three main categories of optimisation techniques. Nonlinear programming techniques are classified into derivative based and derivative free and derivative free techniques can be either deterministic or stochastic. The focus in this study is on stochastic derivative free nonlinear programming techniques such as GA and PSO.

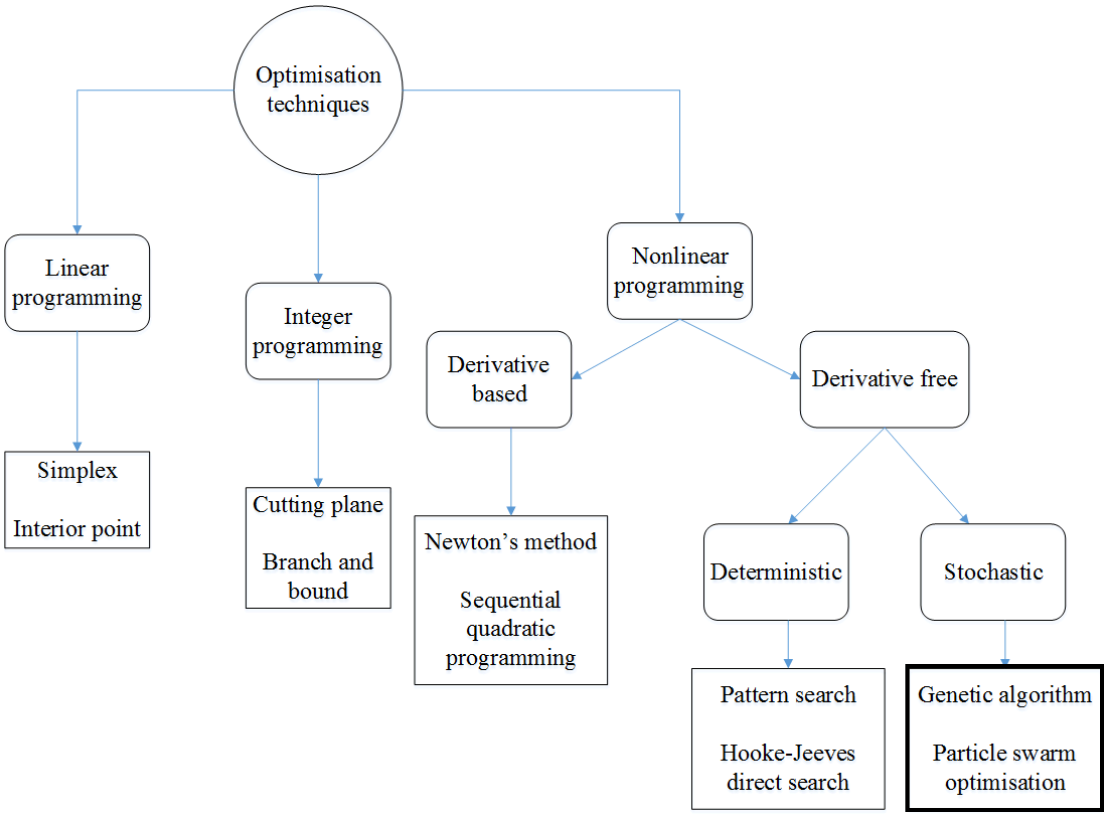

Fig. 2-7: Classification of optimisation techniques

2.6.3.1 Genetic Algorithm (GA)

In 1975, Holland [98] proposed genetic algorithms as motivated by biological evolution. The idea behind this algorithm is natural evolution and genetics with emphasis on the design of robust adaptive systems. Over the last 20 years, this algorithm has attracted much attention from various fields due to its high capability as an optimisation technique to solve complex and nonlinear problems [99].

This algorithm is recognized as an efficient, robust, parallel, and global randomized searching algorithm for managing combinatorial optimisation problems. GA has received extensive attention in the fields of natural science and engineering technology because of the biological background and the applicability for a variety of functions. GA copes with a given problem by investigating and exploiting the search space, and solves the problem through the processing of an aggregation of encoded variable strings (chromosomes). A large number of chromosomes, which comprise the individuals of a population of GA, are processed. To conduct its optimisation process, GA produces its population from one generation (parents) to the next (offspring). The offspring are generated by means of the operations of selection, mutation and crossover [100].

The offspring is selected from the parents through a selection process which plays an important role in the GA method. It is more probable for the chromosomes with higher fitness values to be chosen and they might be selected more often [100].

In the second step (crossover) two parent chromosomes are combined and part of their genetic information is exchanged to produce the offspring. The crossover operator is applied on all the

selected chromosomes around a crossover point which is chosen randomly along their length. After children are produced, those with best calculated fitness values are inserted back into the original population with the remaining parents.

Before inserting the produced offspring back into the initial population, a mutation process based on a mutation operator is completed which causes the GA method to span the search space more thoroughly and bring variety in the population. This process is done through changing the genes of each chromosome sporadically using a small mutation probability. Generally speaking, selection gives higher chance of reproduction to individuals with higher fitness values, crossover speeds up the method's convergence to the optimum, whereas mutation creates variety in the population. Fig. 2-8 shows the evolution flow of GA. Members of a population of GA are evaluated based on their fitness values and through operations of selection, crossover and mutation, the next population is generated. This operation continues until a user-defined stopping criterion is met. It is expected that GA reaches the optimal solution through the combination of these three steps (selection, crossover and mutation) [100]. The operations of crossover and mutation prevent the genetic algorithm from being trapped in one region of the search space [101].

GA has also some disadvantages. There is no guarantee that the algorithm finds the best solution like in any other stochastic method. GA needs a large number of function evaluations depending on the number of individuals and generations and it can be sensitive to the initial guess [101]. Nevertheless, GA has been used in the oil industry more than other evolutionary algorithms [97]. Some of the applications of GA in the oil industry are chronologically reviewed here.

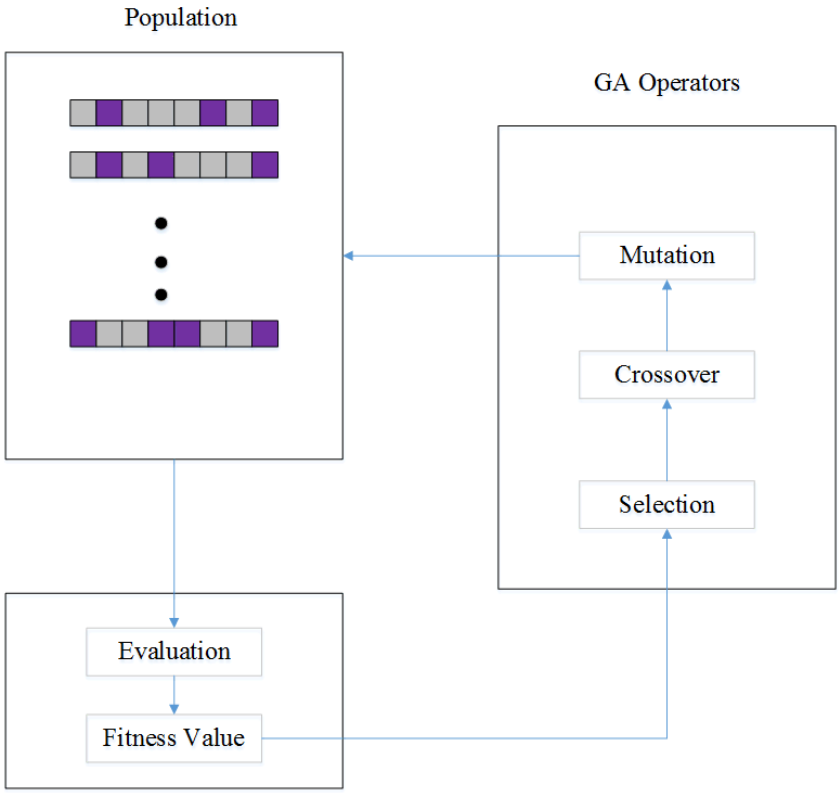

Fig. 2-8: Evolution flow of genetic algorithm [102]

In 1996, Bush and Carter [103] tried to match a simulation model to the production history of a reservoir by adjusting some of the model parameters using a GA. They showed that more than one optimum existed and more than one set of parameters reproduced the production history of the reservoir. The challenge is to identify all the optima by using as few function evaluations as possible.

In 1999, Soleng [104] presented a genetic algorithm that was applied to the problem of modifying the petrophysical rock properties of a reservoir model to match the model with the historical production data. He applied a genetic algorithm to the difficult optimisation problem where each evaluation of the objective function required a flow simulation of the whole

reservoir. Ten independent runs were used to give a prediction with an uncertainty estimate for the total future oil production using two different production strategies.

The work of Romero et al. [105] in 2000 describes the implementation of a GA to carry out hydrocarbon reservoir characterization by conditioning the reservoir simulation model to production data (history matching) on a predefined geological and structural model. They defined the objective function as the weighted sum of the squared errors. The oil production and water injection rates were kept fixed at their measured values and the difference between the measured bottom hole pressures and the simulated values was taken as the error. They tried different operators for crossover and mutation and finally compared the results of their modified GA with simulated annealing which showed the superior performance of GA.

In 2001, Rahman et al. [106] presented an integrated novel model for hydraulic fracturing design optimisation, which recognizes complex interactions between a hydraulically coupled fracture geometry module, a hydrocarbon production module and an investment-return cash flow module. The paper of Tu´pac et al. [107] in 2002 presents a genetic algorithm application for selecting the best alternative for oil field development under uncertainty. In 2003, Yu et al. [108] presented a hybrid GA-fuzzy approach to model reservoir permeability. This approach uses a two-step divide-and-conquer process for modeling.

In 2005, Emera and Sarma [109] developed a new correlation for prediction of the MMP of pure and impure CO_2 streams based on GA. In fact, in this correlation, the constants were obtained

using a GA. The results showed that the proposed correlation outperformed other existing correlations in literature.

In 2007, a new algorithm for the auto-design of neural networks based on GA was used [110]. The new proposed method was evaluated by a case study in South Pars gas field in Persian Gulf. The design of topology and parameters of the artificial neural networks (ANN) as decision variables was done first by trial and error, and then using a genetic algorithm in order to improve the effectiveness of forecasting when ANN is applied to a permeability prediction problem from well logs. Using GA resulted in better performance in terms of prediction error compared to the conventional trial and error method for the ANN model development. In 2008, Mousavi et al. [111] proposed a hybrid neural genetic algorithm (GA-ANN) with the purpose of automating the design of a neural network for a dissimilar type of structures. The results illustrated that the neural genetic model can be applied successfully and afford high accuracy and dependability for MMP forecasting.

In 2009, AlQuraishi [112] proposed a new model to estimate crude oil saturation pressure using linear genetic programming (GP) technique. A total of 131 crudes covering wide ranges of composition and reservoir temperature and different geographic origins were used to build and test the model. In 2013, an integrated framework was constructed to attain the optimal locations of infill wells in coal bed methane reservoirs [113]. This framework consists of a flow simulator (ECLIPSE E100), an optimisation method (genetic algorithm), and an economic objective function. The objective function used was the net present value of the infill project based on an annual discount rate.

In 2014, Ahmadi et al. [114] evaluated and compared the performance of a correlation developed by multivariable regression, back propagation ANN (BP-ANN) and GA-ANN to predict the recovery rate of vapor extraction in heavy oil reservoirs using data obtained from experiments along with additional data in literature. It was claimed that GA-ANN is able to search in different directions simultaneously and this increases the probability of finding the global optimum. The predictions of the three mentioned models were compared with the experimental data in terms of statistical error measures and it was found that the predictive performance of the proposed GA-ANN was better than conventional BP-ANN and regression correlation.

In 2015, Xu et al. [115] developed a modified GA by altering the crossover and mutation rates to history match the simulation data with the experimental results of vapour extraction (VAPEX) heavy oil recovery process. The computational time of the modified approach was reduced by 71% compared to the conventional GA and an excellent match with the error less than 1% was obtained.

The application of GA to the optimisation of WAG performance will be reviewed in the section of WAG optimisation.

2.6.3.2 Particle Swarm Optimisation (PSO)

In 1995, Eberhart and Kennedy [116] introduced particle swarm optimisation (PSO) which was inspired by social behavior and movement dynamics of insects, birds and fish. PSO is a random and probabilistic algorithm and an optimisation technique based on a population which tries to find optimal solutions to problems which have a continuous search space. The original form of PSO was formed through modification of initial simulations [117] and later, Shi and Eberhart produced the standard PSO by introducing the inertia weight [118]. They summarized the swarm adaptation in terms of evaluation, comparison and imitation. A particle in PSO evaluates its surrounding particles, makes a comparison with them and imitates the behavior of those which are better. Hence, the particle's own position and the performance of the particles around it are the two types of information which form its behavior [119]. PSO is designed to find the global optima of possibly nonlinear functions or systems in multidimensional space [117].

PSO is similar to GA, however, PSO uses a collaborative approach rather than a competitive one used in GA [120]. PSO is a swarm intelligence algorithm and follows its basic principles [116, 121]. The particles form a population of random solutions and are stochastically distributed all over the search space. Each particle of the swarm can be a solution to the optimisation problem and the swarm moves towards the global optimum of a function or system. Each particle remembers its position in the search space and its best ever position (called personal best value or p_{best} by Eberhart and Kennedy) and the swarm remembers its best ever global solution (called global best solution or g_{best}) as well as the index of the particle which yields the global best solution. In the optimisation process, and while looking for the optimum in the search space, the velocity of each particle in the next iteration is computed by g_{best} (as the social component), p_{best}

(as the cognitive component) and its current velocity. These components randomly determine the particle position in the next iteration [117].

In the PSO algorithm, a position in the D-dimensional space is allocated to each individual, and the status of each particle is determined by its location and velocity. The position and velocity of particle i at iteration t are specified by [116]

$$V_i^t = [v_{i1}^t, v_{i2}^t, ..., v_{iD}^t], \quad (2.1)$$

$$X_i^t = [x_{i1}^t, x_{i2}^t, ..., x_{iD}^t]. \quad (2.2)$$

Care should be taken that in conventional PSO, no information about the previous velocities of the particles is available. Afterwards, Shi and Eberhart [118] proposed a new parameter, termed inertia weight (ω), to overcome this shortcoming. In this PSO algorithm, each individual modifies its velocity to find the most promising solution based on the following relationship [118]

$$v_{ij}^t = \omega v_{ij}^{t-1} + C_1 r_1 (p_{ij}^t - x_{ij}^t) + C_2 r_2 (p_{gj}^t - x_{ij}^t) \qquad j = 1, 2, ..., D, \quad (2.3)$$

where ω shows the inertia weight and C_1 and C_2 are the cognitive and social learning coefficients, respectively. The quantities r_1 and r_2 represent two random parameters in the range of 0-1. Moreover, P_i^t and P_g^t stand for the local and global best solutions, respectively, and are presented as [118]

$$P_i^t = [p_{i1}^t, p_{i2}^t, ..., p_{iD}^t], \quad (2.4)$$

$$P_g^t = [p_{g1}^t, p_{g2}^t, ..., p_{gD}^t]. \quad (2.5)$$

The linear function of the inertia weight is represented by [118]

$$\omega = \omega_{\max} - \frac{(\omega_{\max} - \omega_{\min})t}{t_{\max}}, \tag{2.6}$$

where $\omega_{\max}$ expresses the maximum magnitude of the inertia weight, $\omega_{\min}$ is the minimum magnitude of the inertia weight, t represents the current iteration, and $t_{\max}$ stands for the total number of iterations.

The range of the particle velocity (e.g., $[-v_{\max}, v_{\max}]$) is prescribed in PSO to keep the velocity at a reasonable level [118].

The relationship between the previous particle position (x_{ij}^{t}) and the new position (x_{ij}^{t+1}) is presented by [118]

$$x_{ij}^{t+1} = x_{ij}^{t} + v_{ij}^{t} \quad j = 1, 2, \ldots D. \tag{2.7}$$

Fig. 2-9 shows how the velocity and position of particles are updated in PSO algorithm. As shown, the velocity of a particle is the resultant of three vectors: its current velocity, its velocity toward the global best and its velocity toward the local best and the resultant velocity determines the particle position at the next iteration.

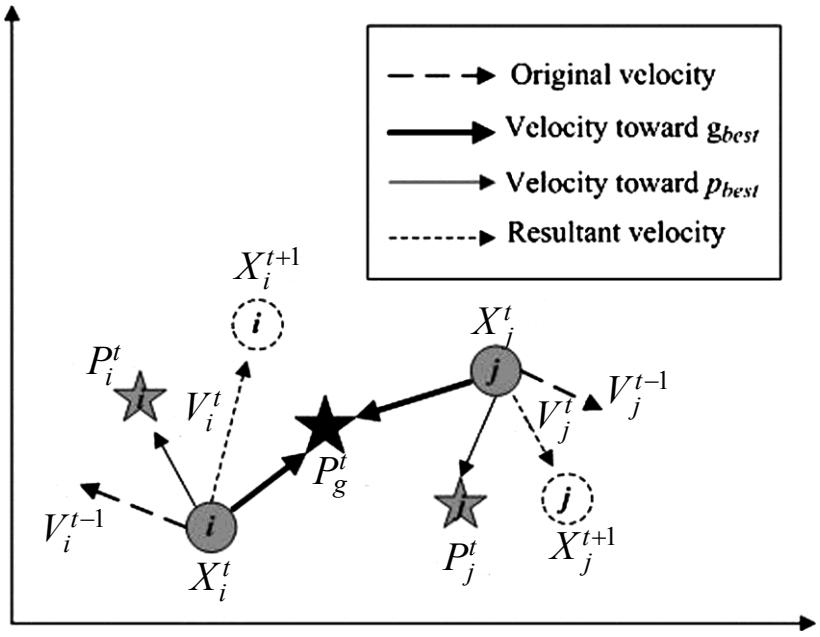

Fig. 2-9: Updating velocities and positions of the particles in PSO [122]

PSO has shown a high search speed in optimisation problems, is easy to implement, has only a few algorithmic parameters and can be efficiently parallelized. On the other hand, the swarm can become trapped in local optima and sometimes suffers from premature convergence [123]. We herein briefly report some of the applications of PSO in oil industry.

In spite of the fact that PSO was first proposed in 1995, its application in oil industry goes only back about five years. In 2010, Onwunalu and Durlofsky [124] applied PSO for determination of the optimal well type and location. The performance of PSO was compared with GA, which showed the superior performance of PSO. Assareh et al. [125] investigated application of PSO and GA to estimate oil demand in Iran in 2010. Both PSO and GA could satisfactorily predict oil demand, however, the results of PSO were more accurate.

In 2012, Zendehboudi et al. [126] proposed an intelligent model based on a feed forward artificial neural network optimised with particle swarm optimisation technique to predict condensate to gas ratio in retrograde gas condensate reservoir. Statistical and graphical error analyses indicated that the proposed PSO-ANN is superior over conventional ANN and empirical correlations.

In 2013, Wang and Qui [127] employed three different PSO algorithms to optimise the ultimate oil recovery of a giant heavy oil reservoir. The performance of these algorithms was evaluated in terms of convergence behavior and the final optimisation results. Conventional PSO gave the best objective function.

In 2013, Humphries et al. [96] investigated the application of PSO combined with the generalized pattern search (GPS) both in a coupled and decoupled (sequential) manner on the joint optimisation of well placement and control problem. They mentioned the possible superiority of decoupling over a fully simultaneous approach although the efficiency of decoupling would depend on the assumed fixed control scheme during the initial stage of well placement optimisation.

In 2014, Zendehboudi et al. [128] linked ANN to PSO for predicting the performance of steam assisted gravity drainage (SAGD) in fractured and unfractured petroleum reservoirs. The results indicated that the developed PSO-ANN can satisfactorily predict the cumulative steam oil ratio and recovery factor of petroleum reservoirs.

In 2015, Jesmani et al. [129] applied PSO to find the optimal location of wells for two simple production cases subjected to realistic field constraints including a minimum inter-well distance, a minimum or maximum well length and orientation of the wells. The net present value (NPV) was selected as the objective function. They used two constraint handling methods, namely a decoder procedure and the penalty method. The decoder procedure was realized to be faster than the penalty method since it does not evaluate infeasible solutions. They also conducted a sensitivity analysis on different field constraints with respect to the optimal solution.

No application of PSO to the problem of WAG optimisation could be found in literature by the author of this thesis.

In the following sections, we briefly introduce some of the other methods which have been used for the optimisation of WAG performance. These methods include optimal control, decision tree analysis, expert systems, design of experiments, Monte Carlo method, Ensemble Kalman filter, simulated annealing and Tabu search. The application of these methods to the optimisation of WAG performance will be reviewed in the section of WAG optimisation.

2.6.3.3 Optimal Control

Optimal control, as a branch of calculus of variations, is a mathematical optimisation method in control theory for calculating control laws. This method is mainly due to the work of Lev Pontryagin [130] and Richard Bellman [131].

In this method, first a desired cost function is defined according to state and control variables and then a set of differential equations is solved to derive the control policies which minimize the cost function. Optimal control finds the control laws for a given system such that a certain optimality criterion is obtained. The optimal control can be either derived from Pontryagin's maximum principle (a necessary condition also known as Pontryagin's minimum principle or simply Pontryagin's Principle) [132], or by solving Hamilton-Jacobi-Bellman equation as a sufficient condition [133].

2.6.3.4 Decision Tree Analysis

A decision tree is composed of different tests on a feature (for example, what comes next in a coin flip) in a flowchart-based structure [134]. The leaf node of the tree is a class label (decision generated after computing all attributes), the branch is the test result and classification rules connect root to leaf. A decision tree and a related influence diagram provide a visual and analytical support tool in decision analysis in which desired values of competing alternatives are calculated. There are three types of nodes in decision tree: decision nodes, chance nodes and end nodes. Decision trees are very common in operations research and management along with other methods such as risk and uncertainty analysis, influence diagrams, utility functions and other decision analysis tools. In case we have incomplete knowledge in online decisions, a probability model or online selection model algorithm is paralleled by the decision tree. This method can also be used as a descriptive tool to calculate conditional probabilities.

2.6.3.5 Expert Systems

An expert system is a decision-making computer system that reproduces the function of a human expert [135]. Instead of using standard procedural code, expert systems utilize the primary knowledge as if-then rules to solve complex problems. They were initiated in the 1970's and their application increased rapidly in the 1980's. Expert systems were considered as one of the first successful methods of artificial intelligence (AI) software [136].

An expert system can be categorized into two sub-systems known as the inference engine and the knowledge base. The facts and rules are provided by the knowledge base while the inference engine obtains new facts by applying the rules to the known facts. Inference engines are also capable of explanation and debugging [137].

2.6.3.6 Design of Experiments

The design of experiments (DOE, DOX or experimental design) is the design of any task which tries to describe the change of information under hypothetical conditions and predict the outcome by introducing a variation in the predictor [138]. Among different methods of design of experiments, we briefly introduce response surface methodology (RSM), optimal design and fractional factorial design.

Response surface methodology (RSM) is a statistical approach introduced by Box and Wilson [139] in 1951 in order to explore the relationships between explanatory and response variables. In this method optimal response is obtained from a sequence of designed experiments using a

polynomial model as an approximation when there is little information available about the process.

Optimal designs are a class of experimental designs in which parameters are being estimated without bias and with minimum variance [140]. This requires a smaller number of experimental runs for estimating statistical models than non-optimal design and practically reduces the costs of experimentation.

In fractional factorial designs, in order to reveal information about the most important features of a problem studied, a fraction of the effort of a full factorial design in terms of experimental runs and resources is used [141]. In this approach, after the experimental runs of a full factorial design, a subset (fraction) of it is carefully chosen to utilize the sparsity-of-effects principle.

2.6.3.7 Monte Carlo Methods

Monte Carlo methods are a broad class of computational algorithms that obtain numerical results by means of repeated random sampling. They are mostly used when other mathematical methods are difficult or impossible to apply to physical or mathematical problems. The applications of these methods can be classified into three categories of optimisation, numerical integration, and generating draws from a probability distribution [142]. If any problem has a probabilistic interpretation, it can be solved by Monte Carlo methods. By the law of large numbers, the empirical mean (the sample mean) of independent samples of some random variable is an approximation to the integrals described by the expected value of the random variable [143].

In oil and gas industry, Monte Carlo simulation has found applications in reserve estimation, production and revenue forecast from a field and comparison of net present values or cash flow from different investments [144]. The most challenging aspect of Monte Carlo simulation is selecting statistical distributions for the input parameters [145].

2.6.3.8 Ensemble Kalman Filter (EnKF)

Bayes theorem is used to obtain the probability density function (PDF) of the state of the modeled system after data likelihood is taken into account. The Monte Carlo implementation of the Bayesian update problem is called Ensemble Kalman Filter (EnKF). As new data is included in the system from time to time, the Bayesian update is combined with advancing the model in time. The original Kalman Filter uses the Bayesian update to formulate the change of the mean and the covariance matrix and advance the covariance matrix in time by assuming Gaussian distribution for linear systems [146]. EnKFs were developed because it was not computationally practical to maintain the covariance matrix for high-dimensional systems. The distribution of the system state is represented by a set of state vectors or an ensemble and EnKF substitutes the covariance matrix by the sample covariance. The ensemble members of a random sample are not independent and the EnKF advances each member of the ensemble to advance the PDF in time [147].

The EnKF recently found application in petroleum science [148] and is mostly used for history matching. The first application was introduced by Lorentzen et al. [148]. In their paper, they tuned the model parameters for a dynamic two-phase fluid flow in a well and improved the predictions of the well pressure behavior. Naevdal at al. [149] used EnKF to update the

permeability field for near-well region of a reservoir model and improvement in the quality of the evaluated permeability was observed as more data was assimilated.

2.6.3.9 Simulated Annealing (SA)

In order to approximate the global optimum of a given function in a large search space (mostly discrete search spaces), a probabilistic technique called simulated annealing was first proposed by Kirkpatrick et al. [150]. This method is preferable to alternatives such as gradient descent when the goal is to find an acceptable local optimum in a limited amount of time instead of the precise global optimum. The method is inspired from annealing in metallurgy as a means to reduce the state of a system to its minimum energy. Slow cooling is similar to a slow reduction in the probability of accepting worse solutions in the search space, which allows for a more exhaustive search for the optimal solution.

2.6.3.10 Tabu Search

Tabu search was first proposed by Glover [151] as a metaheuristic which uses local search for mathematical optimisation. Local search methods check the neighborhood of their current location in the hope of finding a better solution. Tabu search improves the performance of local searches by accepting worse solutions if no better solution is available in the neighborhood. In addition, the points in the search space which have already been checked are marked as tabu (forbidden) in the memory of the algorithm and would not be visited repeatedly.

2.7 WAG Optimisation

In 1988, Mehos and Ramirez [152] used optimal control theory on a simplified black oil model for a two-dimensional flow in a homogeneous porous medium. The theory was applied to optimise the net profit for CO_2 miscible flooding in the three cases of a single slug, simultaneous injection of CO_2 and water and WAG injection. They found wellbore pressure as an important design parameter for carbon dioxide miscible flooding and claimed that the optimal total slug volume of CO_2, the cumulative recovery of oil and the optimal net profit value are nearly the same for all the three cases. They suggested optimal control theory as a good candidate for qualitative discussions on an optimal injection plan.

In 1992, Mackowski et al. [153] employed decision tree analysis to choose the best possible investment and operational plan which would maximize net present value and they found this approach to be more organized and much less time consuming than the cumbersome economic assessment of many single cases. The decision tree was stated to have the ability of involving uncertainties and statistical analysis which would give a range of possible outcomes. They recommended WAG tapering (increasing the WAG ratio), especially at the patterns with the highest incremental GOR.

In 1996, Bedrikovetsky et al. [154] proposed an analytical model for the hyperbolic system of continuity equations (mass conservation). They assumed one-dimensional fractional flow in a three-component two-phase system of oil-water-CO_2 in a homogeneous porous medium and disregarded capillary and diffusive forces, however, they took into account viscous fingering and gravity segregation. Apart from the simplifications, they achieved some semi-qualitative results

on the range of WAG ratio and slug size. The two objectives of maximum displacement efficiency and minimum mobility ratio narrow down the range of the suitable WAG ratio. They also recommended a critical minimum slug size, based on their analytical model, at which the gas becomes unstable, hence the slug size should be selected slightly larger.

Several previous studies only conducted a limited number of simulation runs and suggested field performance surveillance as the means to determine optimal WAG parameters [29, 155-158]. In 2003, Johns et al. [159] completed compositional simulation runs to optimise WAG recovery for gas floods above the minimum miscibility enrichment (MME) and analyzed the influence of WAG parameters, numerical dispersion caused by over-refining the grid-block sizes, the degree of enrichment above the MME and reservoir heterogeneity on displacement and sweep efficiency. They suggested use of coarser grids for estimating the recovery difference between two levels of enrichment above the MME. For heterogeneous reservoirs, when the most permeable layers are at the bottom of the reservoir, over-enrichment above the MME acts best and continuous slug gas injection outperforms WAG with richer gases and lower ratio of vertical to horizontal permeability.

In 2005, Gharbi [160] utilized expert systems, as a subclass of Artificial Intelligence, combined with an economic package, to select the suitable EOR process for a field. Then the method was applied to design the process and optimise the project profitability by sensitivity analysis for chemical as well as WAG flood. WAG ratio, slug size per WAG cycle and then the total slug size were optimised respectively in an iterative manner by changing the variables incrementally in small ranges. They used UTCOMP and UTCHEM as the simulators implemented in the expert

system and also did sensitivity analysis for NPV with respect to its parameters (such as oil price, WAG ratio, etc.).

In 2006, Esmaiel and Heeremans [161] developed a response surface proxy model using optimal design, which reduces the high number of required simulation runs, and then used Monte Carlo simulation to introduce uncertainty in the calculation of NPV and converted the uncertainty to utility for the decision making purpose. This response surface is stated to be fast (although of a polynomial form) compared to the simulator and can be employed for sensitivity analysis and optimisation over the entire design space. In 2008, Ghomian et al. [162] investigated the effect of relative permeability hysteresis based upon correlations, as well as WAG ratio, slug size and heterogeneity on CO_2-WAG recovery and carbon dioxide sequestration via a compositional simulator. The influence of hysteresis is emphasized due to its effect on trapping for the aim of storage and its effect on mobility ratio and sweep efficiency. They did a sensitivity analysis by means of a two-level factorial design and measured the effect of different parameters on the objectives (recovery, storage and NPV) separately and optimised them through response surfaces. In 2012, Ghaderi et al. [163] did similar work on a tight formation, which is a candidate for hydraulic fracturing, however, they neglected hysteresis and quantified the effect of development pattern, fracturing parameters, WAG parameters and the time to switch from primary or water flood to WAG by means of response surfaces. The response surfaces were employed to optimise different combinations of objectives by applying desired weighting multipliers.

In 2010, Odi and Gupta [164] simulated the carbon dioxide core flood results and modeled field scale carbon dioxide WAG on a simple cubic reservoir model. They applied non-adjoint based optimisation algorithms (algorithms which do not need the access to the simulator code) by means of an Ensemble Kalman filter approach to find the optimal WAG configuration (only injection rates) and maximized stored CO_2 and the cumulative oil produced. Their work shows the viability of Ensemble Kalman filter and the importance of WAG design and optimisation in complex reservoir models due to substantial amount of stored carbon dioxide and increase in oil recovery in a simple model. In 2012, Jahangiri [165] developed a new co-optimisation framework based on Ensemble Kalman filter to both take into account the reservoir uncertainties by representing the probability distribution of the model parameters through an ensemble of reservoir trials. The net present value was optimised through coupling the ensemble-based optimisation method with the reservoir trials and controlling the injection rates, bottom hole pressures of the producers and injection pattern as the variables. This method is claimed to be computationally cheap and flexible in the choice of simulator and economic model as a non-adjoint algorithm.

In 2013, Rahmawati et al. [166] solved the mixed-integer nonlinear problem optimisation for different flooding strategies. This problem was a combination of integer variables (choice of injection phases composed of (water/gas)-alternating-(gas/water), continuous gas/water injection and natural depletion) and continuous variables (well pressures, rates and injection volumes). A heuristic simplex algorithm was used to find the maximum NPV and the best injection scenario. This algorithm is a direct search method which does not require the derivatives and can be coupled with the simulator and economic model. They started the iterations with various random

initial guesses and increased the number of the starting guesses with an increased complexity of the injection scenario to avoid the local optimum. They mentioned that the NPV should be tested and maximized for the optimum field production life time (before the negative return of cumulative NPV versus time).

The first application of a genetic algorithm to a WAG optimisation was in 2000 by Daoyong et al. [167]. They optimised the multivariate production-injection system for WAG miscible flooding using net present value as the objective function. They only assumed two cycles of WAG injection and linked the economic model, reservoir model, production well and choke model for the optimisation task. Their decision variables included bottom hole pressures of the producers and gas/water injection rates. They put some constraints on pressures, material balance calculations and development strategies such as the ultimate recovery and the average rate of oil production. They claimed that GA showed stability and efficiency for their optimisation purpose. In a similar work in 2002 [168], they tried simulated annealing as well as GA and mentioned the capability of both of the techniques for WAG process optimisation. The results with optimisation showed more stable flooding front, improved sweep efficiency and a delayed high water-cut stage by up to 5 years compared to the unoptimised case. In 2010, Chen et al. [54], used a genetic algorithm hybridized with Tabu search method and an experimental design technique to optimise the controlling variables (WAG ratio, cycle time, injection rates and bottom hole pressures of the producers) of a CO_2-miscible flooding in field scale. The genetic algorithm was criticized for its low convergence speed in their research. Hence an orthogonal array was used to obtain a better initial generation for the optimisation process and Tabu search was applied through a mutation operator, which helps the procedure avoid the local optimum, and this was

mentioned to have increased the convergence speed to a large extent. Their optimal WAG design could increase recovery factor and NPV by 9.9% and 11.4%, respectively.

The above applications of different optimisation methods for the purpose of WAG optimisation are listed in Table 2-2. For each reference investigated in this study, the optimisation method, the decision making variables included and the main observations are tabulated.

Table 2-2: WAG optimisation methods, the optimisation variables and observations found in the literature

Reference	**Optimisation method**	**WAG Optimisation variables**	**Main observations**
Mehos and Ramirez [152]	Optimal control	Injection rates	Importance of wellbore pressure as a design parameter Applicability of optimal control to optimise injection plan
Mackowski et al. [153]	Decision tree analysis	WAG ratio, Slug size	Organization and speed of decision tree analysis Ability of involving uncertainties Recommendation of WAG tapering, especially for high incremental GOR
Bedrikovetsky et al. [154]	Analytical model	WAG ratio, Slug size	Deriving ranges for WAG ratio and slug size Recommendation of a critical minimum slug size
Johns et al. [159]	Trial and error	WAG ratio, number of cycles	Applicability of coarser grids for estimating recovery above MME Superiority of continuous gas injection over WAG when permeability is higher at the bottom layers of the reservoir
Gharbi [160]	Expert system	WAG ratio, Slug size per WAG cycle, Total slug size	Applicability of expert systems to select the suitable EOR process and optimise its parameters

Esmaiel and Heeremans [161]	DOE + Monte Carlo simulation	Status of completions, Slug size	Speed of DOE and its applicability to sensitivity analysis and optimisation
Ghomian et al. [162]	DOE	WAG ratio, Slug size	Influence of hysteresis on mobility ratio and sweep efficiency
Ghaderi et al. [163]	DOE	Development pattern, Hydraulic fracture geometry, WAG ratio, Slug size, WAG timing	Applicability of response surfaces to optimise different combinations of objective functions
Odi and Gupta [164]	EnKF	Injection rates	Viability of EnKF to optimise WAG recovery and carbon storage
Jahangiri [165]	EnKF	Injection rates, bottom hole pressures of producers, Injection pattern	Flexibility of EnKF in the choice of simulator and economic model and its low computational cost
Rahmawati et al. [166]	Mixed-integer nonlinear programming	Recovery method, Injection pressures, Oil production rates, Time to switch between recovery methods, Total time	Necessity of NPV optimisation for the optimum field production life time
Daoyong et al. [167]	GA	Bottom hole pressures of producers, Injection rates	Stability and efficiency of GA for NPV optimisation
Daoyong et al. [168]	SA	Bottom hole pressures of producers, Injection pressures	more stable flooding front, improved sweep efficiency and a delayed high water-cut stage compared to the unoptimised case
Chen et al. [54]	GA + Tabu search	Bottom hole pressures of producers, Injection rates, WAG ratio, Cycle time	Low convergence speed of GA without hybridizing with Tabu search Increase in NPV and oil recovery by 9.9% and 11.4%, respectively, compared to the reference case

2.8 Summary

WAG performance needs to be optimised to obtain either the maximum oil recovery or NPV within the economic limits and the problem of WAG optimisation in the field scale needs to be investigated more thoroughly under field constraints.

The problem of WAG optimisation on field scale is a complex nonlinear problem with a rough surface and probably multiple local optima. A genetic algorithm (GA) and a particle swarm optimisation (PSO) are employed as the optimisation techniques. These techniques are derivative free, non-invasive (non-adjoint) or black box global randomized search strategies which do not require access to the simulator code and gradient information. These algorithms have the potential of leaving the local optima in the search space and finding the global optimum. GA and PSO both have proved their capability in the area of optimisation in petroleum science which was supported by literature. GA has already been used for the purpose of WAG optimisation on field scale, however PSO is tested on this type of problem for the first time.

In this study, we optimise over bottom hole pressures of the producers, injection rates, cycle ratio, cycle time, total WAG time and the injection gas composition. The gas composition, which involves the effect of miscibility on production performance, is included for the first time in the area of WAG optimisation research to the best of the author's knowledge.

Chapter 3: Methodology

A methodology for a WAG optimisation on the E-segment of the Norne field is presented in this chapter. The presented methodology includes a brief description of the field and the rock and fluid properties, optimisation framework, history matching, definition of the objective functions, along with the optimisation variables and constraints and the design of the experiments which will be conducted in this study.

3.1 Norne Field

In this section, the E-segment and the rock and fluid properties are briefly described. A short explanation on the geological simulation model of the E-segment as well as the description of the active wells are presented. Then fluid properties, relative permeabilities and the results of slim tube tests are discussed.

3.1.1 Field description

The Norne field, located about 80 km north of the Heidrun field in the Norwegian Sea, is composed of two separate oil compartments, namely Norne main structure (C, D and E-segments) which contains 97% of the oil in place and the North-East Segment (Norne G-segment).

In this thesis, we only consider the E-segment where we separate it from the rest of the field.

The E-segment contains 8733 active cells. The sizes of the blocks are between 80 m to 100 m in the horizontal direction. In total, 8 wells have been drilled in the E-segment. These include one observation well, two injection wells and five production wells. The reservoir initial pressure was about 273 bar at 2639 m TVD. The rock is of mixed wettability and pore compressibility is 4.84×10^{-5} 1/bar at 277 bar [11].

At the end of 2006, the E-segment contains two active injectors, namely F-1H and F-3H, and three active producers, namely E-2AH, E-3CH, and E-3H as shown in Fig. 3-1. The description of the wells in the E-segment is included below.

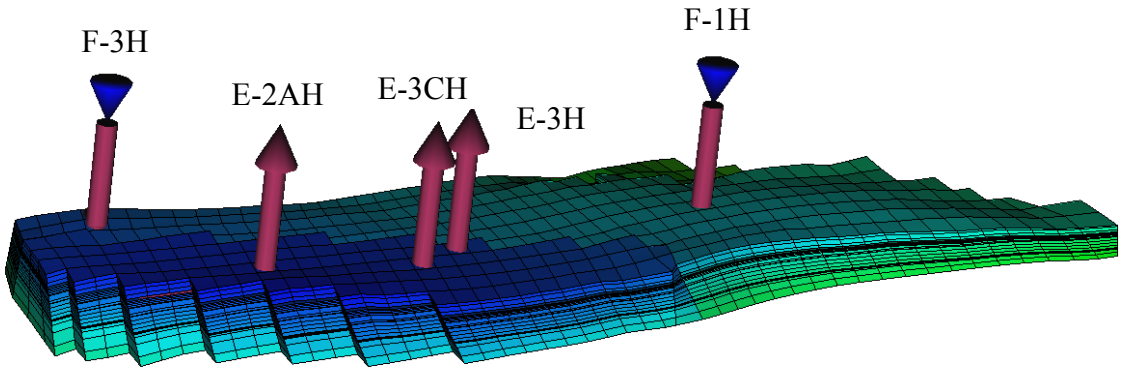

Fig. 3-1: The E-segment of the Norne field at the end of 2006

Injector Well 6608/10-F-1 H: Well 6608/10-F-1 H was the fourth water injector to be drilled, located in the north of the Norne E-Segment. The well was designed to inject water in the water leg of the northern part of the field. All wells on the F-template can easily be converted from

water to gas injection. The well was perforated approximately 23 m TVD below the oil-water contact in the Ile and Tofte formations. Injection into this well started in September 1999 [169].

Injector Well 6608/10-F-3H: This was the sixth water injector drilled on the field, located in the south-western part of the E-segment. The well was drilled with an angle of up to 50° in the top-hole section and less than 20° in the reservoir. It was perforated in the Tofte and Tilje Formations. Injection started in September 2000. It is easy to convert well F-3H from water to gas injection.

Well 6608/10-E-2AH: The objective for this well was to drain the remaining oil from the E-segment. The well trajectory was planned as a horizontal section below the top Ile Formation, over the oil-water contact (OWC) at approximately 2606 m TVD mean sea level (MSL). It was drilled deeper than planned and penetrated higher than the anticipated OWC, before it was steered back through Ile 2.1 Formation. The well started to produce oil in August 2005.

Well 6608/10-E-3CH: This well was perforated in Ile formation and started oil production in April 2005.

Well 6608/10-E-3H: Well 6608/10-E-3 H was the eighth development well and first production well planned in the northern part of segment E. The central part of the E-segment was the target for draining. The well was designed to contribute to a low GOR oil production and provide a reference point in the northern part of the field to confirm reservoir communication. Well completion has been done in Ile and upper Tofte formations [169].

3.1.2 Rock and Fluid Properties

The composition of the Norne oil and gas as reported by Statoil are presented in Table 3-1 [170]. Fig. 3-2 shows the P-T diagram of the oil with the above composition obtained from PVTsim

with the three-parameter Peng-Robinson equation of state (PR-Peneloux EOS) before any regression and tuning.

Table 3-1: Compositional analysis of the reservoir oil and gas

Component	Reservoir oil (mol%)	Reservoir gas (mol%)
N_2	0.272	0.027
CO_2	0.874	1.306
C_1	47.749	89.242
C_2	3.921	4.850
C_3	2.085	1.940
i-C_4	0.445	0.361
n-C_4	0.878	0.609
i-C_5	0.429	0.131
n-C_5	0.467	0.128
C_6	0.871	0.161
C_7	2.505	0.282
C_8	4.071	0.319
C_9	2.992	0.185
C_{10+}	32.441	0.459

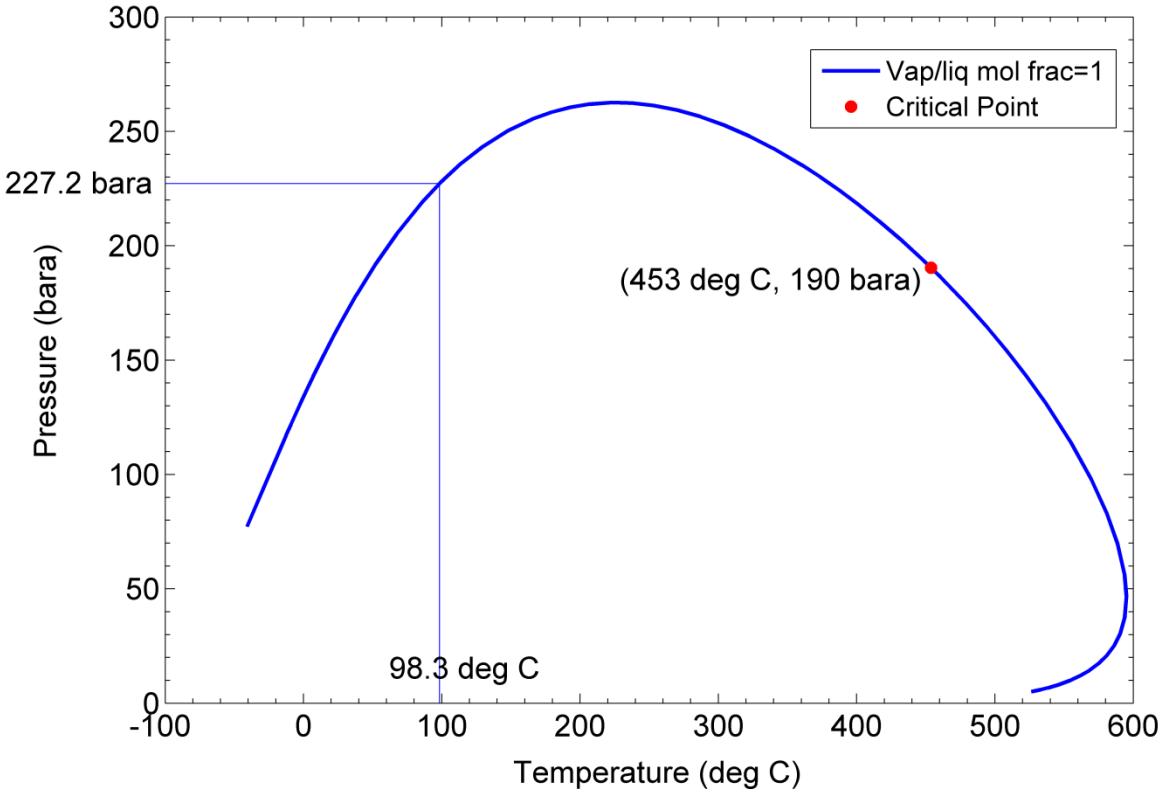

Fig. 3-2: P-T diagram of Norne reservoir oil with PR-Peneloux EOS (before tuning)

As can be seen from the above figure, PR-Peneloux EOS predicts a bubble point pressure of about 227 bar at the reservoir temperature (98.3°C) which is below the actual value (251 bar). This indicates the necessity of tuning of the EOS for improvement in the predictions of compositional simulations.

Fig. 3-3 and Fig. 3-4 regenerated from [169] represent the oil-water and gas-oil relative permeability curves of the E-Segment, respectively. Connate water saturation varies from 0.05 to 0.38 among different curves.

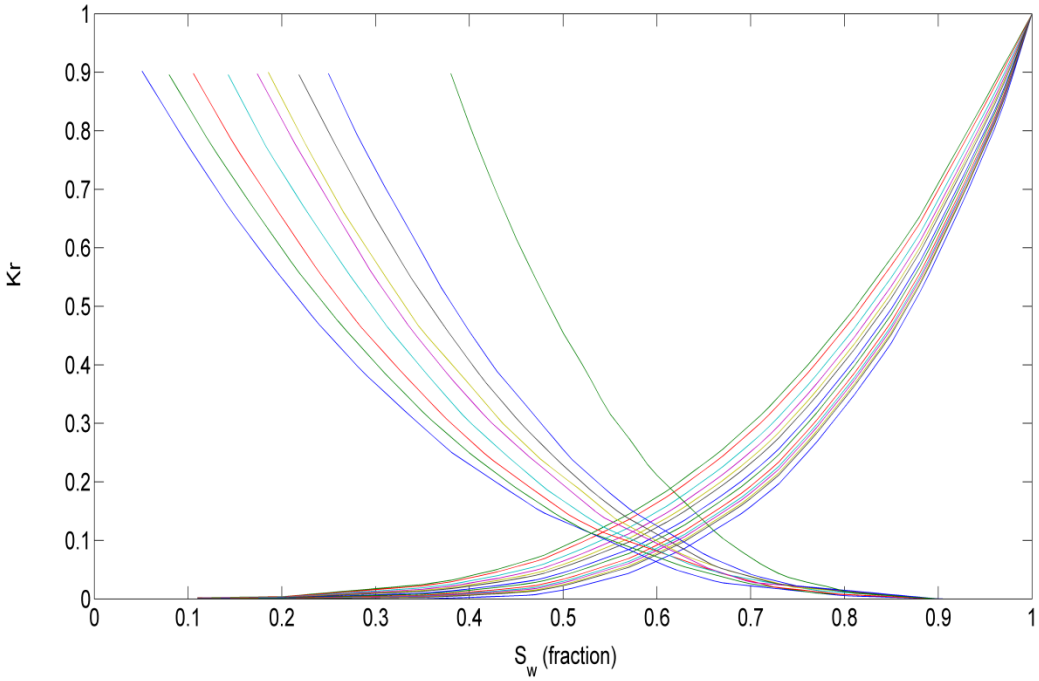

Fig. 3-3: Oil-water relative permeability for the E-segment of the Norne field [169]

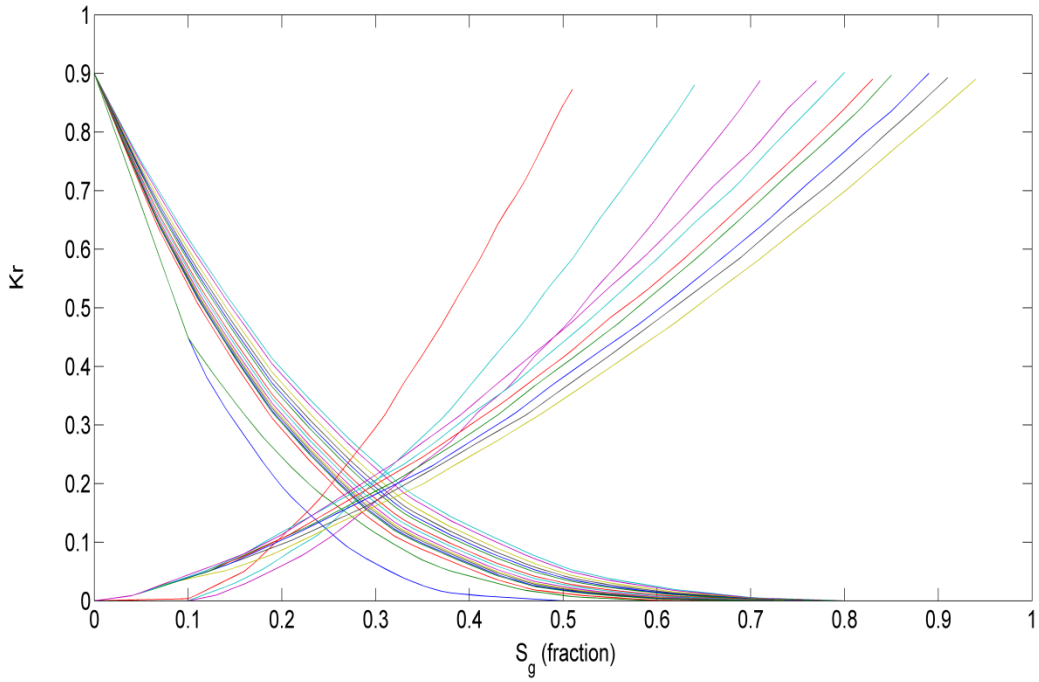

Fig. 3-4: Gas-oil relative permeability for the E-segment of the Norne field [169]

The minimum miscibility pressure (MMP) is a function of reservoir pressure and temperature as well as the injected gas composition. Usually, the separator gas is re-injected into the reservoir for pressure maintenance and EOR purposes. Since no data could be found in literature on the composition of the separator gas for the Norne field, the normalized composition of the reservoir gas containing only C_1 to C_4 (92% C_1, 5% C_2, 2% C_3 and 1% C_4) was chosen as the base injecting gas. The MMP between the crude oil with the base injecting gas and with the enriched gas containing 65% C_1, 20% C_2, 10% C_3 and 5% C_4 was obtained by means of PVTsim [171] and the results are shown in Tables 3-2 and 3-3, respectively.

Table 3-2: Slim tube results using the base injecting gas (92% C_1, 5% C_2, 2% C_3 and 1% C_4)

Slim Tube Recovery at 98 °C	
Pressure (bar)	**Recovery (%)**
270	12.87
300	18.90
350	30.23
400	44.06
450	62.01
500	86.38
550	96.92
600	98.19

Table 3-3: Slim tube results using the enriched gas composition (65% C_1, 20% C_2, 10% C_3 and 5% C_4)

Slim Tube Recovery at 98 °C	
Pressure (bar)	**Recovery %**
270	73.23
300	89.12
350	95.65
400	98.24
450	99.46
500	99.79

MMP is usually defined as the pressure at which approximately 95% of the oil is recovered during slim tube test [172]. The effect of enrichment on the results of slim tube tests is quite clear. Enriching the gas from 8% to 35% of the intermediate components, the MMP is reduced from about 550 bar to about 350 bar. Since the initial reservoir pressure of the Norne field is about 273 bar, miscible and near miscible injection might occur in some portions of the reservoir if the injecting gas is enriched enough and the injection pressure and bottom hole pressure of the producers are kept sufficiently high.

3.2 Optimisation

In this section, the optimisation framework is detailed. The methodology used for history matching of the reservoir model is discussed. The objective functions used in this study are introduced. The optimisation variables, constraints and techniques employed to solve the WAG optimisation problem are presented. Finally, the detailed optimisation procedure and the experiments conducted in this study are described.

3.2.1 Optimisation Framework

Fig. 3-5 shows the flowchart for the WAG optimisation framework in this study. After the reservoir model is history matched, the initial guesses of well control parameters for starting the optimisation technique(s) are generated. Then the reservoir simulator is called to run the simulation data file and calculate the production profiles. The results of production are read from the output of the simulator and the objective function(s) are computed for each particle (point in the solution space). A stopping criterion (usually based on the computational budget or

maximum CPU time) is defined. If the criterion is not met, the optimisation techniques generate the particles for the next iteration according to their built-in rules and theories and the above process of simulation runs and objective function calculations continues until the stopping criterion is met. Then the process is terminated and the saved results can be viewed.

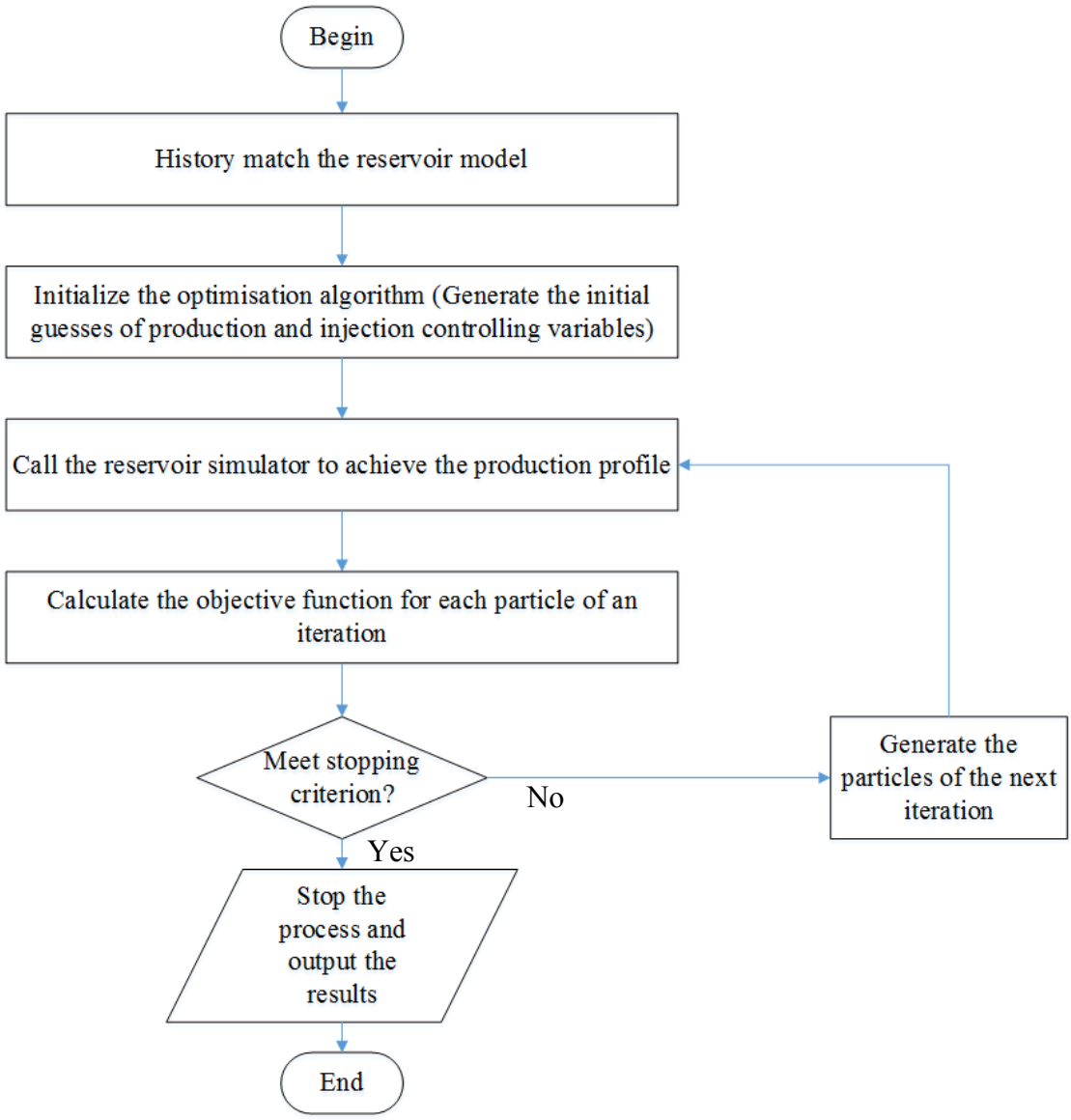

Fig. 3-5: Flowchart of the WAG optimisation process

3.2.2 Reservoir Simulation

Reservoir, production and injection subsystems must be taken into account as a whole for the purpose of production optimisation.

The reservoir simulator is generally regarded as a black box with the injected fluids as the input and the produced fluids as the output. Due to the complexities of fluid flow in porous media, reservoir simulation has to be employed as an inseparable part of the production forecast and optimisation. In this study, the compositional simulator, module E300 of Schlumberger reservoir simulation software, has been used. Unlike the black oil simulator, the compositional simulator takes into account the changes in the composition of the fluids as the field is produced. PVT properties of oil and gas are fitted to an equation of state (EOS) and the tuned EOS is used to dynamically track the movement of phases and components in the reservoir [173].

The production subsystem starts with the inflow performance relationship (IPR) between the bottom hole pressure (BHP) and the production rate and continues with multiphase flow calculations in the production string. The BHP of the producer will be selected as an optimisation variable in this study.

In the injection subsystem, the injection rates of gas and water, cycle (WAG) ratio, the injection period (cycle time and total WAG duration) and composition of the injected gas can be regarded as the optimisation variables.

3.2.2.1 History Matching

The first step to have a reliable prediction of the performance of various EOR methods during reservoir simulation is history matching. Due to errors and uncertainties in the simulation model, the simulated results rarely match with reality [174]. The errors usually result from the uncertainties in the description data (such as the geological model) and the inaccuracies in the historical production and injection data [175]. In history matching, reservoir engineers try to adjust the reservoir parameters with a higher degree of uncertainty, such as permeabilities, layering structure, fault transmissibilities, etc., to match the simulation results (usually production rates) with the production history during a specific period of time [174].

This task can be complex and time consuming. Reservoir engineers usually perform this task by means of trial and error. Initially, a sensitivity study is conducted and then one or more of the most sensitive reservoir parameters are changed and modified during several iterations to match the simulation and history as closely as possible. History matching is usually performed manually in the industry although automatic methods are gaining attention and popularity nowadays [12]. A few examples of the application of optimisation techniques to history matching are briefly mentioned in sections 2.6.3.1 and 2.6.3.8.

In this study, history matching is conducted up to December 2006 (on the available data) by adjusting the relative permeabilities in order to match the simulated oil production rates of the wells with the history. History matching can be regarded as an optimisation problem. A genetic algorithm (GA) is used to solve this optimisation problem. Only one set of oil-gas and one set of oil-water relative permeability has been used for the whole field. A Corey model is fitted to the

relative permeability data. Corey correlations for two-phase oil-water and gas-oil relative permeabilities are presented below [176, 177]

$$S_{wn} = \frac{S_w - S_{wc}}{1 - S_{wc} - S_{or}}, \tag{3.1}$$

where

S_{wn} = Normalized water saturation
S_w = Water saturation
S_{wc} = Critical (irreducible) water saturation
S_{or} = Residual oil saturation.

Then the correlations of water and oil relative permeability in a two-phase oil-water system are defined as below

$$K_{rw} = K^{\circ}_{rw}(S_{wn})^{N_w},$$
$$K_{row} = K^{\circ}_{row}(1 - S_{wn})^{N_{ow}}, \tag{3.2}$$

where

K_{rw} = Water relative permeability
K_{row} = Oil relative permeability (in a two-phase oil-water system)
K°_{rw} = The endpoint of water relative permeability
K°_{row} = The endpoint of oil relative permeability (in a two-phase oil-water system)
N_w = Exponent of water relative permeability
N_{ow} = Exponent of oil relative permeability (in a two-phase oil-water system).

Similar correlations were defined for oil and gas relative permeabilities in a two-phase gas-oil system as below

$$S_{gn} = \frac{S_g - S_{gc}}{1 - S_{wc} - S_{gc}}, \tag{3.3}$$

where

S_{gn} = Normalized gas saturation
S_g = Gas saturation
S_{gc} = Critical gas saturation.

Then the correlations of gas and oil relative permeability in a two-phase gas-oil system are defined as below

$$K_{rg} = K^{\circ}_{rg}(S_{gn})^{N_g},$$
$$K_{rog} = K^{\circ}_{rog}(1 - S_{gn})^{N_{og}}, \tag{3.4}$$

where

K_{rg} = Gas relative permeability
K_{rog} = Oil relative permeability (in a two-phase gas-oil system)
K°_{rg} = The endpoint of gas relative permeability
K°_{rog} = The endpoint of oil relative permeability (in a two-phase gas-oil system)
N_g = Exponent of gas relative permeability
N_{og} = Exponent of oil relative permeability (in a two-phase gas-oil system).

The endpoint values and exponents of the model are selected for optimisation. The objective function is defined to be the square of the weighted sum of the differences between the history and the simulated oil production rates of the wells and higher weights are applied to the simulated rates which are further from the history. To minimize the error between the simulated and historical total oil production data is one of the main concerns of reservoir engineers in

history matching, so the objective function (Error) was selected to be defined in the following form

$$Error = \int_0^{T^{sim}} \sum_{i=1}^{N_{well}} w_i (q_{oi}^{sim} - q_{oi}^{hist})^2 \, dt, \tag{3.5}$$

where

T^{sim} = total simulation time [day]
N_{well} = Number of production wells (3 in this study)
w_i = Weight applied to production well *i*
q_{oi}^{sim} = Simulated oil production rate of well *i*
q_{oi}^{hist} = Historical oil production rate of well *i*
t = time [day].

The initial population (vectors of the coefficients and exponents) are generated randomly by means of GA. The oil-water and gas-oil relative permeability data required for the reservoir simulation are provided using equations (3.2) and (3.4) and then written in a file included in the main simulation data file. The oil production rates are then read for each particle in an iteration from the simulation output. The objective function is calculated for each of the particles. The next population is generated by the operators of selection, crossover and mutation of GA. This process is set to 2000 simulation runs. The results of the history matching are presented in Chapter 4.

Water flooding is performed on the history matched model with sufficiently low rates in the two injectors to reach the value of 90% for the field water cut in May 2015. The production wells are kept at bottom hole pressures of 240 bar which is a little less than the bubble point pressure (the

bubble point pressure of the reservoir oil is 251 bar) since production with a pressure much lower than the bubble point pressure leads to early gas breakthrough and oil recovery reduction. The end of water flood up to May 1st 2015 is used in the form of restart file as the initial point for all WAG simulations for optimisation in this study.

3.2.3 Objective Functions for WAG Optimisation

It is necessary to choose a suitable objective function for the optimisation procedure. In production optimisation, the ultimate recovery factor or NPV is usually chosen as the objective (fitness) function which needs to be maximized. In this study, we optimise both of the NPV and recovery factor separately. Although NPV, as an economic measure, is not the only influencing factor, it is a proper indication of the project's profitability and helps in decision making.

NPV is defined as the sum of the present values of incoming and outgoing cash flows over a period of time. NPV for a WAG process can be calculated as follows:

$$
\begin{aligned}
NPV(X) = \sum_{i=1}^{n} \Big\{ & Q_o^{prod}(i) c_o - \left[Q_g^{inj}(i) - Q_g^{prod}(i-1) \right] c_g - Q_g^{prod}(i-1) c_g^{'} \ldots \\
& - \left[Q_w^{inj}(i) - Q_w^{prod}(i-1) \right] c_w - Q_w^{prod}(i-1) c_w^{'} \Big\} (1+r)^{-i} \ldots \\
& + [Q_g^{prod}(n)(c_g - c_g^{'}) + Q_w^{prod}(n)(c_w - c_w^{'})](1+r)^{-n}, \qquad (3.6)
\end{aligned}
$$

where n is the total number of evaluation years, i is the year number, c_o is the price of produced oil, c_g and c_w are the price for purchasing gas and water for injection, $c_g^{'}$ and $c_w^{'}$ are the cost of treating and recycling the produced gas and water, Q is the total volume of the produced or

injected fluid and r is the interest rate. Clearly, the volumes are functions of the optimisation vector X.

NPV is highly affected by the assumed prices. Different economic models would greatly influence the results. Operators define their economics differently and the prices also depend on the source and availability of the injection fluids. In spite of these differences, the optimisation procedure remains the same. Table 3-4 shows the economic parameters used in this study along with their values. To study the effect of assumed prices on the NPV to some extent, a sensitivity analysis on the economic parameters will be conducted in Chapter 4.

Table 3-4: Economic parameters used in the simulations

Parameter	**Value**
Oil price [\$ / Sm^3]	377
Methane price [\$ / Sm^3]	0.1
Ethane price [\$ / Sm^3]	0.21
Propane price [\$ / Sm^3]	0.79
Butane price [\$ / Sm^3]	1.7
Gas recycling cost [\$ / Sm^3]	70% of gas price
Water price [\$ / Sm^3]	6
Water recycling cost [\$ / Sm^3]	38
Interest rate [-]	5%

The oil price used in this study is \$377 / Sm^3 (\$60 / STB) which is based on WTI crude oil price in May 2015. The injection gas is composed of methane (C_1) plus different percentages of ethane, propane and butane (C_2, C_3 and C_4). The prices used are \$0.1, \$0.21, \$0.79 and \$1.7 per Sm^3 for C_1, C_2, C_3 and C_4, respectively, based on [178]. The cost of gas recycling is roughly

assumed to be 70% of the gas purchase price. The price of water purchase is \$6 / Sm^3 (\$1 / STB) and the cost of water recycling and disposal is \$38 / Sm^3 (\$6 / STB).

In addition to NPV, the total oil production in terms of incremental recovery factor (IRF) after the start of WAG is the second objective function in this study. IRF is defined in the following form.

$$IRF = \frac{\int_0^T q_o dt}{OIIP}, \tag{3.7}$$

where

$T =$ total WAG duration [day]
$q_o =$ total oil production rate [Sm^3/day]
$t =$ time [day]
$OIIP =$ Oil initially in place [Sm^3].

3.2.4 Optimisation Variables and Constraints

The decision variables, which should be optimised, are the production and injection settings. They usually consist of surface and reservoir variables. Wellhead pressure, injection and production rates are the surface variables [179]. The net to gross ratio of reservoir rock, fluid saturations, reservoir architecture, faults and fractures parameters, reservoir properties, pressure-volume-temperature (PVT) relation, relative permeability, compaction and compressibility of the reservoir rock compose the reservoir variables.

In this study, **total WAG duration**, **WAG cycle time**, **cycle ratio**, **injection rates** and **bottom hole pressure (BHP)** for the producers as well as the **composition** of the injected gas can be potentially chosen as the decision variables to achieve the optimal production (See Table 3-5 below).

Table 3-5: Variables of WAG process

Decision Variables	**Controllability**	**Type**
Total WAG duration	Y	Discrete
WAG cycle time	Y	Discrete
Cycle ratio	Y	Discrete
Injection rate	Y	Continuous
BHP	Y	Continuous
Gas composition	Y	Continuous

As shown above, all the input (decision variables) are controllable. The total WAG duration, cycle time and cycle ratio are chosen as discrete variables in the WAG simulations. The number of WAG cycles is the ratio of the total WAG duration to the cycle time. In this study, the cycle ratio is defined as the ratio of the time of water injection to the cycle time. So, the to-be-optimised variables in this study consist of water and gas injection rates for the two injectors, bottom hole pressures for the three producers, cycle ratio, cycle time, total WAG duration, mole fractions of ethane, propane and butane added to the base injectant. This gives 13 possible variables in total.

The ranges of the input variables in optimisation are chosen based on physical and/or economic constraints. Selecting a wider range for the variables increases the chance of not missing the

optimal solution, however, it makes the optimisation more expensive and may not be even physically feasible.

The minimum and maximum water injection rates are selected as 500 and 2700 Sm^3/day in the injectors. Gas injection ceased in the field in 2005 and there has been no gas injected into either of these wells. According to a previous simulation study [12] on the Norne field, 1000 and 1,000,000 Sm^3/day are the minimum and maximum limits for gas injection rates.

The upper limit for bottom hole pressures is set a little lower than the bubble point pressure (240 bar) and the lower limit is set equal to 150 bar to cover a wide range. Too low of a limit value for BHP might lead to early gas breakthrough and oil recovery reduction. It is expected that the optimisation algorithms will find the optimal bottom hole pressure for each producer.

The cycle ratio is between 0 and 1 and is discretized into steps of 0.05. A cycle ratio of 0 indicates a gas flood which might result in gas breakthrough. A cycle ratio of 1 indicates a water flood which may cause oil trapping, insufficient contact of solvent with oil and high water cut [12]. So, finding the optimal cycle ratio is obviously of importance.

Cycle time is set between two and 12 months in steps of 1 month. The lower limit for the total WAG duration is set at 30 months and since the field is to be abandoned in 2020, 60 months is selected as the upper limit.

The mole fractions of C_2-C_4 are the three remaining variables. The ranges for the optimisation variables in this study have been tabulated in Table 3-6.

Table 3-6: The optimisation variables along with their ranges in this study

Optimisation Variable	**Range**
Water injection rates [Sm^3/day]	500-2700
Gas injection rates [Sm^3/day]	1000-10^6
Producers bottom hole pressures [bar]	150-240
Cycle ratio [-]	0-1 in steps of 0.05
Cycle time [month]	2-12 in steps of 1 month
Mole fraction of C_2 [-]	0.05-0.2
Mole fraction of C_3 [-]	0.02-0.1
Mole fraction of C_4 [-]	0.01-0.05
Total WAG duration [month]	30-60 in steps of 1 month

There are numerous safety, capacity and economic constraints on the operations of oil and gas production. For safety reasons, a maximum/minimum pressure constraint may be required at the bottom of a well due to injectivity and fracture pressure. An upper or lower limit for the flow rate might have to be imposed on some of the production wells or facilities for economic reasons. The economic reasons may include the volume of gas available or the gas composition and enrichment and the control of fluid velocities to avoid excessive corrosion or erosion. The capacity constraints mainly include the processing capacities of surface facilities like surface pumps and separators for handling the water and gas produced with the hydrocarbons [180].

There are two types of constraints within this optimisation problem, namely general bound and economic (and/or safety) constraints. The bound constraints are of the simple inequality type as shown in Table 3-6. The economic constraints consist of lower limit on oil production (10 Sm^3/day) and upper limits on water cut (95%) and GOR (500 Sm^3/Sm^3) for all the production wells' perforations. If the limits are violated, the worst offending perforation will be shut and the

simulation continues until at least one perforation is open. The maximum liquid production rate of 6000 Sm^3/day (in each producer) and maximum injection pressure of 600 bar (in each injector) are also placed in the reservoir simulation data file. The limits of these safety and economic constraints are shown in Table 3-7.

Table 3-7: Upper and lower limits of economic constraints

Parameter	**Limit**
Well oil production rate [Sm^3/day]	10 (min)
Well water cut [-]	95% (max)
Well GOR [Sm^3/ Sm^3]	500 (max)
Well liquid production rate [Sm^3/day]	6000 (max)
Well injection pressure [bar]	600 (max)

3.2.5 Optimisation Techniques

Due to the complexities of the field-scale WAG optimisation, powerful optimisation techniques should be employed. Among the direct optimisation algorithms we will use GA and PSO. A brief description of these optimisation techniques has already been presented in Chapter 2. These are global derivative free optimisation techniques which do not need to extract the gradient information from the simulator code and have shown their capability in the optimisation area for different objectives in oil and gas engineering.

3.2.6 Experimental Setup

Two issues are discussed in this section. The first is to describe the different experiments which will be conducted in this study and the second is how to obtain the initial guesses for starting the optimisation process. Three experiments are designed for optimisation of NPV in this study.

In experiment 1, two water and two gas injection rates, three BHPs of the production wells, cycle ratio and cycle time (nine variables) are optimised. The mole fractions of injecting gas components are fixed at their lower bounds. The gas injection is immiscible in this case since the minimum miscibility pressure of the reservoir oil and injecting gas is calculated to be about 550 bar using PVTsim software, which is far above the reservoir pressure. In experiment 2, the injecting gas composition (mole fractions of C_2, C_3 and C_4) are added to the optimisation variables giving a total of 12 variables. The MMP between the reservoir oil and the most enriched gas is calculated to be about 330 bar, so miscibility could be achieved in the reservoir. In experiments 1 and 2, the total WAG simulation time is fixed at 30 months. We include it as a variable in experiment 3, that is we optimise over all 13 variables.

The decision and fixed variables for the three NPV optimisation experiments are shown in Table 3-8. The rationale behind the progressive experiments is to investigate the effect of increasing the number of variables on the quality of the resulting optimal solution and to evaluate and compare the efficiency of the two optimisation techniques.

Table 3-8: Optimisation and fixed variables for the three different experiments of NPV optimisation

	Experiment 1	**Experiment 2**	**Experiment 3**
Optimisation variables	• 2 water injection rates • 2 gas injection rates • 3 BHPs • Cycle ratio • Cycle time	• 2 water injection rates • 2 gas injection rates • 3 BHPs • Cycle ratio • Cycle time • Mole fractions of C_2,C_3 and C_4	• 2 water injection rates • 2 gas injection rates • 3 BHPs • Cycle ratio • Cycle time • Mole fractions of C_2,C_3 and C_4 • Total time
Fixed variables	• Mole fraction of C_2=0.05 • Mole fraction of C_3=0.02 • Mole fraction of C_4=0.01 • Total time=30 months	• Total time=30 months	None

For the purpose of oil recovery optimisation, only one experiment is conducted with the 12 decision variables of experiment 2 at the fixed total WAG simulation time of 60 months.

In this study, design of experiments (DOE, see section 2.6.3.6) is used to obtain the initial guess for the optimisation algorithms. DOE is a widely used method to specify the optimum input vectors in order to span the search space with considerably fewer runs than a full factorial design [163]. Optimal design (as a class of experimental designs) allows the parameters to be estimated without bias and with minimum variance and can reduce the cost of experimentation compared to a non-optimal design [140]. In experiment 3, for example, there are 10 variables with two levels (two gas injection rates, two water injection rates, three BHPs and mole fractions of C_2, C_3 and C_4) and three discrete variables with three levels (cycle ratio, cycle time and total WAG duration), hence a full factorial design requires $2^{10} \times 3^3 = 27648$ simulation runs. Optimal design is able to search the solution space with only 110 runs. For experiments 1 and 2, with nine and 12 variables, respectively, optimal design only requires 60 and 96 simulation runs. The best run

for each experiment will be selected as the reference (unoptimised) case to be compared with the optimisation results, and the runs from each experiment which result in higher objective function values will be used as the initial guess for that experiment to improve the convergence speed of the algorithms.

3.2.7 Optimisation Procedure

In this study, model-based production optimisation (optimisation on a fixed history-matched reservoir model) as shown in the flowchart (see Fig. 3-5) will be conducted. The best simulation runs from the design of experiment results are used to initialize the search process. The variables will be written in a file included in the main simulation data file and the reservoir simulator (E300) will be called to calculate the oil recovery and profiles of cumulative oil, gas and water for each scheme by integrating over the field production and injection rates. Cumulative oil production is calculated directly for the purpose of oil recovery optimisation. NPV for each individual scheme will be computed using equation (3.6) coded in the economic module. GA generates the next population by means of selection, crossover and mutation operators and PSO updates the velocity and position of the particles using equations (2.3) and (2.7). The aforementioned process will be iterated for the new population until the number of iterations reaches a pre-defined value. The whole optimisation process will be done automatically and without any manual interruption.

Due to the stochastic nature of the optimisation techniques, multiple trials are required for each experiment. The compositional simulations are time consuming, so the objective function calculations are costly and demanding. Four trials with 2000 function evaluations (simulation

runs) will be performed for each experiment of NPV optimisation and three trials with the same number of function evaluations for oil recovery optimisation using both GA and PSO. Each trial will be run with 50 particles for 40 iterations. For experiment 3, an exhaustive search on only the discrete variables (cycle ratio, cycle time and the total WAG time) requires about 6000 function evaluations.

The global optimisation toolbox of MATLAB R2012a is used for GA. For PSO, the following parameters (see equations (2.3) and (2.6)) are selected. These parameter values have shown good convergence results in literature [181, 182].

$C_1 = 0.5,$
$C_2 = 1.25,$
$\omega_{\max} = 0.9,$
$\omega_{\min} = 0.4.$

Chapter 4: Results and Discussion

The optimisation methodology explained in the Chapter 3 is utilized here to optimise the well control parameters in a field-scale hydrocarbon WAG process on the E-segment of the Norne field. Three experiments for NPV optimisation with different numbers of controlling variables sampled from the set of gas and water injection rates, bottom hole pressures of the producers, cycle ratio, cycle time, total WAG duration and mole fractions of C_2, C_3 and C_4 added to the base injectant are considered. One experiment for IRF optimisation including the same variables with a fixed total WAG duration is also investigated. GA and PSO algorithms are used to optimise NPV/IRF for each experiment. The results from the two algorithms are analyzed and compared within and among the experiments. As the global optimality cannot be guaranteed for stochastic methods such as GA and PSO, multiple trials are required to yield an estimate of the optimal solution. The multiple trials also allow us to assess the reliability of the optimisation methods. Hence we will conduct four trials for each of the experiments of NPV optimisation and three trials for the experiment of IRF optimisation.

Field operations far from an optimal point or inappropriate selection of the well control parameters may result in operational difficulties such as early gas breakthrough, increase in the cost of facilities and lower ultimate recovery factor. This leads to a reduction in NPV causing the project to be less economical. In other words, an optimisation algorithm is designed to help us find the operational point which results in more oil production from the point of oil recovery

optimisation or earning more money in a shorter period of time from the point of NPV optimisation. WAG optimisation on a field scale including all the above parameters has never been done before to the best of the author's knowledge. We will discuss the performance of the optimisation algorithms (GA and PSO) for the optimisation of NPV and oil recovery factor.

4.1 Fluid Characterization

All the simulation studies already done on the Norne field have been run in Black Oil mode (E100). The fluid properties presented in Table 4-1 are the only data which could be found in literature [139]. These data points were used for the PVT regression and match with the module PVTi of Eclipse and then the output file was included in the reservoir simulation data file for compositional simulation runs using module E300 of the Schlumberger reservoir simulation software Eclipse. The critical temperature of the plus fraction was selected as the regression parameter and PR-Peneloux EOS was used for tuning purposes.

Table 4-1: Characteristic fluid properties for the Norne field

Fluid property	**Value**
P_b [bar]	251
GOR at P_b [Sm^3/Sm^3]	111
B_o at P_b [Rm^3/Sm^3]	1.347
Oil density at P_b [g/cm^3]	0.712
Oil viscosity at P_b [cP]	0.58
B_o at P_i [Rm^3/Sm^3]	1.3185
B_g [Rm^3/Sm^3]	0.0047

Fig. 4-1 shows the P-T diagram of the reservoir oil before and after tuning of the EOS. After the regression and tuning, PR-Peneloux EOS predicts a bubble point pressure of about 250.8 bar which is quite close to the actual value (251 bar) and this shows the improvement in the EOS prediction after the tuning.

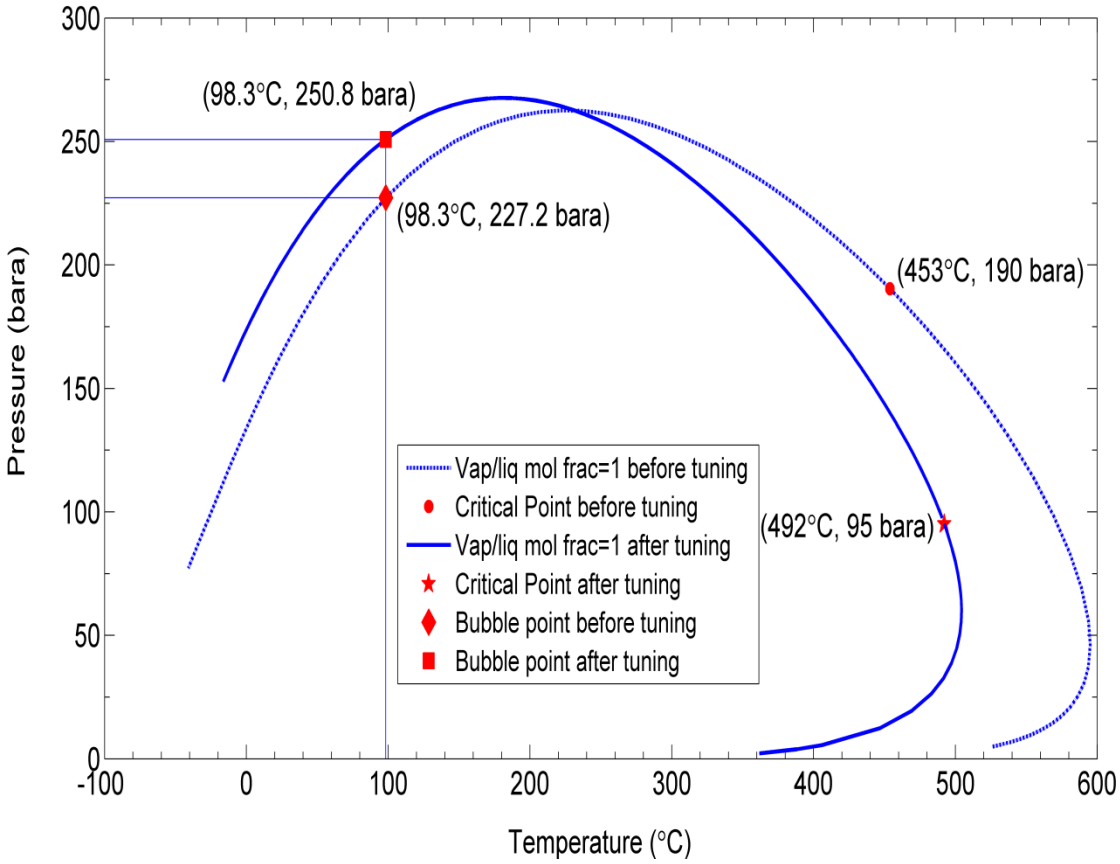

Fig. 4-1: P-T diagrams of Norne reservoir oil with PR-Peneloux equation of state (before and after tuning)

4.2 History Matching

History matching is a means for reducing the uncertainty between the reservoir simulator's predicted production and actual field production (history). This work is done on a fixed history matched model and multiple reservoir realizations are not considered in this study. The

methodology explained in Chapter 3 (see section 3.2.1) was used to reduce the discrepancy between the simulation results and the history. The coefficients and exponents of Corey models were optimised using a genetic algorithm. The Corey models obtained by curve fitting before the history matching are as follows

$$K_{rw} = 0.3662 S_w^{2.2108}$$
$$K_{row} = 0.9273(1 - S_w)^{3.9227}$$
$$K_{rg} = 0.9795 S_g^{2.1458}$$
$$K_{rog} = 0.7953(1 - S_g)^{4.0085}.$$

The following Corey models are the results of history matching.

$$K_{rw} = 0.9507 S_w^{4.9140}$$
$$K_{row} = 0.8577(1 - S_w)^{2.3976}$$
$$K_{rg} = 0.5773 S_g^{3.8121}$$
$$K_{rog} = 0.7922(1 - S_g)^{1.7102}.$$

The relative permeability curves before and after history matching are shown versus normalized water and normalized gas saturation in Fig. 4-2 and 4-3 for oil-water and oil-gas system, respectively. As shown, after history matching the reservoir rock wettability has changed from neutral wet to water wet since the endpoint value of water relative permeability has increased and the intersection of relative permeability curves of oil and water has shifted to the right (greater water saturation) in Fig. 4-2 and also the residual oil saturation shows reduction in Fig. 4-3.

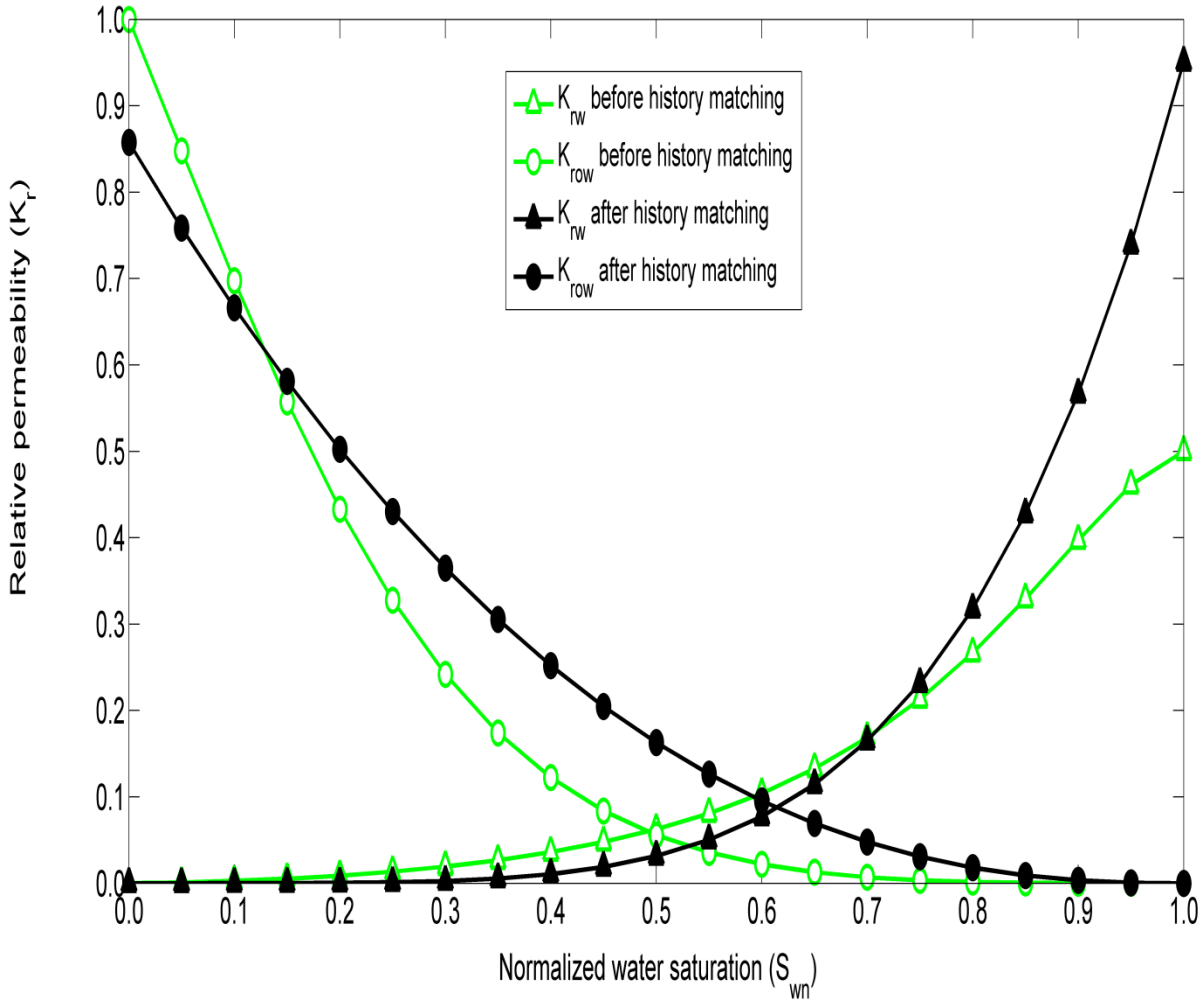

Fig. 4-2: Oil-water relative permeability curves before and after history matching

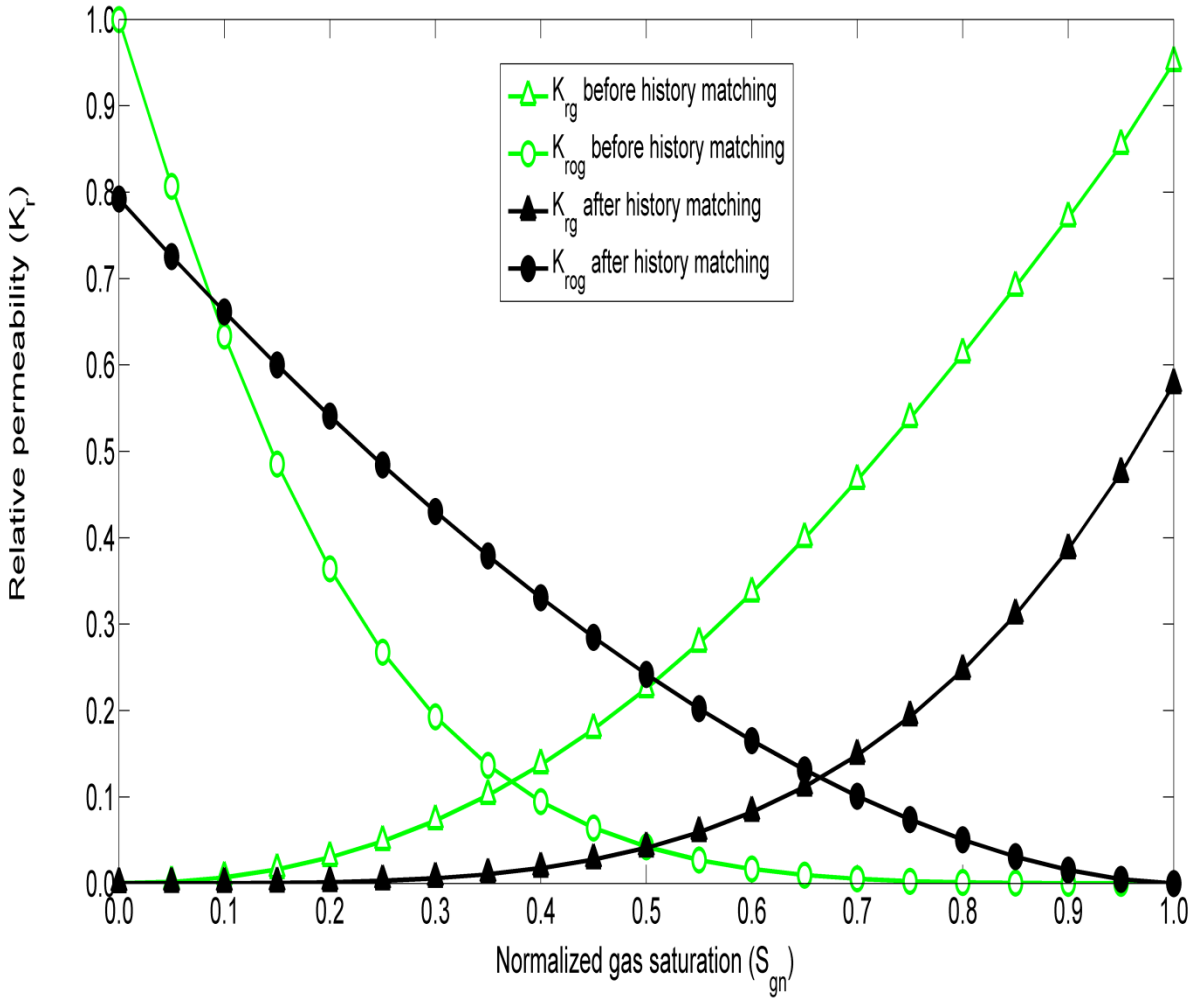

Fig. 4-3: Oil-gas relative permeability curves before and after history matching

The plots of oil production rates from the three active producers of the E-segment (E-2AH, E-3CH and E-3H) are presented in Fig. 4-4 to 4-6. In each figure, the simulation results before and after history matching as well as the historical recorded production rates are plotted. It is expected that by adjusting the reservoir parameters (relative permeabilities in this work) during history matching and making the simulation results closer to the history, more reliable predictions would be achieved. Fig. 4-4 to 4-6 show that in general the simulated wells' oil production rates have approached the historical data after history matching.

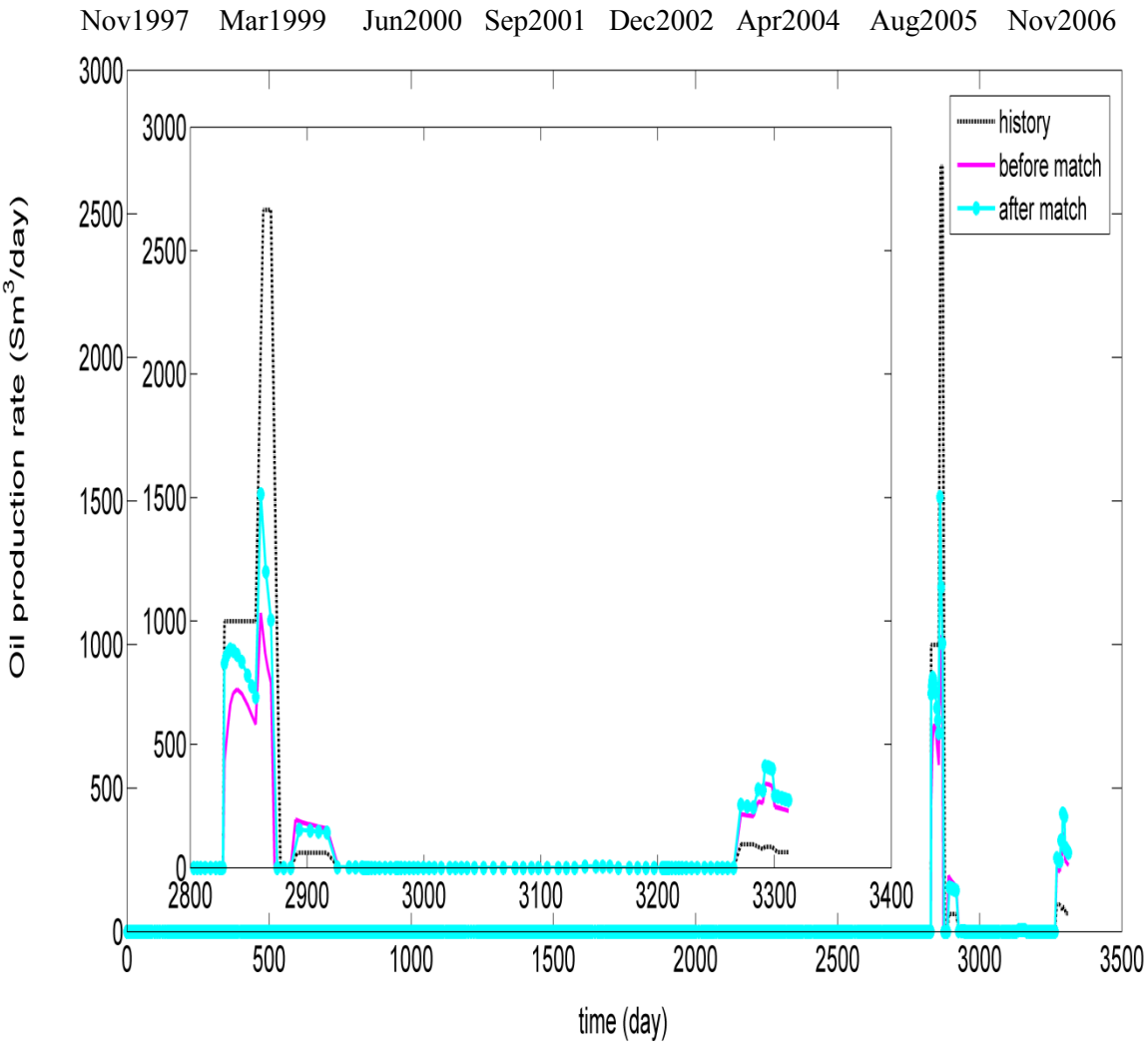

Fig. 4-4: History matching results of well E-2AH

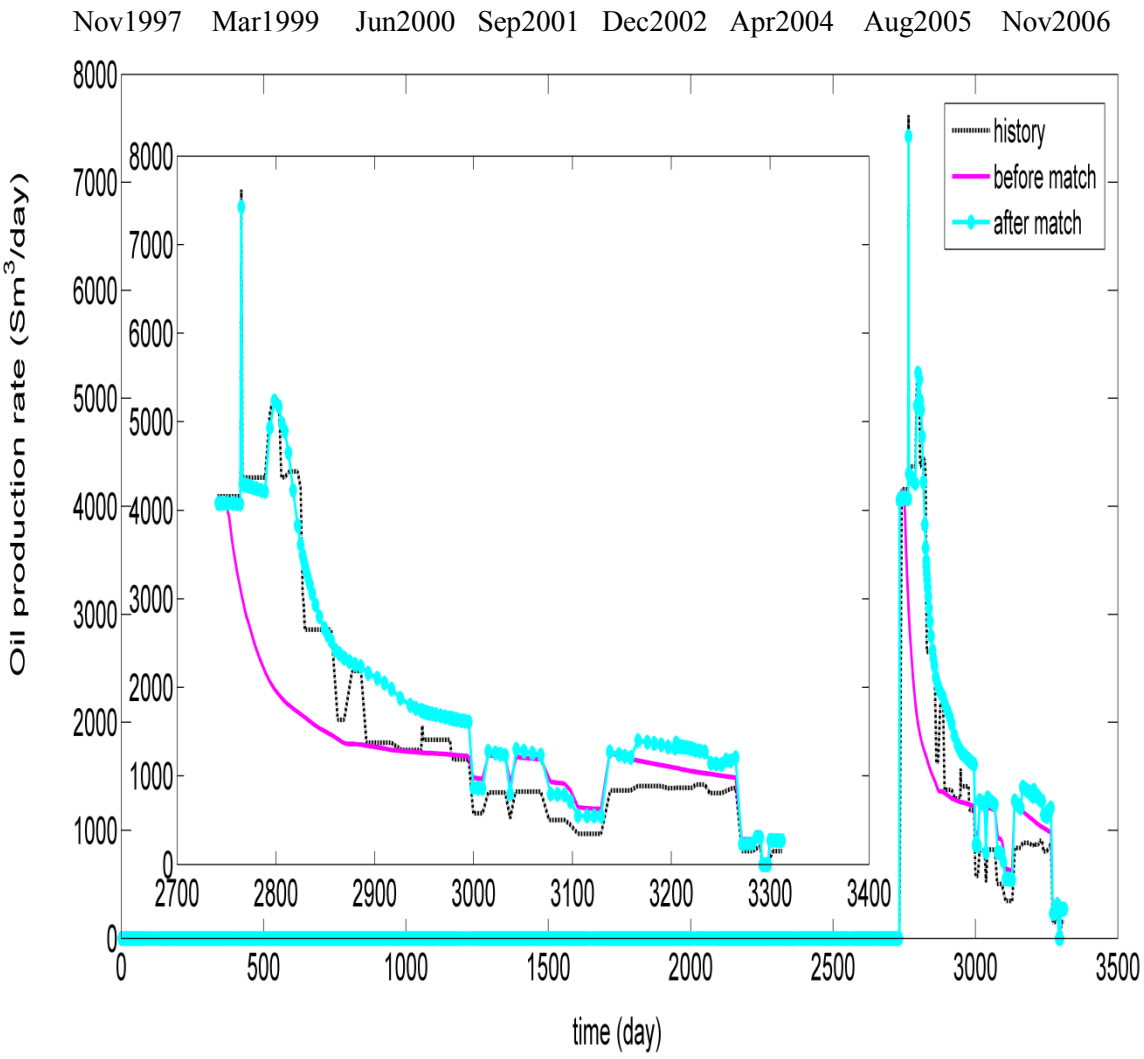

Fig. 4-5: History matching results of well E-3CH

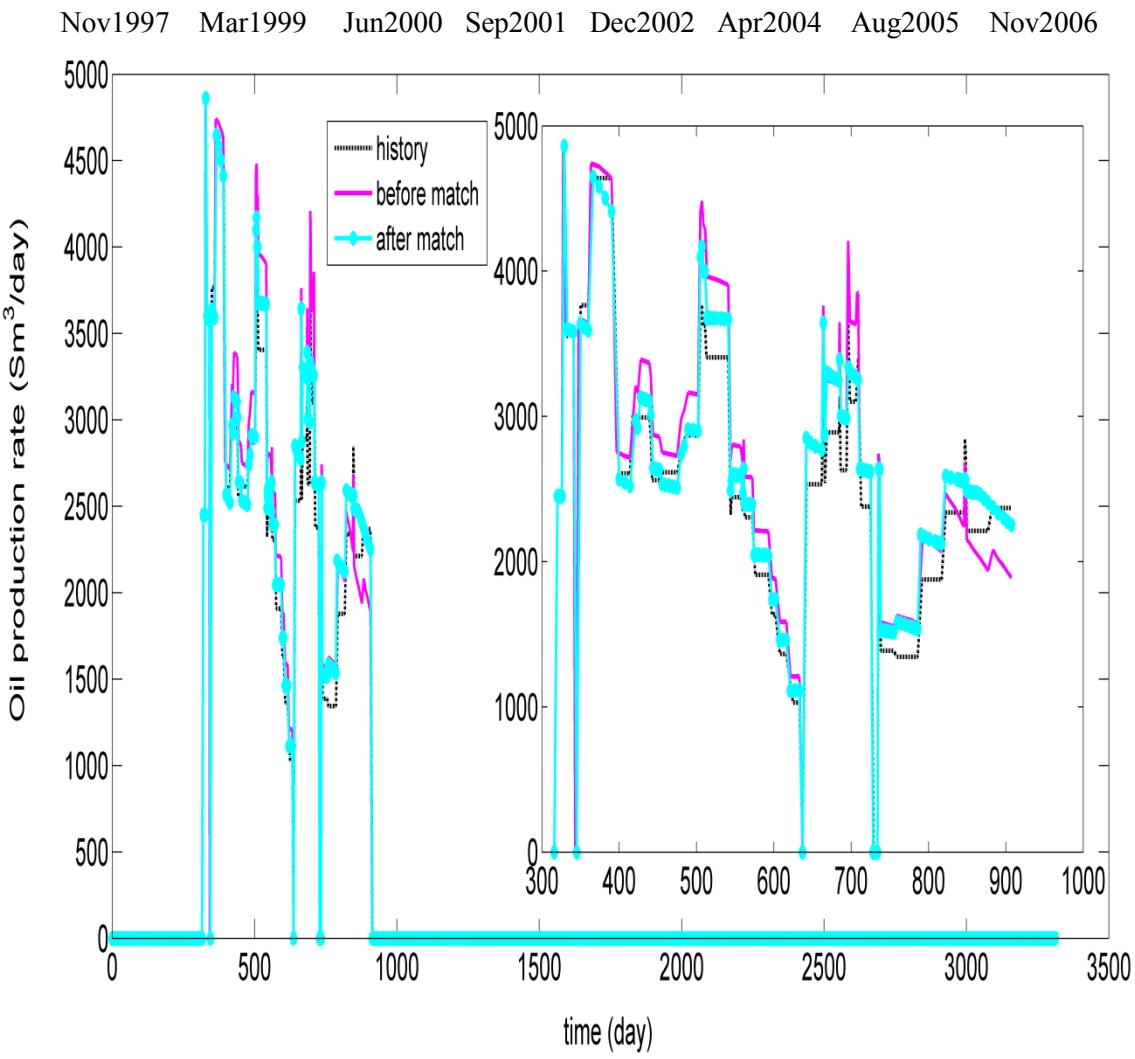

Fig. 4-6: History matching results of well E-3H

As mentioned, the objective function for history matching was defined to be the square of the weighted sum of the differences between the history and the simulated oil production rates of the wells (see equation (3.5)). Therefore, as expected, the simulated oil production rates of the wells have in general approached the recorded data after history matching. The effect of adjusting the relative permeabilities (history matching) on water and gas cumulative productions are shown in Fig. 4-7 and Fig. 4-8, respectively. These figures indicate that the degree of adjustment to the

relative permeabilities is in an acceptable range since the cumulative production curves follow the same trend as the history and the total gas and water production at the end of simulation time have approached the history for both gas and water. History matching can be improved taking into account other tuning parameters such as fault transmissibilities, flow capacity (product of horizontal permeability and thickness), vertical to horizontal permeability ratio, etc. For the purpose of developing this optimisation methodology, the history match is considered adequate.

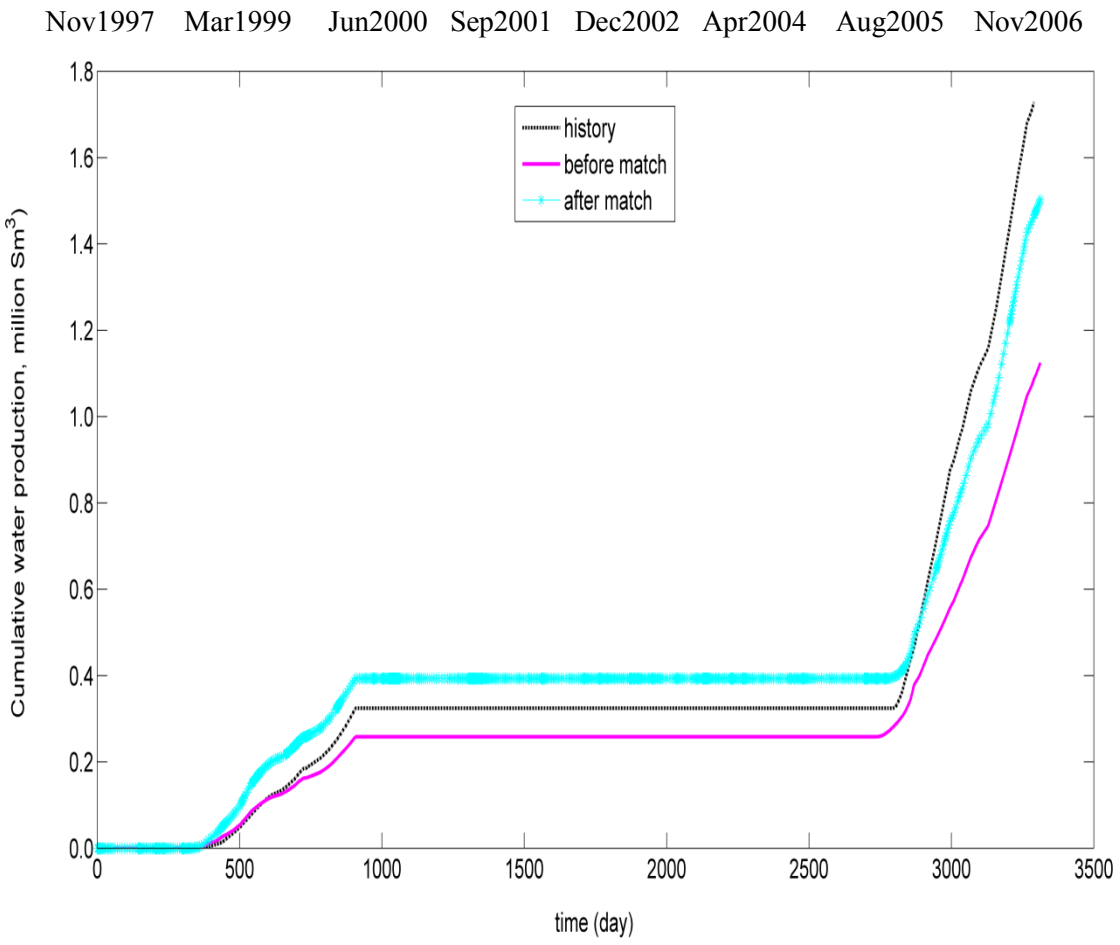

Fig. 4-7: History matching results of cumulative water production

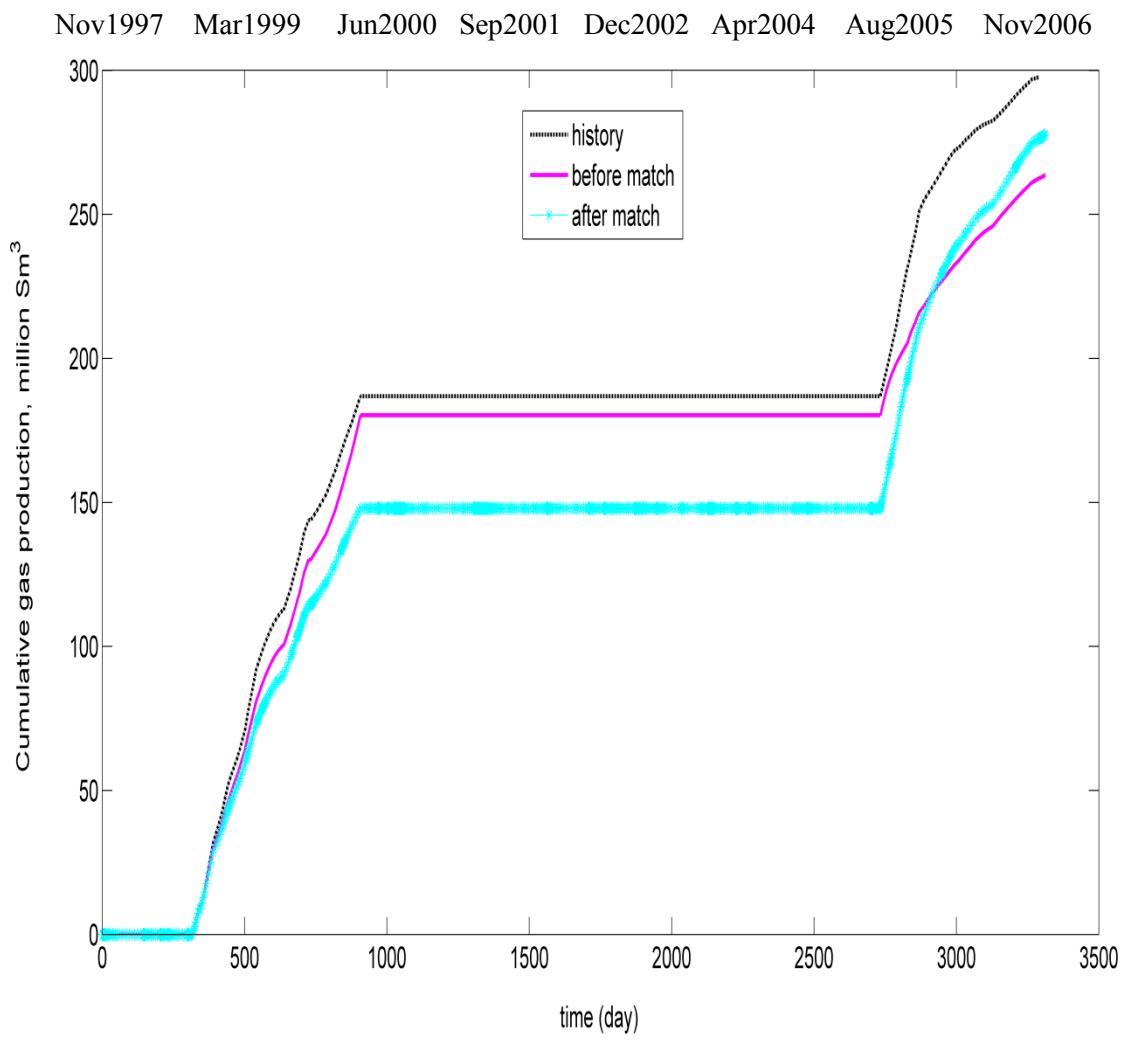

Fig. 4-8: History matching results of cumulative gas production

4.3 Optimisation of NPV

The three experiments already described in Chapter 3 are discussed and the results are presented in this section. For each experiment, four trials are run. The performance of the optimisation techniques are analyzed and compared among and within the experiments.

4.3.1 Experiment 1

In experiment 1, two water injection rates, two gas injection rates, three BHPs of the producers, cycle ratio and cycle time are the nine optimisation variables. The total WAG duration is fixed at 30 months and the mole fractions of C_2 to C_4 are fixed at 0.05, 0.02 and 0.01, respectively. The top 50 results out of 60 simulation runs from the design of experiments are used as the initial guess for both of the optimisation algorithms (GA and PSO) and the best of the 50 (the best vector of the initial guess matrix) is chosen as the reference (unoptimised) case for comparison. Each row of the initial guess matrix corresponds to a particle and the columns in that row are the different variables of that particle.

4.3.1.1 Reference Case

The reference case for experiment 1 has the maximum water injection rates, minimum gas injection rates, minimum BHPs in the producers, a cycle ratio of 0.65 and a cycle time of 4 months. These values as well as the NPV calculated from the start of the WAG (as time zero) are shown in Table 4-2.

Table 4-2: Variables of the reference case with their values for experiment 1

Variable	Reference case
Q_w (F-1H)	2700
Q_g (F-1H) [Sm^3/day]	1000
Q_w (F-3H)	2700
Q_g (F-3H) [Sm^3/day]	1000
BHP (E-2AH) [bar]	150
BHP (E-3CH) [bar]	150
BHP (E-3H) [bar]	150
Cycle ratio [-]	0.65
Cycle time [month]	4
NPV [$ million]	135.45

4.3.1.2 Optimisation Results

The optimisation results for the four trials of GA and four trials of PSO for experiment 1 are presented in Fig. 4-9 and 4-10, respectively. In Fig. 4-10 the results of iterations 11 to 40 of PSO are plotted as an inset for better visualization. The results of all the eight trials of GA and PSO are shown in Fig. 4-11. In these figures, the best NPV of each iteration (among the 50 particles) is plotted versus the iteration index.

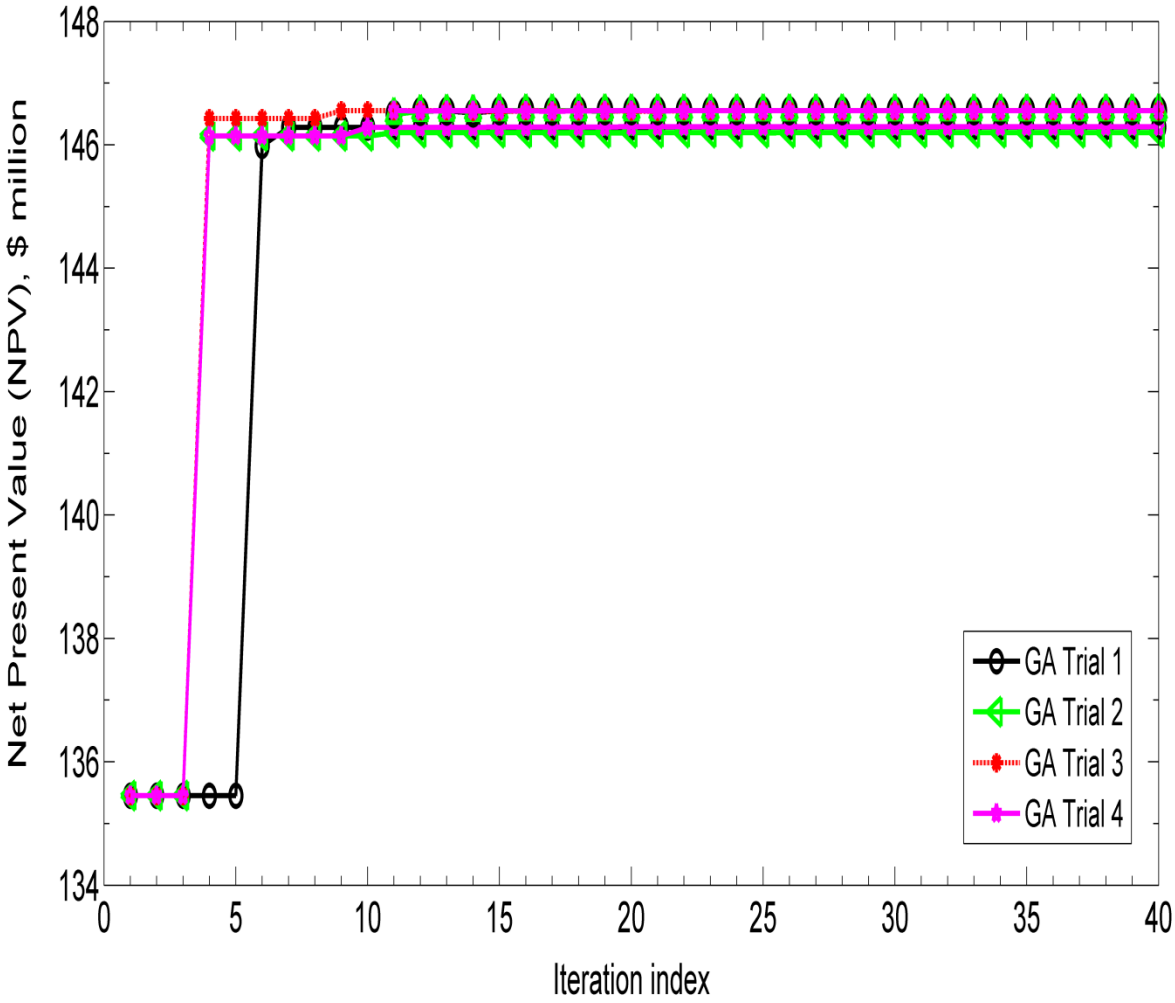

Fig. 4-9: NPV vs. iteration index per trial for GA (experiment 1)

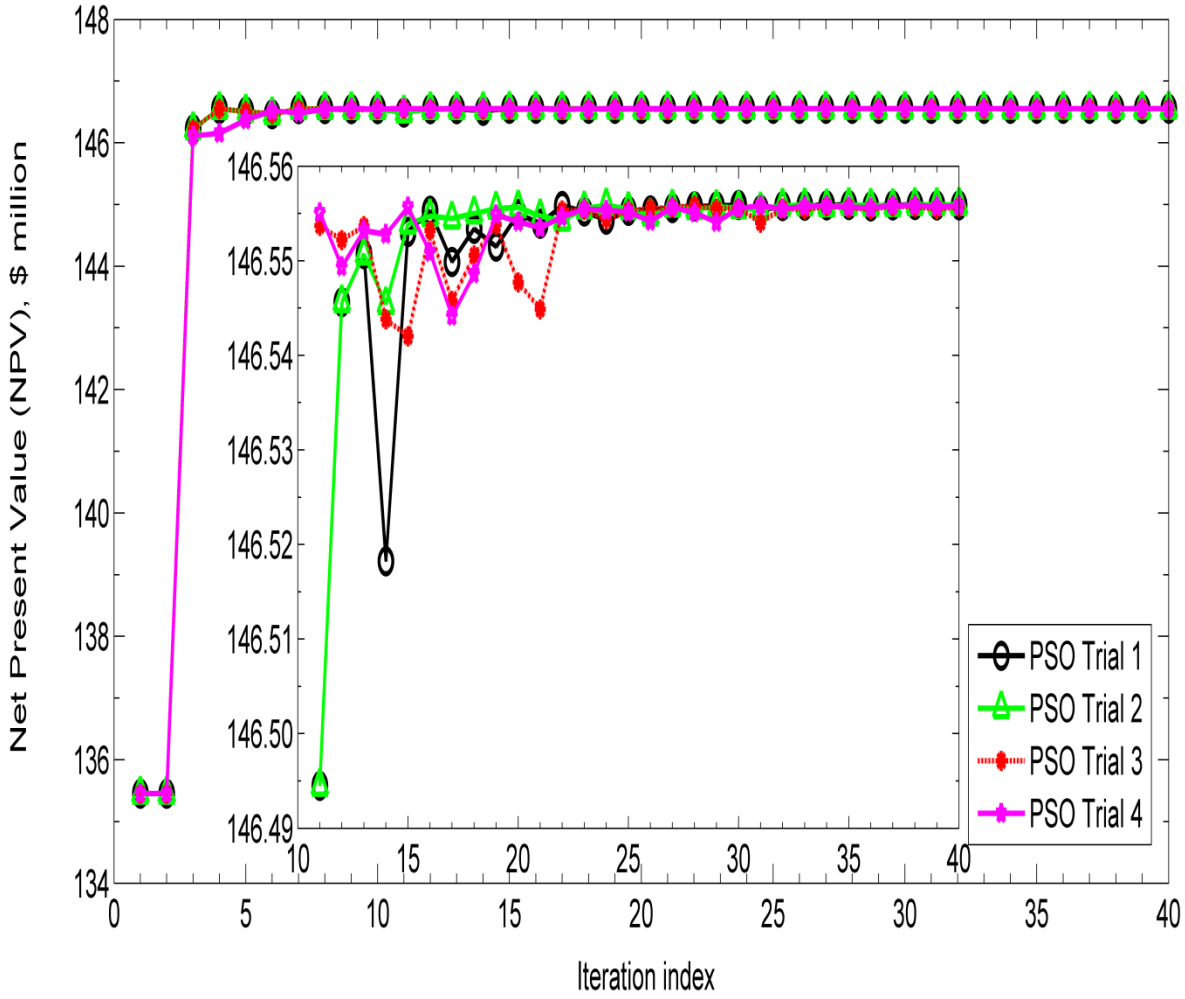

Fig. 4-10: NPV vs. iteration index per trial for PSO (experiment 1)

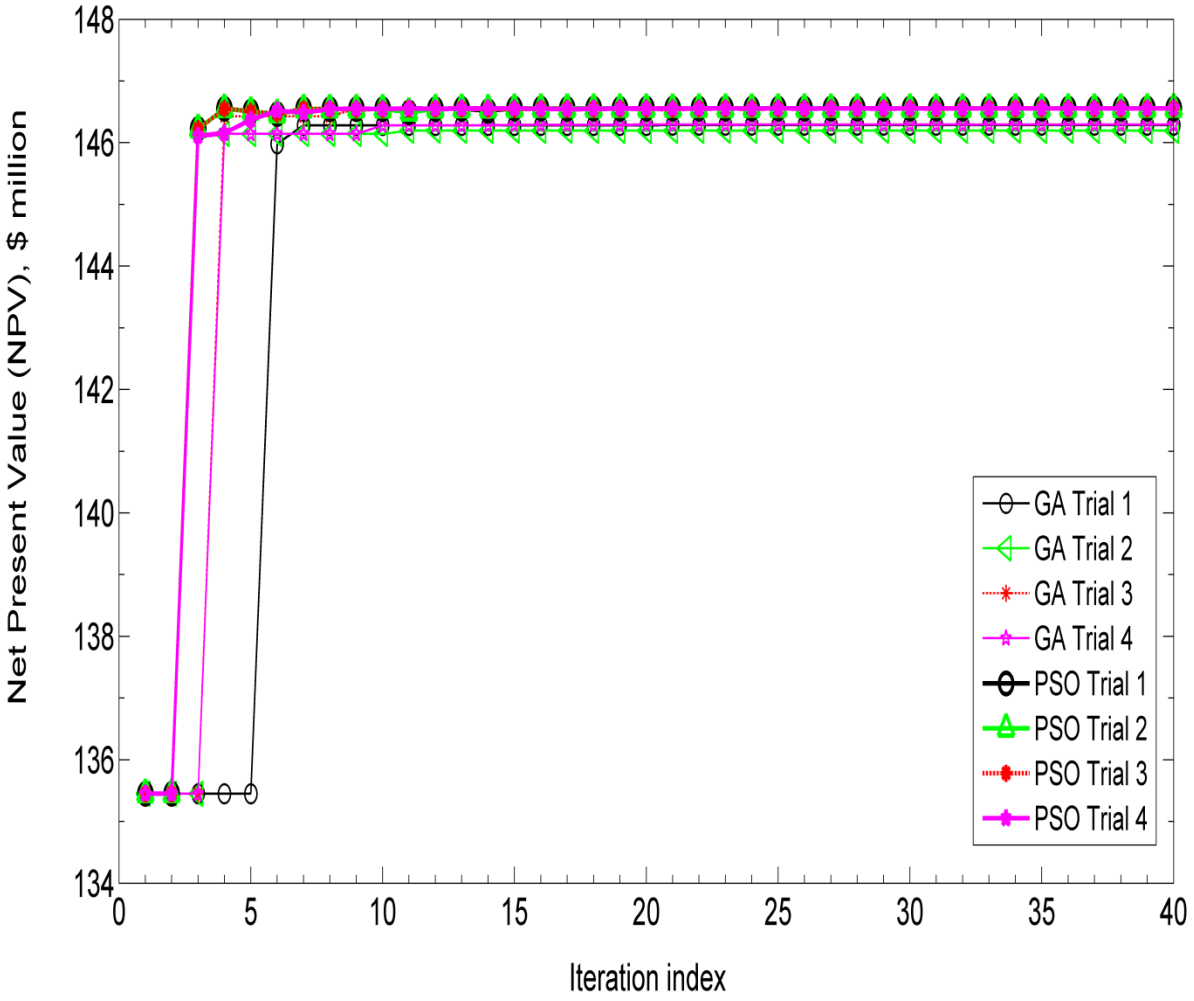

Fig. 4-11: NPV vs. iteration index per trial for GA and PSO (experiment 1)

Fig. 4-9 shows that the best NPVs found by GA are steadily increasing, however GA does not converge to the same solution in all the trials. Fig. 4-10 shows the convergence of PSO to the same optimal solution in its four trials and the inset magnifies its fluctuations. Fig. 4-11 represents the superiority of PSO over GA in most of the trials.

The values of the variables for the reference case and the best operational points from each trial of the two algorithms and the values of the maximum NPVs found for experiment 1 are shown in Table 4-3 and 4-4 for GA and PSO, respectively. The values of the optimised variables which differ from the reference case have been asterisked for each trial.

Table 4-3: The reference case and best operational points of four trials of GA (experiment 1)

Variable	**Reference case**	**GA Trial 1**	**GA Trial 2**	**GA Trial 3**	**GA Trial 4**
Q_w (F-1H) [Sm^3/day]	2700	2700	2700	2700	2700
Q_g (F-1H) [Sm^3/day]	1000	1000	1000	1000	1000
Q_w (F-3H) [Sm^3/day]	2700	2700	2700	2700	2700
Q_g (F-3H) [Sm^3/day]	1000	1000	1000	1000	1000
BHP (E-2AH) [bar]	150	155.8*	171*	158.8*	156*
BHP (E-3CH) [bar]	150	150	150	150	150
BHP (E-3H) [bar]	150	150	150	150	150
Cycle ratio [-]	0.65	0.9*	0.9*	0.9*	0.9*
Cycle time [month]	4	4	4	5*	4
NPV [$ million]	135.45	146.29	146.20	146.56	146.29

Table 4-4: The reference case and best operational points of four trials of PSO (experiment 1)

Variable	Reference case	PSO Trial 1	PSO Trial 2	PSO Trial 3	PSO Trial 4
Q_w (F-1H) [Sm^3/day]	2700	2700	2700	2700	2700
Q_g (F-1H) [Sm^3/day]	1000	1000	1000	1000	1000
Q_w (F-3H) [Sm^3/day]	2700	2700	2700	2700	2700
Q_g (F-3H) [Sm^3/day]	1000	1000	1000	1000	1000
BHP (E-2AH) [bar]	150	158.8*	158.8*	158.8 *	158.8*
BHP (E-3CH) [bar]	150	150	150	150	150
BHP (E-3H) [bar]	150	150	150	150	150
Cycle ratio [-]	0.65	0.9*	0.9*	0.9*	0.9*
Cycle time [month]	4	5*	5*	5*	5*
NPV [$ million]	135.45	146.56	146.56	146.56	146.56

As indicated by asterisks in Table 4-3 and 4-4, one of the BHPs (well E-2AH) has changed from 150 bar to 158.8 bar, the cycle ratio has changed from 0.65 to 0.9 and the cycle time has changed from 4 months to 5 months in the optimal configuration found by the algorithms compared to the initial reference case. The overall optimal solution is about 8.2% higher in NPV.

As can be seen from Fig. 4-9 to Fig. 4-11 and Table 4-3 and 4-4, PSO converges to the same optimal solution in all the four trials which shows its consistency, while GA has only been able to find the same optimal solution in the third trial. While the NPV found by the GA is always increasing throughout its search, it usually converges to a marginally lower solution. The inset in Fig. 4-10 shows small fluctuations in the performance of PSO. This could be a feature of PSO by which it tries to escape from local optima.

GA finds a solution with an NPV in the vicinity of 0.01% of the optimum solution for the first time in iteration 9 of the third trial and fails to find such an answer in the other trials. PSO gives a solution in the specified range for the first time in iteration 7 of trials 1 to 3 and iteration 8 of trial 4.

To compare GA and PSO from the perspective of average performance, the average NPVs of the four trials of GA and four trials of PSO versus the iteration index are plotted in Fig. 4-12. The figure also shows error bars indicating the standard deviations. The average shown here is the average over all particles and all trials (200 particles in total).

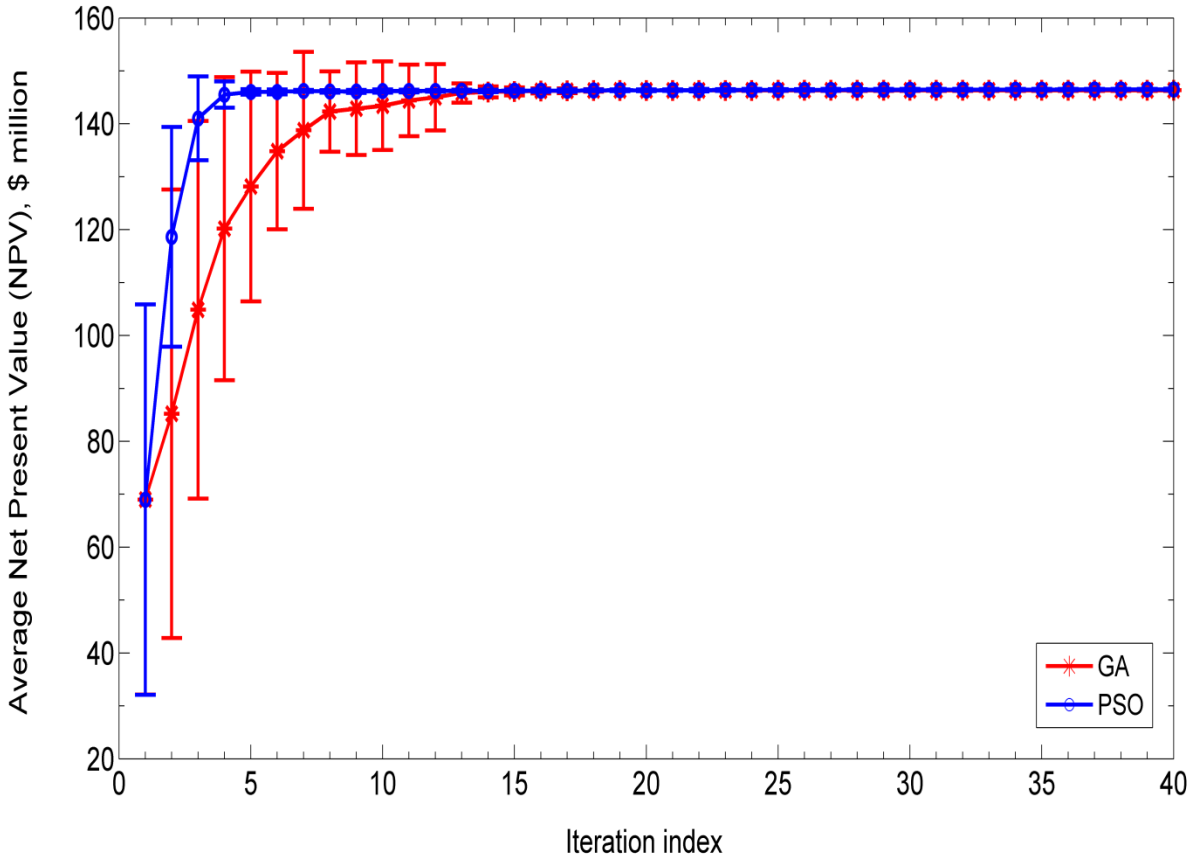

Fig. 4-12: Average performance of GA and PSO for all the four trials (experiment 1)

As can be seen from Fig. 4-12, the average NPV found by PSO for every iteration of the four trials is higher than the corresponding value found by GA. The standard deviations of PSO are lower than the standard deviations of GA indicating that the particles of PSO are closer to the average values. Since the average values of PSO are greater than those of GA, particles of PSO are always closer to a better point in the search space.

To realize which of the algorithms finds a better solution within a limited number of iterations, the residual NPV is defined as below

$$NPV_{residual} = 1 - \frac{\max\left\{NPV\right\}_{i=1}^{n}}{NPV_{\max}}, \tag{4.1}$$

where n is the number of iterations of a trial included in the calculations and $NPV_{\max}$ is the maximum overall NPV.

Residual NPVs of the first 10, 20, 30 and all the 40 iterations ($n = 10, 20, 30$ and 40) for each trial of GA and PSO are shown in the form of bar charts in Fig. 4-13 to Fig. 4-16. A smaller value on the vertical axis is an indication of better performance of the algorithm since it shows that the maximum NPV found by the algorithm is closer to the best overall NPV.

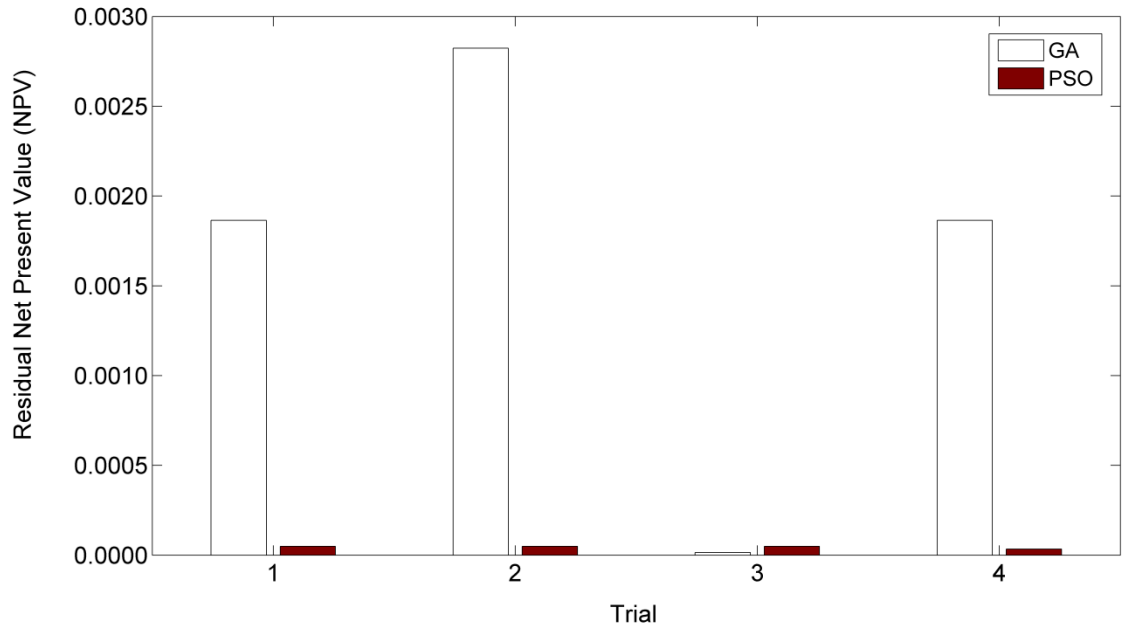

Fig. 4-13: Residual NPV comparisons per trial for iterations 1 to 10 (experiment 1)

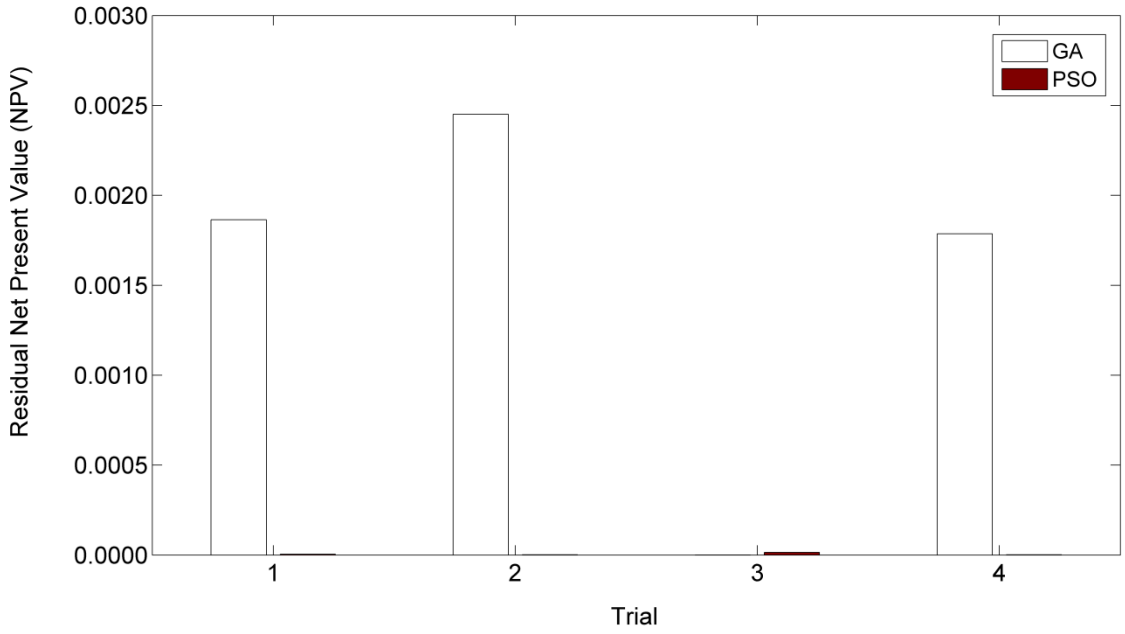

Fig. 4-14: Residual NPV comparisons per trial for iterations 1 to 20 (experiment 1)

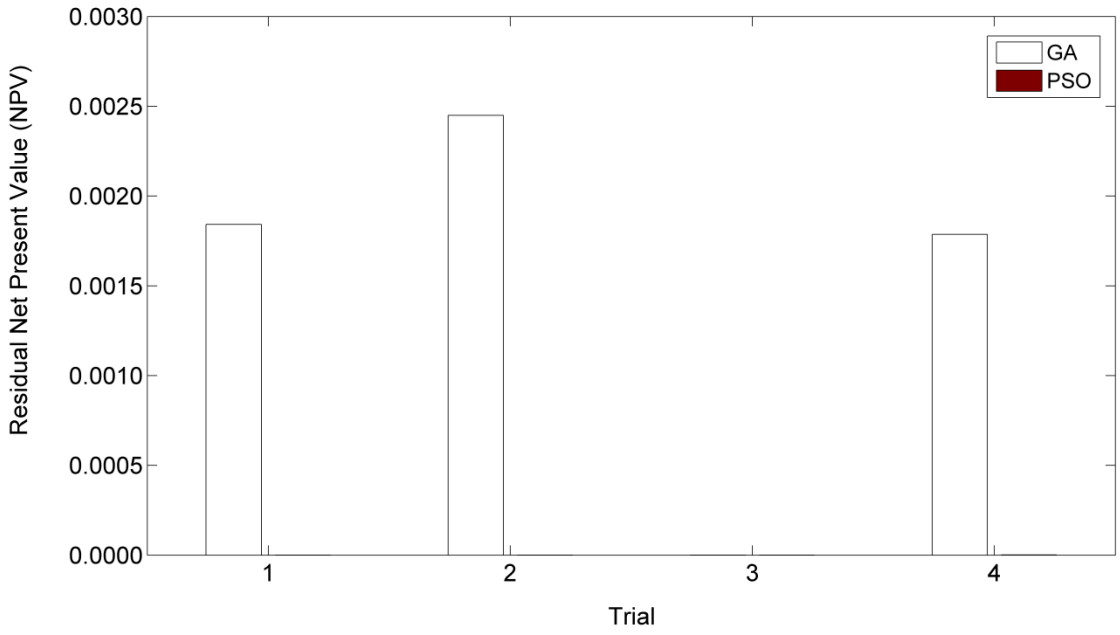

Fig. 4-15: Residual NPV comparisons per trial for iterations 1 to 30 (experiment 1)

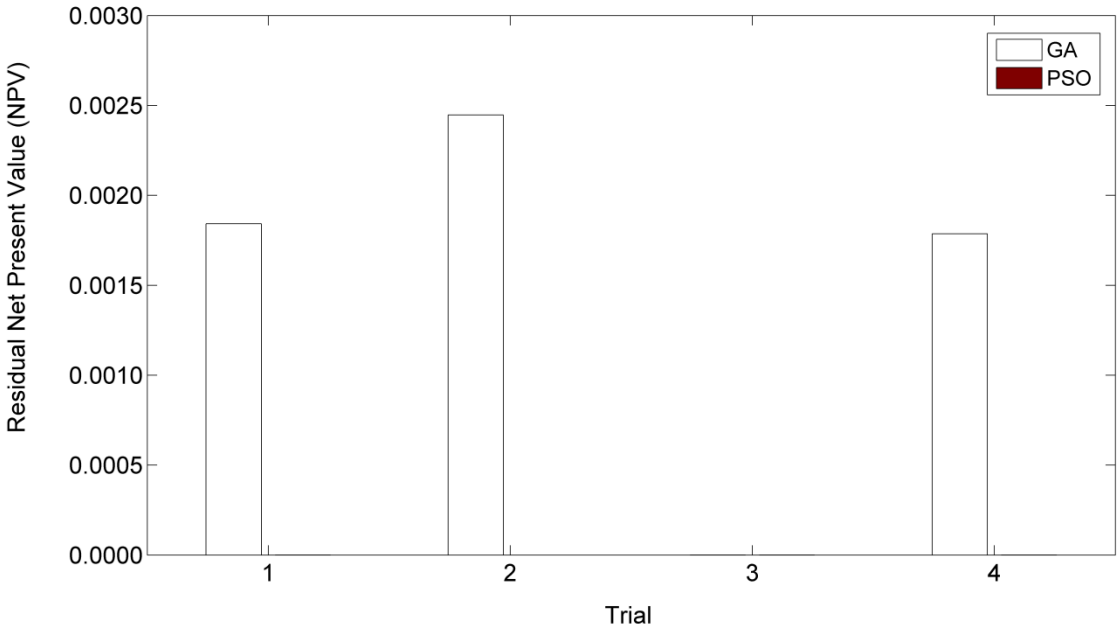

Fig. 4-16: Residual NPV comparisons per trial for iterations 1 to 40 (experiment 1)

As shown in Fig 4-13 to 4-16, in trials 1, 2 and 4, PSO shows a better performance than GA and in trial 3, GA acts better only in the first 10 and 20 iterations. For example, as represented in Fig. 4-13, the best NPV found by PSO in the first 10 iterations is closer to the optimal solution of experiment 1 than any NPV found by GA for trials 1, 2 and 4. A value of 4×10^{-5}, for example, for residual NPV of PSO in Fig. 4-13 indicates that the best NPV found by PSO in its first 10 iterations is 99.995% of the best overall NPV for experiment 1. So, if there is a restriction due to computational time or resources, trying PSO would appear to be a better approach since it could find a solution closer to the optimum sooner.

4.3.2 Experiment 2

In experiment 2, two water injection rates, two gas injection rates, three BHPs of the producers, cycle ratio, cycle time and mole fractions of C_2 to C_4 added to the base injecting gas are the 12 optimisation variables. The total WAG duration is fixed at 30 months. The top 50 results out of 96 simulation runs from the design of experiments are used as the initial guess for both of the optimisation algorithms (GA and PSO) and the best of the 50 is chosen as the reference (unoptimised) case for comparison.

4.3.2.1 Reference Case

The operational point which results in the highest NPV among the 96 simulation runs of design of experiments is the reference case. The values of the variables for the reference case and the resulting NPV are shown in Table 4-5. The reference case of experiment 2 yields a lower NPV compared to experiment 1. In spite of the fact that in experiment 2 more simulation runs are conducted for the design of experiments than in experiment 1 (96 compared to 60), the design of

experiments is not effectively able to cover the search space and provide a good initial guess since experiment 2 is more complex and has a higher dimensional search space (12 variables in experiment 2 compared to nine variables in experiment 1).

Table 4-5: Variables of the reference case with their values for experiment 2

Variable	Reference case
Q_w (F-1H) [Sm^3/day]	2700
Q_g (F-1H) [Sm^3/day]	380620
Q_w (F-3H) [Sm^3/day]	2700
Q_g (F-3H) [Sm^3/day]	1000
BHP (E-2AH) [bar]	150
BHP (E-3CH) [bar]	150
BHP (E-3H) [bar]	201.3
Cycle ratio [-]	0.7
Cycle time [month]	2
Mole fraction of C_2 [-]	0.05
Mole fraction of C_3 [-]	0.1
Mole fraction of C_4 [-]	0.05
NPV [$ million]	132.09

4.3.2.2 Optimisation Results

The results of the performance of GA and PSO for the four trials of experiment 2 are shown in Fig. 4-17 and 4-18, respectively. In Fig. 4-18 the results of iterations 11 to 40 of PSO are plotted as an inset for better visualization. The results of all the eight trials of the optimisation algorithms are presented in Fig. 4-19. In these figures, the best NPV of each iteration (among

the 50 particles) is plotted versus the iteration index for all the iterations from the four trials of the algorithms.

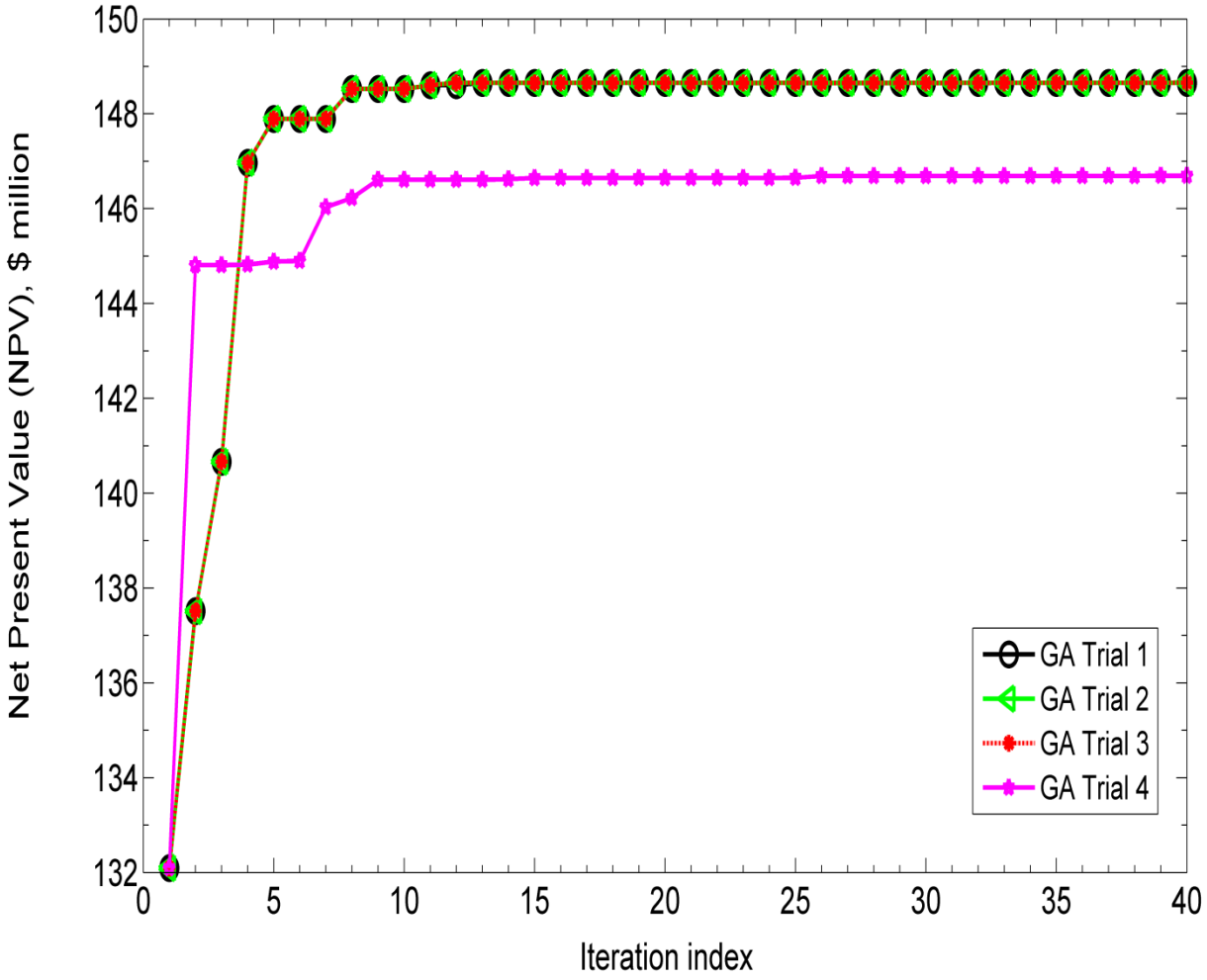

Fig. 4-17: NPV vs. iteration index per trial for GA (experiment 2)

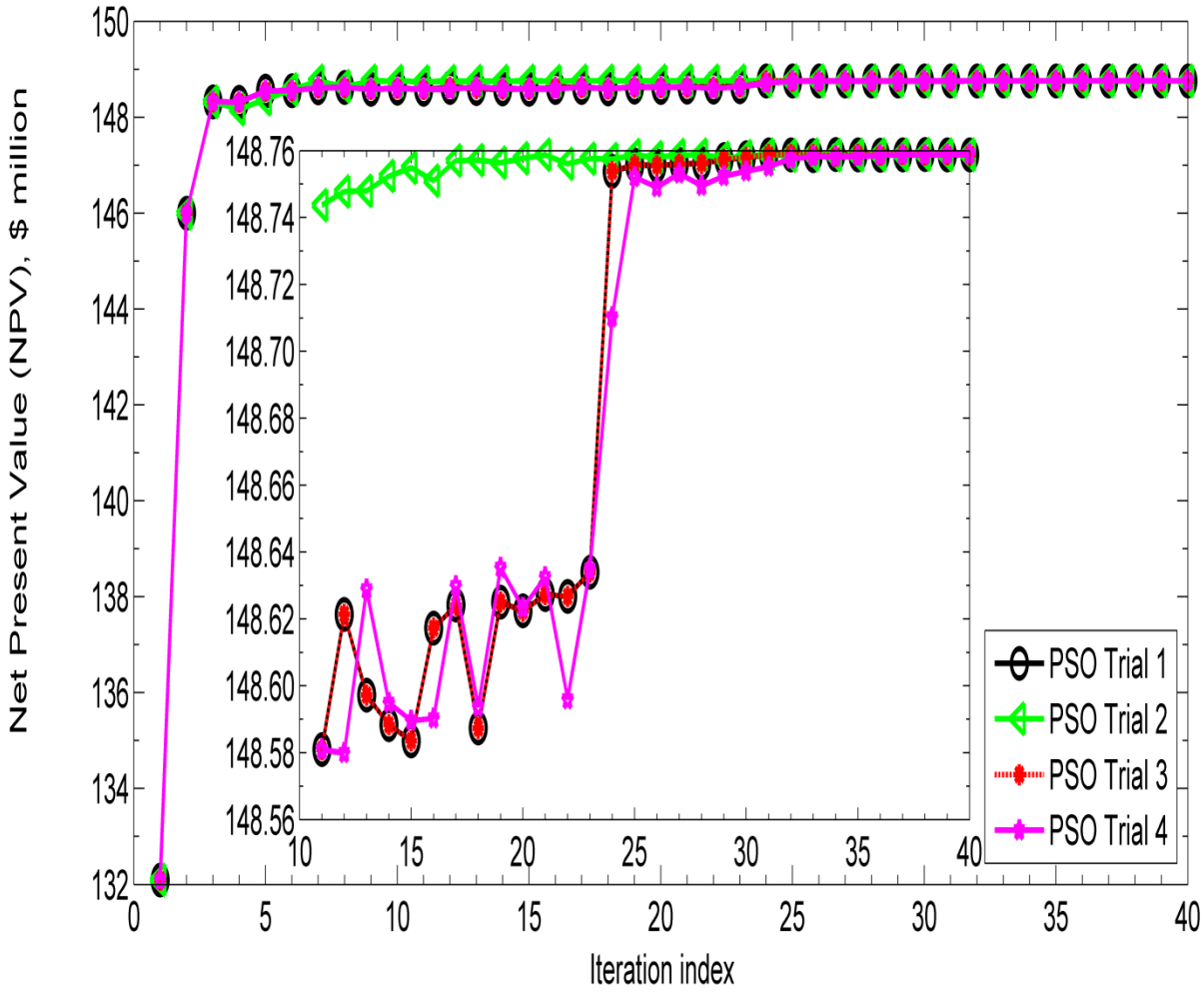

Fig. 4-18: NPV vs. iteration index per trial for PSO (experiment 2)

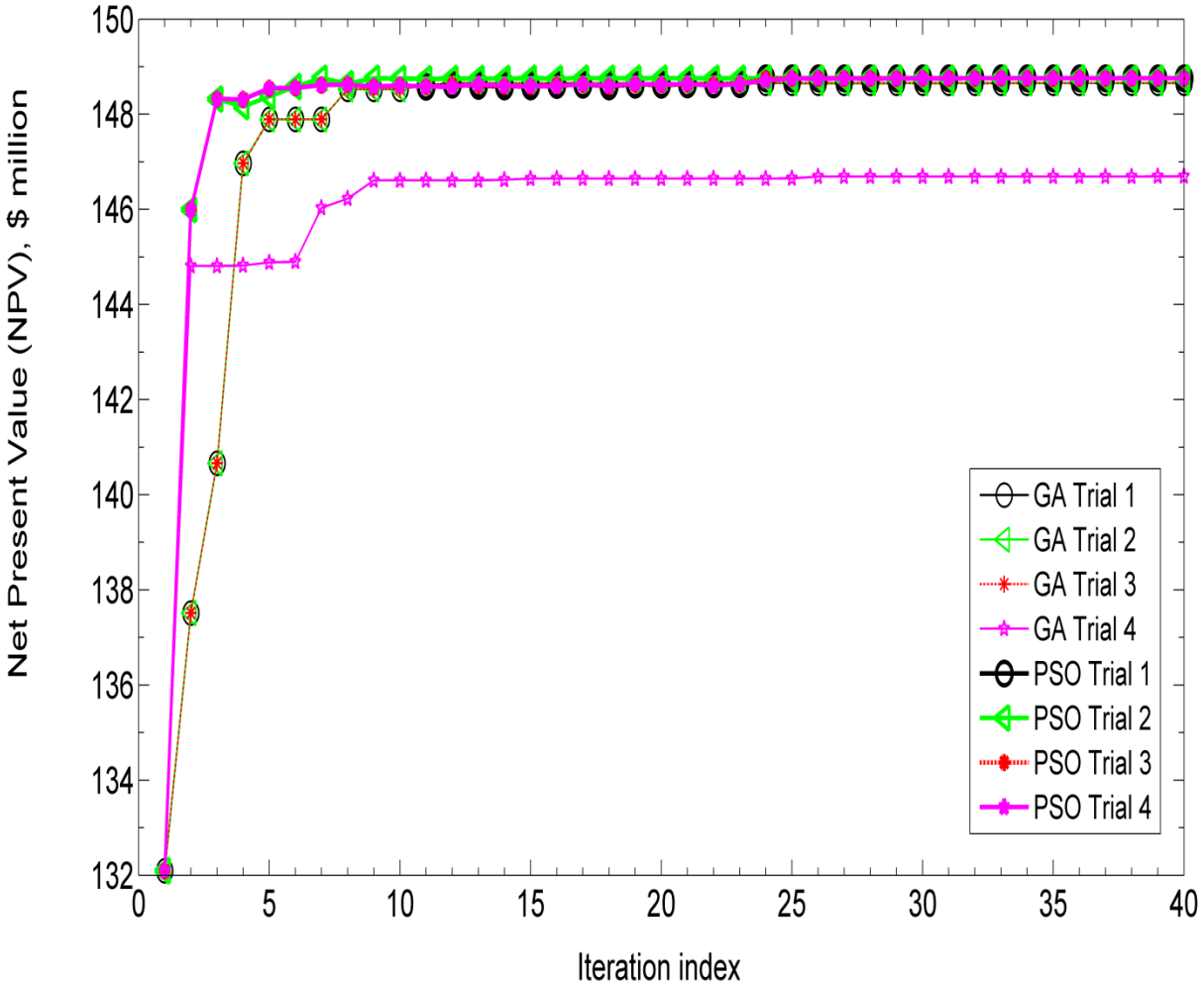

Fig. 4-19: NPV vs. iteration index per trial for GA and PSO (experiment 2)

Fig. 4-17 shows that the best NPV found by GA is steadily increasing and except for trial 4, GA converges to approximately the same optimal solution. Fig. 4-18 shows that PSO converges to the same optimal solution in all the four trials, however it shows fluctuations and sometimes finds lower NPVs compared to its prior iterations. Fig. 4-19 shows the better performance of PSO compared to GA for all the trials of experiment 2.

The values of the variables for the reference case and the best operational points and corresponding NPVs found from each of the four trials of GA and PSO for experiment 2 are given in Table 4-6 and 4-7, respectively. The values of the optimised variables which differ from the reference case have been asterisked for each trial.

Table 4-6: The reference case and best operational points of four trials of GA (experiment 2)

Variable	**Reference case**	**GA Trial 1**	**GA Trial 2**	**GA Trial 3**	**GA Trial 4**
Q_w (F-1H) [Sm^3/day]	2700	2700	2700	2700	2700
Q_g (F-1H) [Sm^3/day]	380620	1000*	1000*	1000*	110768*
Q_w (F-3H) [Sm^3/day]	2700	2700	2700	2700	2700
Q_g (F-3H) [Sm^3/day]	1000	1000	1000	1000	1000
BHP (E-2AH) [bar]	150	159.4*	158.9*	158.9*	152*
BHP (E-3CH) [bar]	150	150	150	150	150
BHP (E-3H) [bar]	201.3	150*	150*	150*	150*
Cycle ratio [-]	0.7	0.9*	0.9*	0.9*	0.9*
Cycle time [month]	2	2	2	2	2
Mole fraction of C_2 [-]	0.05	0.2*	0.2*	0.2*	0.2*
Mole fraction of C_3 [-]	0.1	0.1	0.1	0.1	0.1
Mole fraction of C_4 [-]	0.05	0.05	0.05	0.05	0.05
NPV [$ million]	132.09	148.65	148.66	148.66	146.69

Table 4-7: The reference case and best operational points of four trials of PSO (experiment 2)

Variable	Reference case	PSO Trial 1	PSO Trial 2	PSO Trial 3	PSO Trial 4
Q_w (F-1H) [Sm^3/day]	2700	2700	2700	2700	2700
Q_g (F-1H) [Sm^3/day]	380620	1000*	1000*	1000*	1000*
Q_w (F-3H) [Sm^3/day]	2700	2700	2700	2700	2700
Q_g (F-3H) [Sm^3/day]	1000	1000	1000	1000	1000
BHP (E-2AH) [bar]	150	158.8*	158.8*	158.8*	158.8*
BHP (E-3CH) [bar]	150	150	150	150	150
BHP (E-3H) [bar]	201.3	150*	150*	150*	150*
Cycle ratio [-]	0.7	0.9*	0.9*	0.9*	0.9*
Cycle time [month]	2	5*	5*	5*	5*
Mole fraction of C_2 [-]	0.05	0.2*	0.2*	0.2*	0.2*
Mole fraction of C_3 [-]	0.1	0.1	0.1	0.1	0.1
Mole fraction of C_4 [-]	0.05	0.05	0.05	0.05	0.05
NPV [$ million]	132.09	148.76	148.76	148.76	148.76

As indicated by asterisks in Table 4-7, PSO has been able to reduce the gas injection rate of well F-1H to its minimum (1000 Sm^3/day), increase the BHP of well E-2AH from 150 to 158.8 bar and decrease the BHP of well E-3H to the minimum (150 bar), change the cycle ratio from 0.7 to 0.9 and increase the mole fraction of ethane in the injecting gas from 0 to the maximum (0.2). The optimal NPV (found by PSO) is about 12.6% higher compared to the NPV value of the reference case.

Table 4-6 shows that GA fails to change the cycle time in all the four trials and gets stuck at the value of the reference case. GA is not able to find a solution comparable in quality to the solution found by PSO. PSO, unlike GA, gives the same optimal solution in all the trials. However, the

difference between the best answers of GA and PSO is negligible and mainly due to the effect of different cycle times. The NPV of the optimal point from the first trial of GA is a little lower than the solutions found in trials 2 and 3.This is due to the higher value of BHP for well E-2AH. In trial 4, GA changes the value of the gas injection rate of well F-1H and the BHP of well E-2AH to the values which result in the lowest NPV of all the trials of the optimisation techniques. In other words, GA has the worst performance in trial 4.

The first nine variables of the optimal solution of experiment 2 are the same as those from experiment 1, while a better NPV has been achieved due to enriching the gas and a more miscible injection which increases oil recovery. The optimal NPV of experiment 2 is about 1.5% higher than the value for experiment 1. So even though the reference case for experiment 2 has a lower NPV compared to experiment 1, the optimisation techniques, especially PSO, have been able to find an optimal solution better than that of experiment 1.

PSO finds a solution with an NPV in the vicinity of 0.01% of the optimal solution for the first time in iteration 24, 7, 24 and 25 of trials 1 to 4, respectively. GA totally fails to achieve such a solution. A worse initial guess compared to the optimum definitely influences the number of iterations required to find a solution closer to the optimal solution, hence the effect of problem complexity by adding more variables is difficult to discern.

The average NPV versus the iteration index for the four trials of GA and four trials of PSO (200 particles in each iteration of each algorithm) with the standard deviations is shown in Fig. 4-20 for GA and PSO. PSO always shows a better performance and a lower standard deviation than

GA in every single iteration. A lower standard deviation for PSO indicates the closeness of its particles to its higher average value. PSO is monotonically increasing, while GA shows some reductions in the average value of NPV before the final increase and convergence. Fluctuations are observed in the best values for PSO and in the average values for GA. This could be attributed to the basic differences in the random structures of the optimisation algorithms.

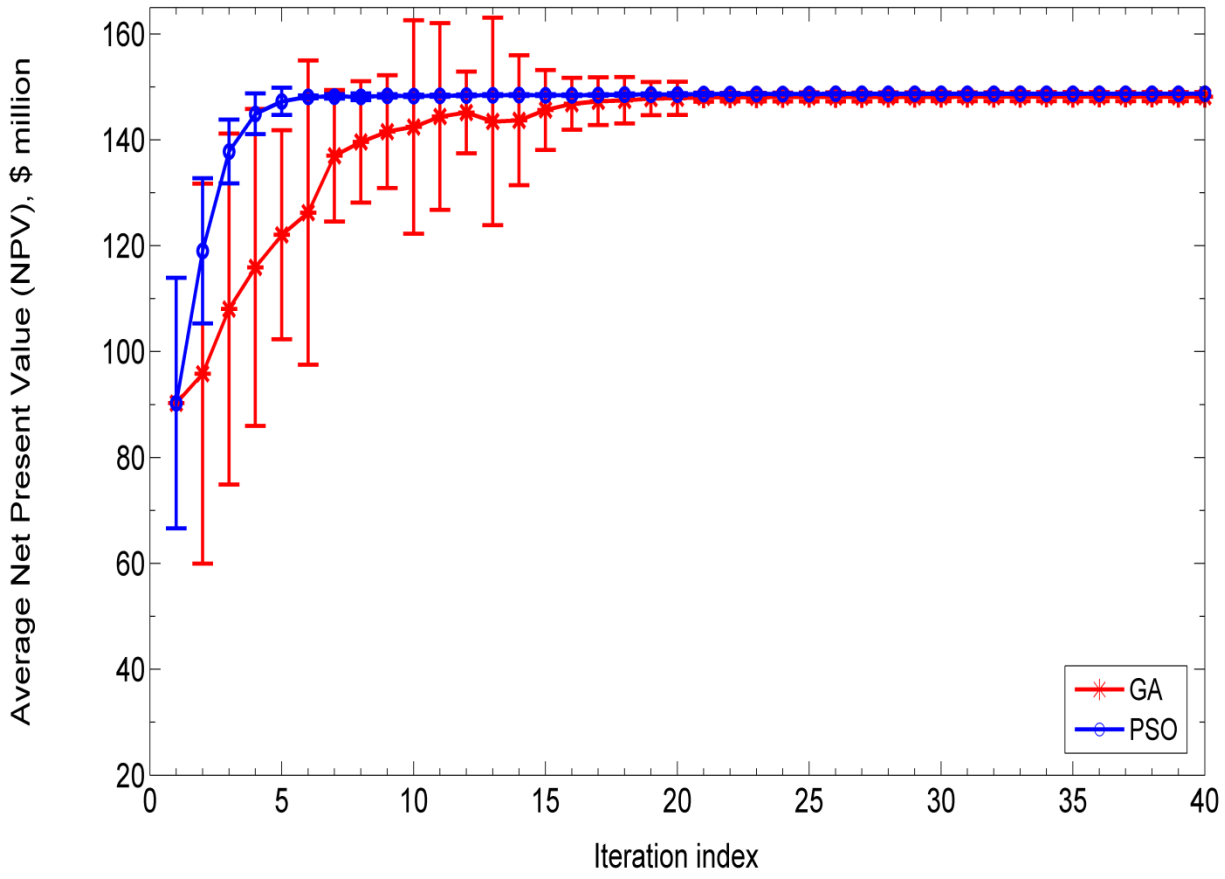

Fig. 4-20: Average performance of GA and PSO for all the four trials (experiment 2)

Bar charts of residual NPV (see equation (4.1)) for the first 10, 20, 30 and 40 iterations of the four trials of GA and PSO are presented in Fig. 4-21 to 4-24. These figures help choose the better

algorithm if there is a restriction in computational time and the best possible solution would be required with the fewest possible number of function evaluations.

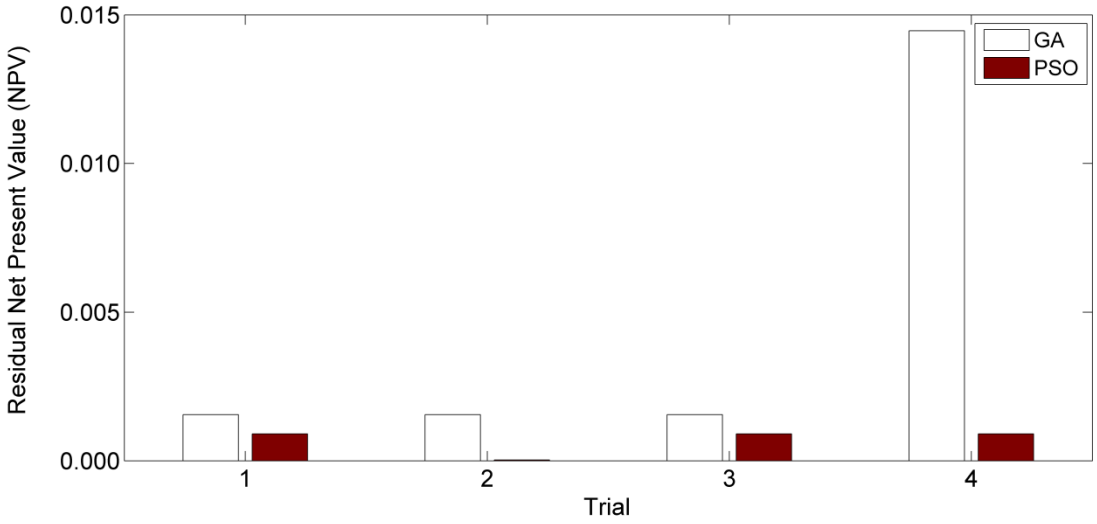

Fig. 4-21: Residual NPV comparisons per trial for iterations 1 to 10 (experiment 2)

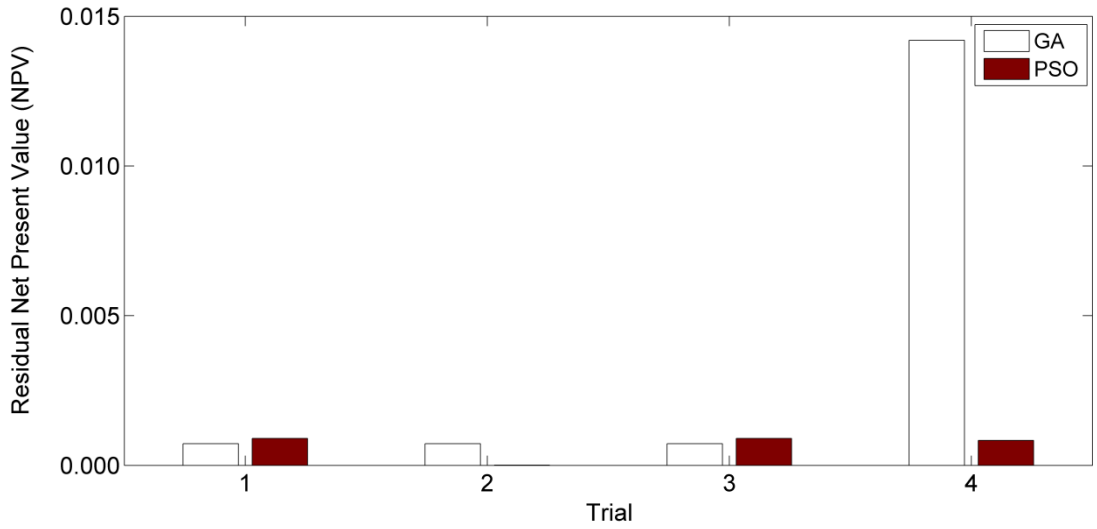

Fig. 4-22: Residual NPV comparisons per trial for iterations 1 to 20 (experiment 2)

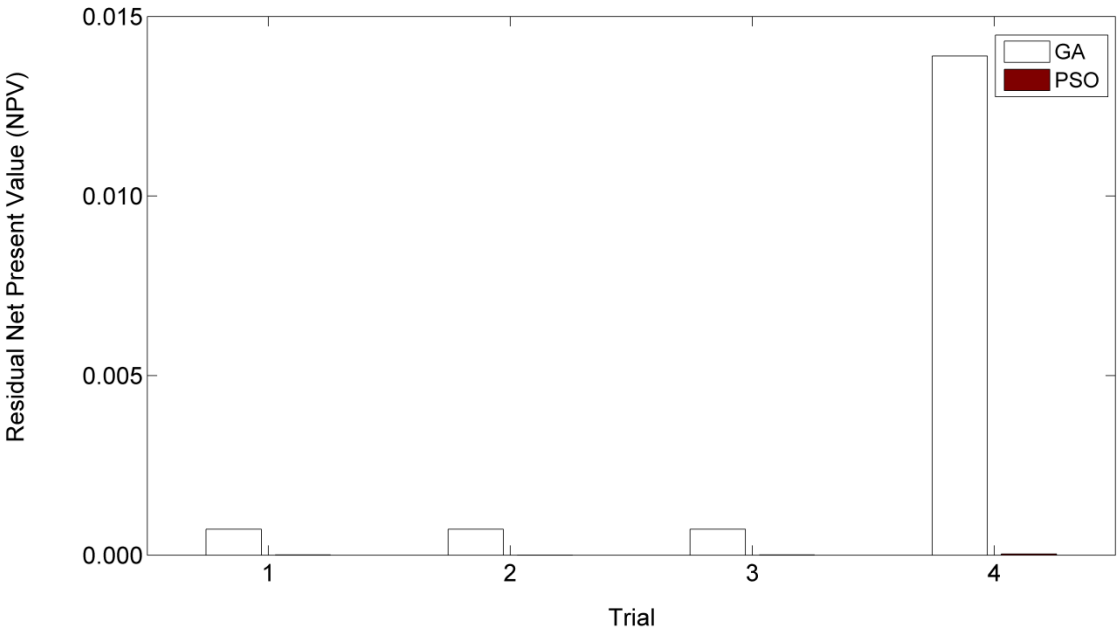

Fig. 4-23: Residual NPV comparisons per trial for iterations 1 to 30 (experiment 2)

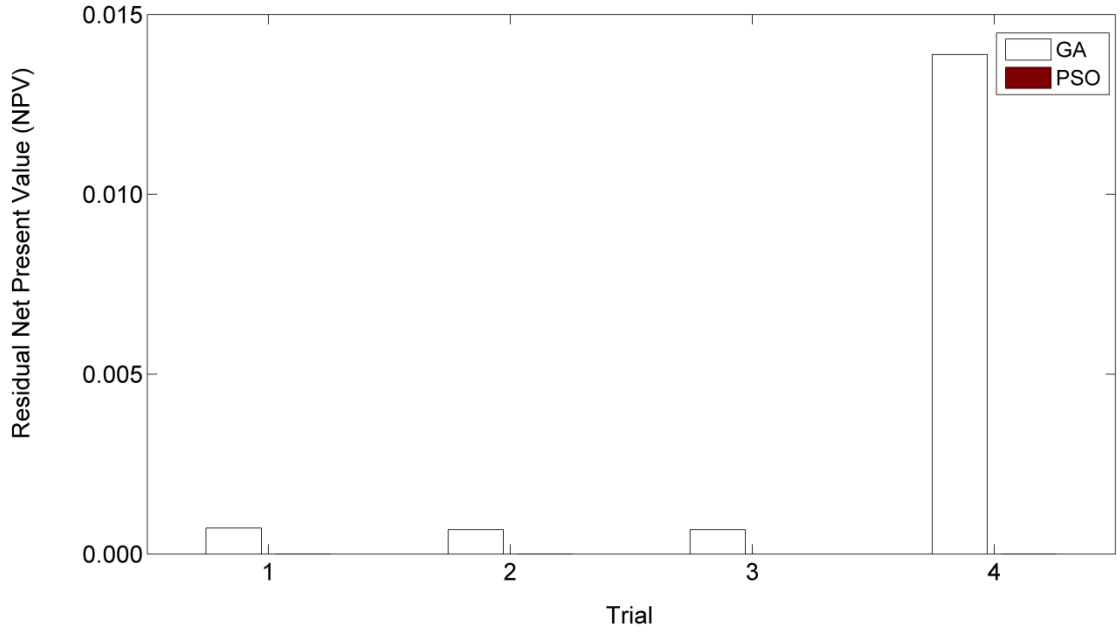

Fig. 4-24: Residual NPV comparisons per trial for iterations 1 to 40 (experiment 2)

As shown in Fig. 4-21 to 4-24, GA outperforms PSO only in the first 20 iterations of trials 1 and 3 and after the 20th iteration, PSO always gives a solution closer to the optimum. The random structure of the algorithms is definitely an influencing parameter on the performance of the algorithms. It is worth recalling that the maximum NPV found by GA in all the trials is less than the optimal solution found by PSO and PSO has been able to find the same answer in every trial.

4.3.3 Experiment 3

In experiment 3, two water injection rates, two gas injection rates, three BHPs of the producers, cycle ratio, cycle time, mole fractions of C_2 to C_4 added to the base injecting gas and the total WAG duration are chosen as the optimisation variables. This gives 13 variables in total. The top 50 results out of 110 simulation runs from the design of experiments are used as the initial guess for both of the optimisation algorithms (GA and PSO) and the best of the 50 is chosen as the reference (unoptimised) case for comparison.

4.3.3.1 Reference Case

The operational point which results in the highest NPV among the 110 simulation runs is the reference case. The variables along with their values and the NPV for the reference case of experiment 3 are shown in Table 4-8. The reference case for experiment 3 gives a higher NPV than experiments 1 and 2. This is mainly due to a longer total WAG duration and a higher total oil production.

Table 4-8: Variables of the reference case with their values for experiment 3

Variable	Reference case
Q_w (F-1H) [Sm^3/day]	2700
Q_g (F-1H) [Sm^3/day]	1000
Q_w (F-3H) [Sm^3/day]	2700
Q_g (F-3H) [Sm^3/day]	1000
BHP (E-2AH) [bar]	150
BHP (E-3CH) [bar]	150
BHP (E-3H) [bar]	150
Cycle ratio [-]	0.55
Cycle time [month]	2
Total time [month]	60
Mole fraction of C_2 [-]	0.2
Mole fraction of C_3 [-]	0.02
Mole fraction of C_4 [-]	0.05
NPV [$ million]	194.72

4.3.3.2 Optimisation Results

The best NPV of each iteration (among the 50 particles) from the four trials of experiment 3 tested with GA and PSO are plotted versus the iteration index for all the iterations in Fig. 4-25 and Fig. 4-26, respectively. The results of iterations 11 to 40 of PSO are plotted as an inset in Fig. 4-26 for better visualization. The results of all the eight trials of the optimisation algorithms are presented in Fig. 4-27.

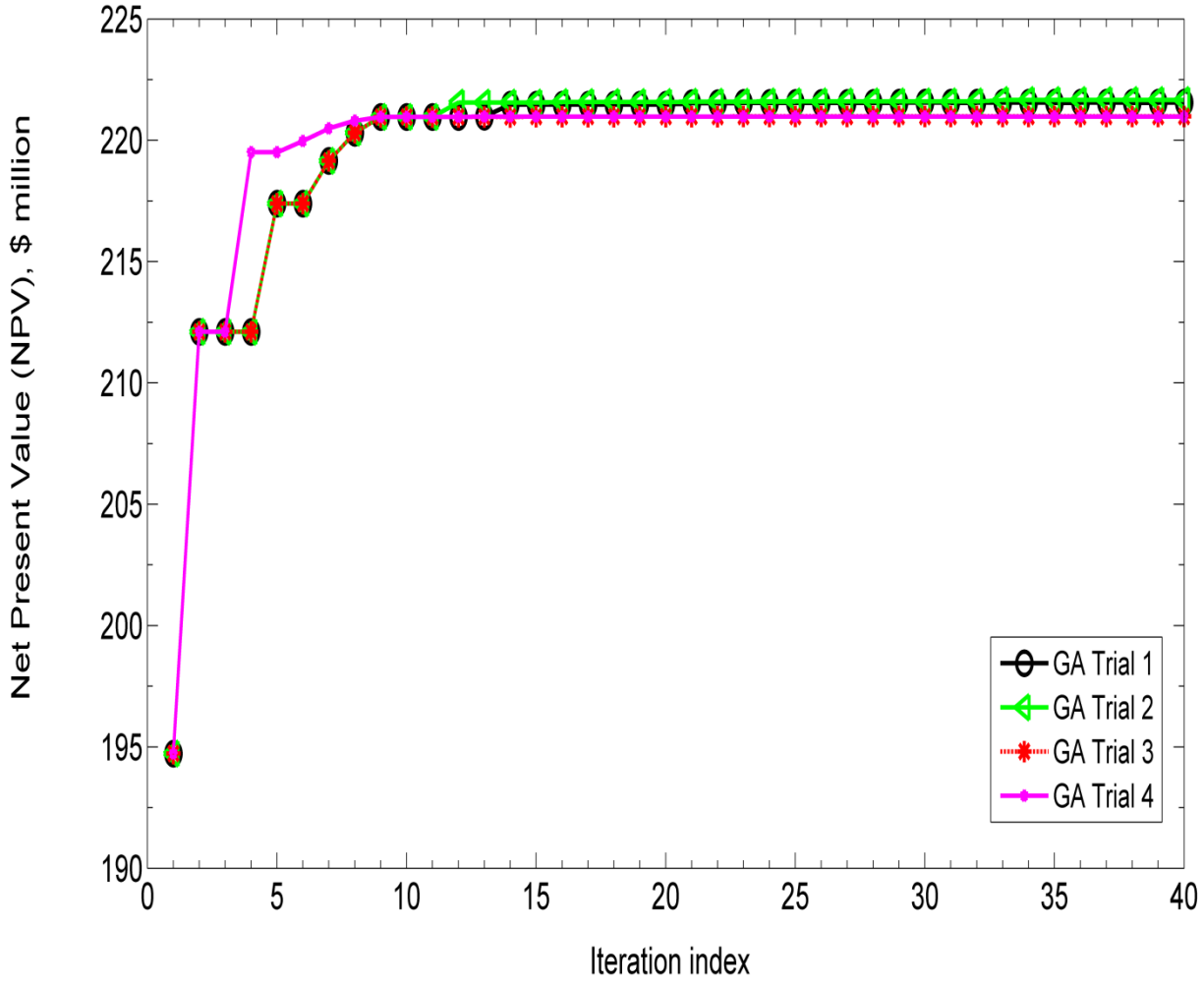

Fig. 4-25: NPV vs. iteration index per trial for GA (experiment 3)

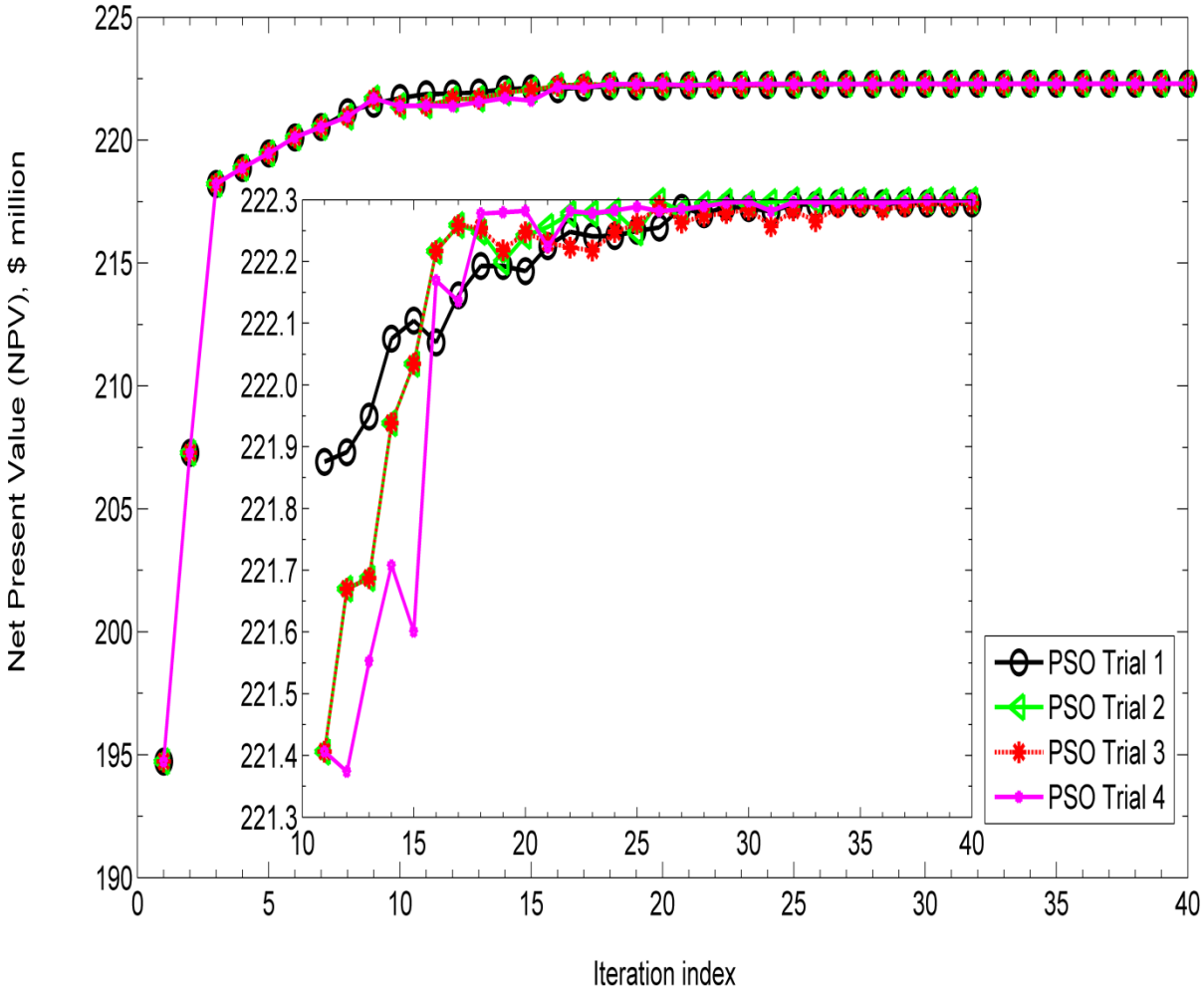

Fig. 4-26: NPV vs. iteration index per trial for PSO (experiment 3)

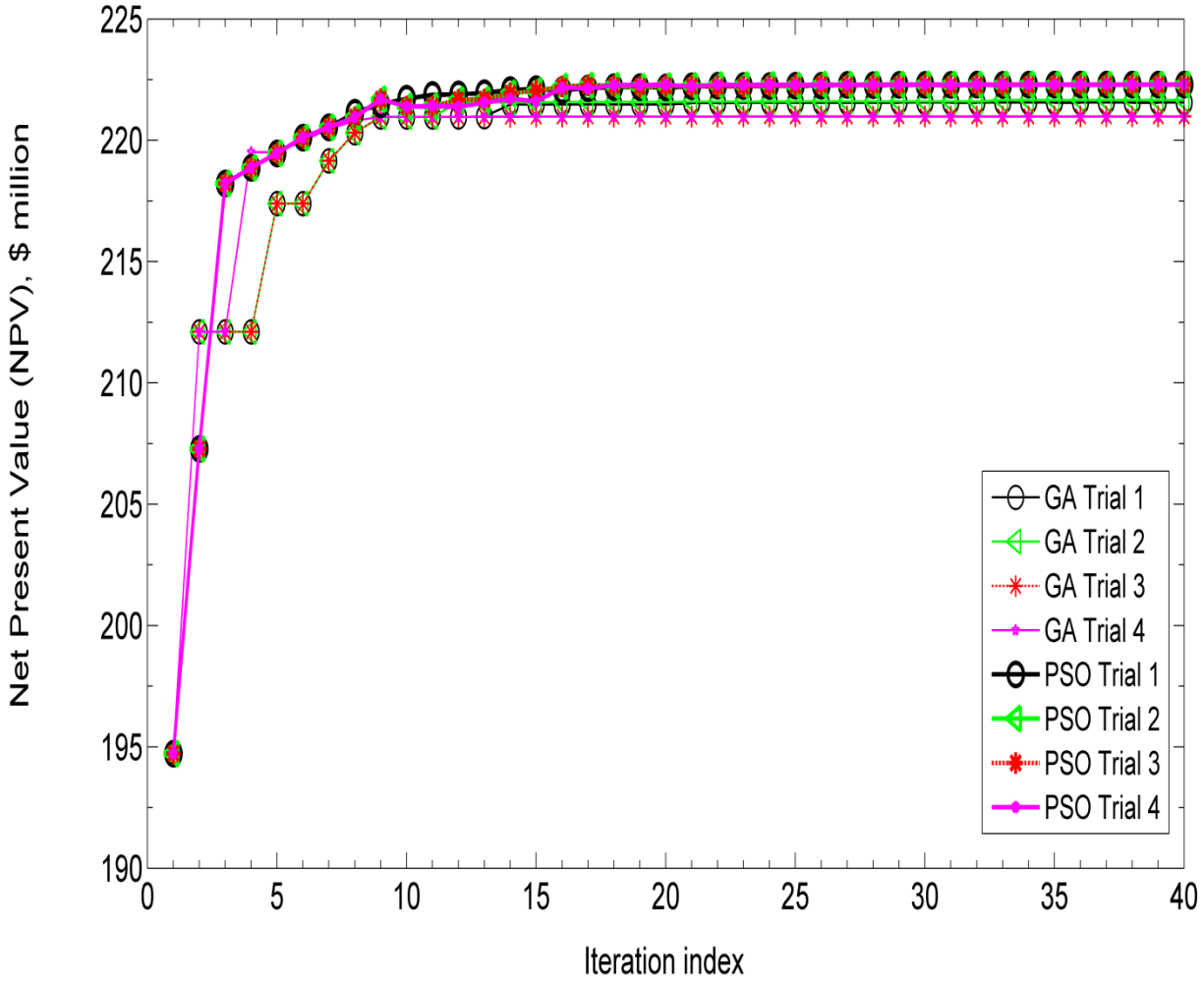

Fig. 4-27: NPV vs. iteration index per trial for PSO (experiment 3)

Fig. 4-25 shows the monotonic behaviour of GA and its convergence to different solutions. Fig. 4-26 shows the consistency of PSO in converging to the same optimal solution and fluctuations in its performance. Fig. 4-27 indicates the better performance of PSO in all the trials compared to GA.

The values of the variables for the reference case of experiment 3 along with the optimal solutions and the corresponding NPVs from each of the four trials of GA and PSO are presented in Table 4-9 and 4-10, respectively. The values of the optimised variables which differ from the reference case have been asterisked for each trial.

Table 4-9: The reference case and best operational points of four trials of GA (experiment 3)

Variable	**Reference case**	**GA Trial 1**	**GA Trial 2**	**GA Trial 3**	**GA Trial 4**
Q_w (F-1H) [Sm^3/day]	2700	2700	2700	2700	2700
Q_g (F-1H) [Sm^3/day]	1000	1000	1000	1000	1000
Q_w (F-3H) [Sm^3/day]	2700	2700	2700	2700	2700
Q_g (F-3H) [Sm^3/day]	1000	1000	1000	1000	1000
BHP (E-2AH) [bar]	150	150	150	150	150
BHP (E-3CH) [bar]	150	150	150	150	150
BHP (E-3H) [bar]	150	237*	237.5*	239.8*	240*
Cycle ratio [-]	0.55	0.9*	0.9*	0.9*	0.9*
Cycle time [month]	2	5*	7*	3*	3*
Total time [month]	60	60	60	60	60
Mole fraction of C_2 [-]	0.2	0.2	0.2	0.2	0.2
Mole fraction of C_3 [-]	0.02	0.1*	0.1*	0.1*	0.1*
Mole fraction of C_4 [-]	0.05	0.05	0.05	0.05	0.05
NPV [$ million]	194.72	221.55	221.65	220.98	220.98

Table 4-10: The reference case and best operational points of four trials of PSO (experiment 3)

Variable	Reference case	PSO Trial 1	PSO Trial 2	PSO Trial 3	PSO Trial 4
Q_w (F-1H) [Sm^3/day]	2700	2700	2700	2700	2700
Q_g (F-1H) [Sm^3/day]	1000	1000	1000	1000	1000
Q_w (F-3H) [Sm^3/day]	2700	2700	2700	2700	2700
Q_g (F-3H) [Sm^3/day]	1000	1000	1000	1000	1000
BHP (E-2AH) [bar]	150	150	150	150	150
BHP (E-3CH) [bar]	150	150	150	150	150
BHP (E-3H) [bar]	150	226.2*	226.2*	226.2*	226.2*
Cycle ratio [-]	0.55	0.9*	0.9*	0.9*	0.9*
Cycle time [month]	2	8*	8*	8*	8*
Total time [month]	60	60	60	60	60
Mole fraction of C_2 [-]	0.2	0.2	0.2	0.2	0.2
Mole fraction of C_3 [-]	0.02	0.1*	0.1*	0.1*	0.1*
Mole fraction of C_4 [-]	0.05	0.05	0.05	0.05	0.05
NPV [$ million]	194.72	222.29	222.29	222.29	222.29

As shown in the Fig. 4-25 to 4-27 and Table 4-9 and 4-10, GA always converges to a suboptimal solution and is never able to find the solution found by PSO in any of the trials. GA has found quite different values for the cycle time in the trials, neither of which yields the optimum NPV found by PSO. However, the best NPV found by PSO is only 0.29% higher than the optimal NPV of GA and this is due to different BHPs for well E-3H and different cycle times. In the optimal solution found by PSO, the BHP of well E-3H has increased from 150 bar to 226.2 bar, cycle ratio has changed from 0.55 to 0.9, the cycle time has shifted from 2 months to 8 months and the mole fraction of C_3 has changed from 0 to 0.1. This has resulted in about 14.2% increase in NPV compared to the reference case. PSO converges to the same solution in all the trials.

PSO finds a solution with an NPV in the vicinity of 0.01% of the optimum solution for the first time in iteration 27, 22, 26 and 18 of trials 1 to 4, respectively. GA never finds such a point in any of the trials.

After three experiments, fluctuations in the best solutions found by PSO seem to be a feature of this technique, while GA has usually proved to be continuously increasing in the value of the objective function. GA keeps the best ever solution and if the GA operations (selection, crossover and mutation) do not result in a better solution, the global best solution would be transferred to the next iteration. In PSO, however, the positions of all the particles are updated by a random factor of the position of the global best solution, hence the best found solution may not carry over to the next iteration. These fluctuations probably help PSO escape from local optima.

The main difference between experiment 3 and experiments 1 and 2 is the addition of the total time as a variable and setting 60 months as its upper bound. This has resulted in two major differences in the optimal operational points. In experiments 1 and 2, the optimal BHP of well E-2AH is about 158.8 bar and wells E-3CH and E-3H would give a higher NPV if produced at the lower pressure bound (150 bar). In experiment 3, the optimal BHP of well E-2AH and E-3CH is the minimum (150 bar) and well E-3H would produce optimally at around 226.2 bar. The other distinction is the cycle time. The optimal cycle time of experiments 1 and 2 lies at 5 months, while it was found to be 8 months for experiment 3. The optimal NPV of experiment 3 is about 49.4% and 51.7% higher in value compared to the optimal NPVs of experiments 1 and 2, respectively.

The average NPV of the 200 particles in each iteration of all the four trials of GA and four trials of PSO are plotted versus the iteration index in Fig. 4-28 for both of the algorithms along with the error bars showing the standard deviations.

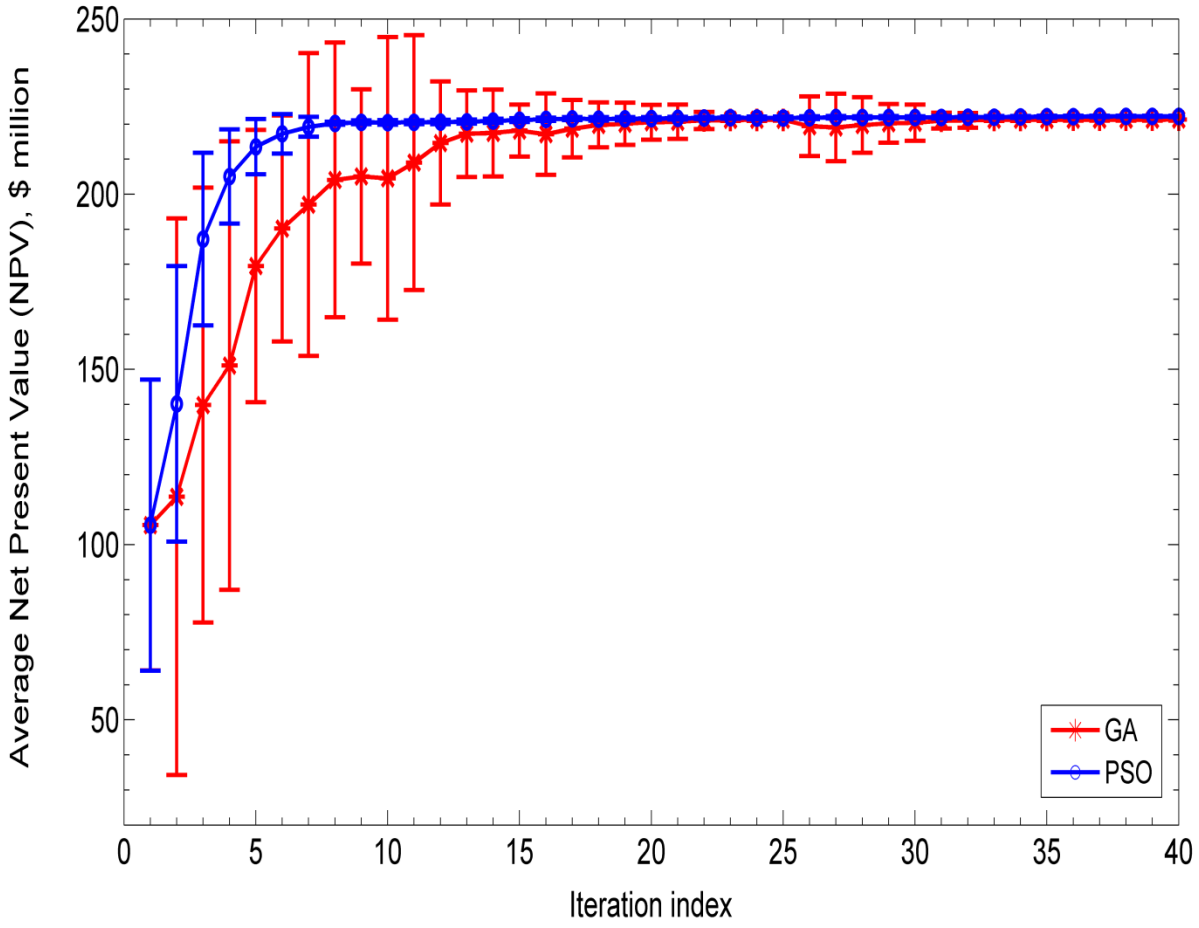

Fig. 4-28: Average performance of GA and PSO for all the four trials (experiment 3)

As shown in Fig. 4-28, the average NPV of all the four trials of GA is lower than the corresponding average NPV found by PSO for every iteration which indicates the superior performance of PSO. The solutions found by PSO are also located closer to their average indicated by the lower standard deviations of PSO. We see monotonicity in the PSO results and fluctuations in the GA results from the perspective of average performance.

The bar charts in Fig. 4-29 to 4-32 show the relative difference between the best NPV found in the first 10, 20, 30 and 40 iterations and the maximum overall NPV of the problem (see equation (4.1)) for the four trials of GA and PSO.

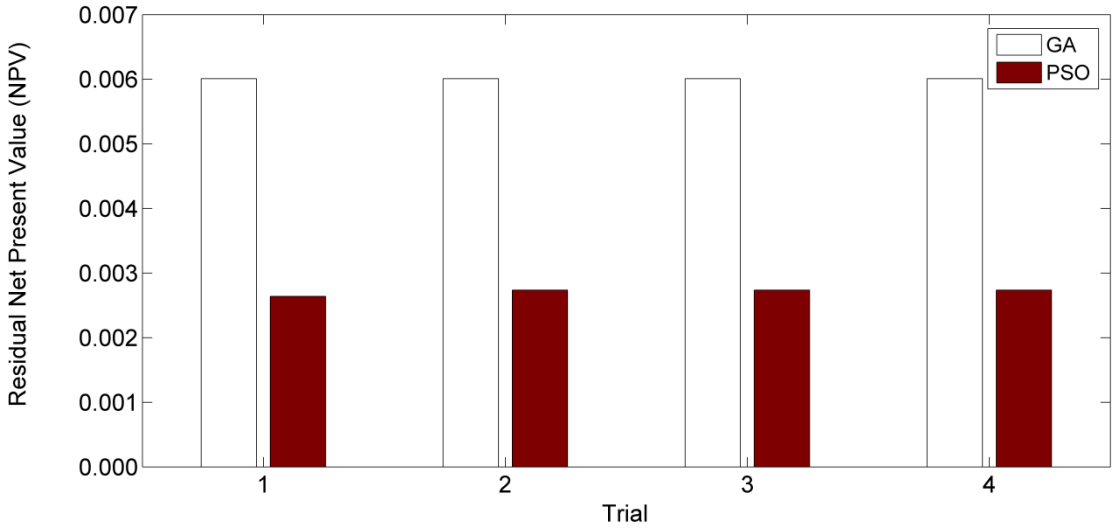

Fig. 4-29: Residual NPV comparisons per trial for iterations 1 to 10 (experiment 3)

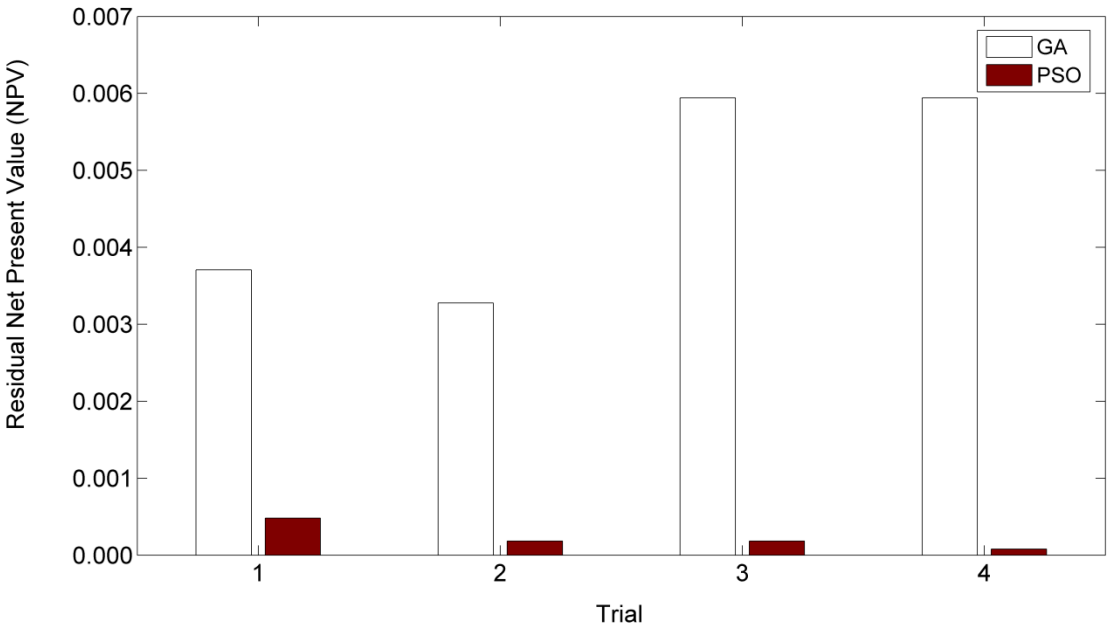

Fig. 4-30: Residual NPV comparisons per trial for iterations 1 to 20 (experiment 3)

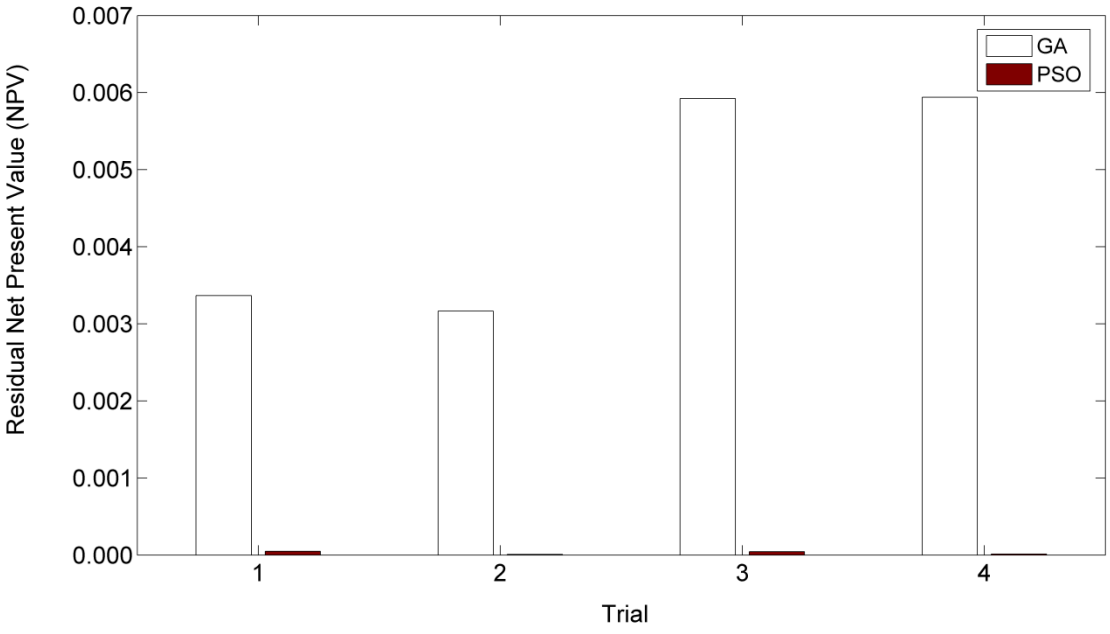

Fig. 4-31: Residual NPV comparisons per trial for iterations 1 to 30 (experiment 3)

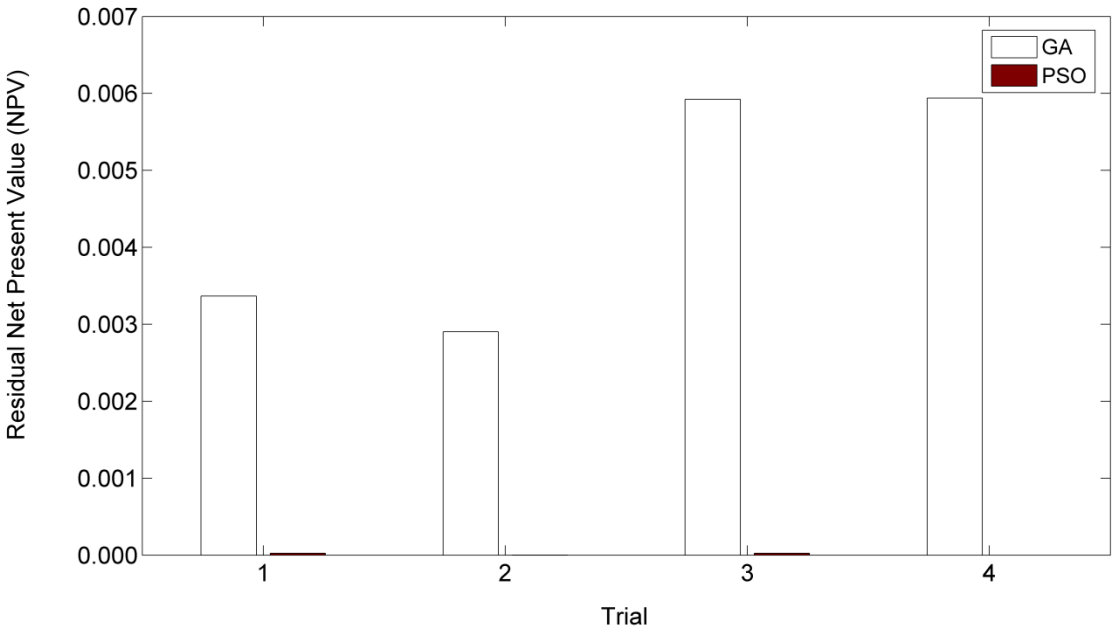

Fig. 4-32: Residual NPV comparisons per trial for iterations 1 to 40 (experiment 3)

For this experiment, PSO always outperforms GA in all the trials regardless of the number of iterations. PSO shows better performance and a greater improvement compared to GA as the number of iterations increases. Since this experiment was designed to be the most complex, this indicates the general superiority of PSO over GA for the case of NPV optimisation for WAG on this field.

The bar charts show that the best solution of PSO in most iterations of each trial is better than the corresponding value found by GA and the plots of average NPV demonstrate that the particles in each single iteration of PSO are always located closer to the optimum than the individuals in the same iteration of GA.

4.3.4 Sensitivity Studies on NPV

A sensitivity analysis is a means to measure the effect of independent parameters on the objective function. In this study, to examine the effect of one WAG operational parameter on NPV, all the other parameters are kept constant at their optimal values. This method is called one-factor-at-a-time and is the most common approach to investigate the effect of input variables on the output. This method does not take into account the interactions between the input variables [183]. Other methods such as local methods, scatter plots, regression analysis, variance-based methods and screening, to name a few, can be used for sensitivity analysis. We limit ourselves to one-factor-at-a-time in this study. The normalized NPV (the ratio of NPV to the maximum NPV found by the optimisation algorithms for experiment 3) is plotted versus the normalized variables (the ratio of each variable to its optimal value). The trend and slope of each curve shows how that parameter affects the objective function.

In Fig. 4-33, we consider the normalized water injection rate on the interval [0.8, 0.95] in steps of 0.05 and the normalized gas injection rate on the interval [1.05, 1.2] in steps of 0.05.

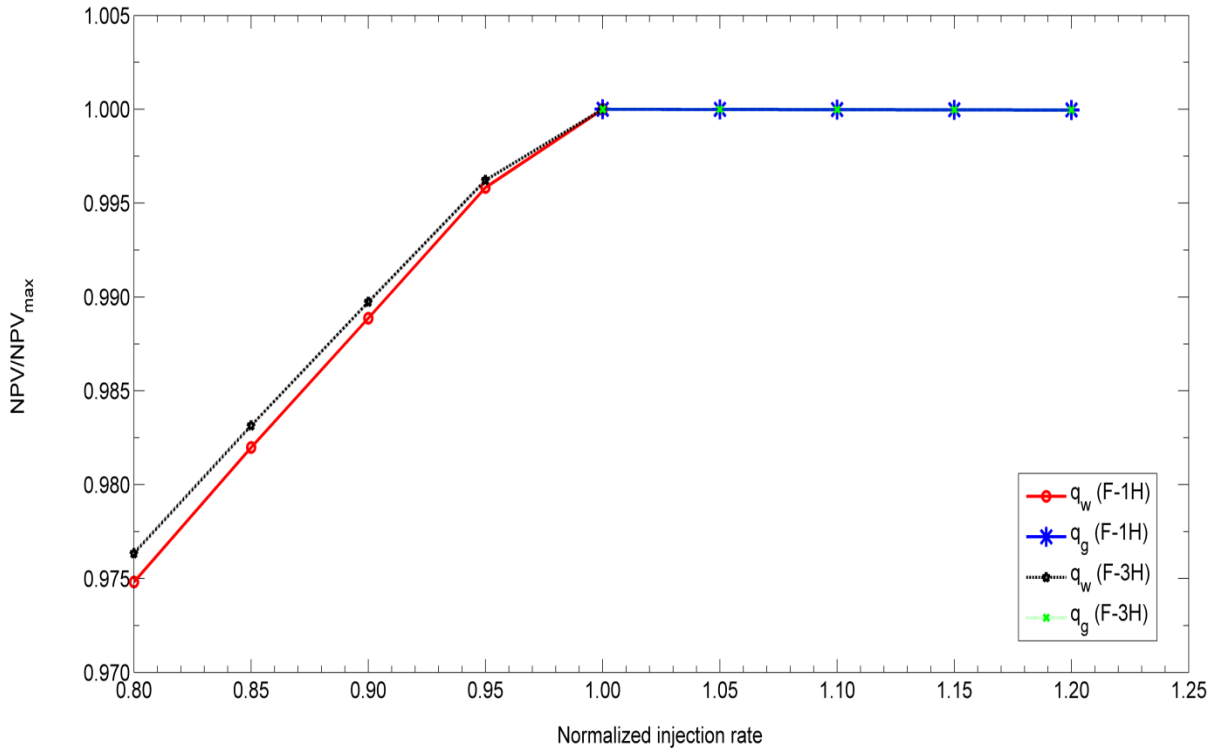

Fig. 4-33: Effect of water and gas injection rates on NPV

As shown in Fig. 4-33, at low injection rates of gas and high injection rates of water, the effect of change in water injection rates on NPV is much higher than that of the gas injection rates which indicates the better response of the reservoir to water injection and its greater effect on oil recovery as compared to gas injection. The slope of the line related to well F-1H is greater than that of well F-3H which means that water injection in well F-1H is more influential on NPV and likely oil recovery. The slopes of the lines related to gas injection rates are negative but very small for both wells. This shows that increasing the gas injection rate is not cost effective and the increase in oil recovery due to enhancing the gas injection rates is not justified economically.

In Fig. 4-34 the effect of the BHP of the producers on NPV is shown.

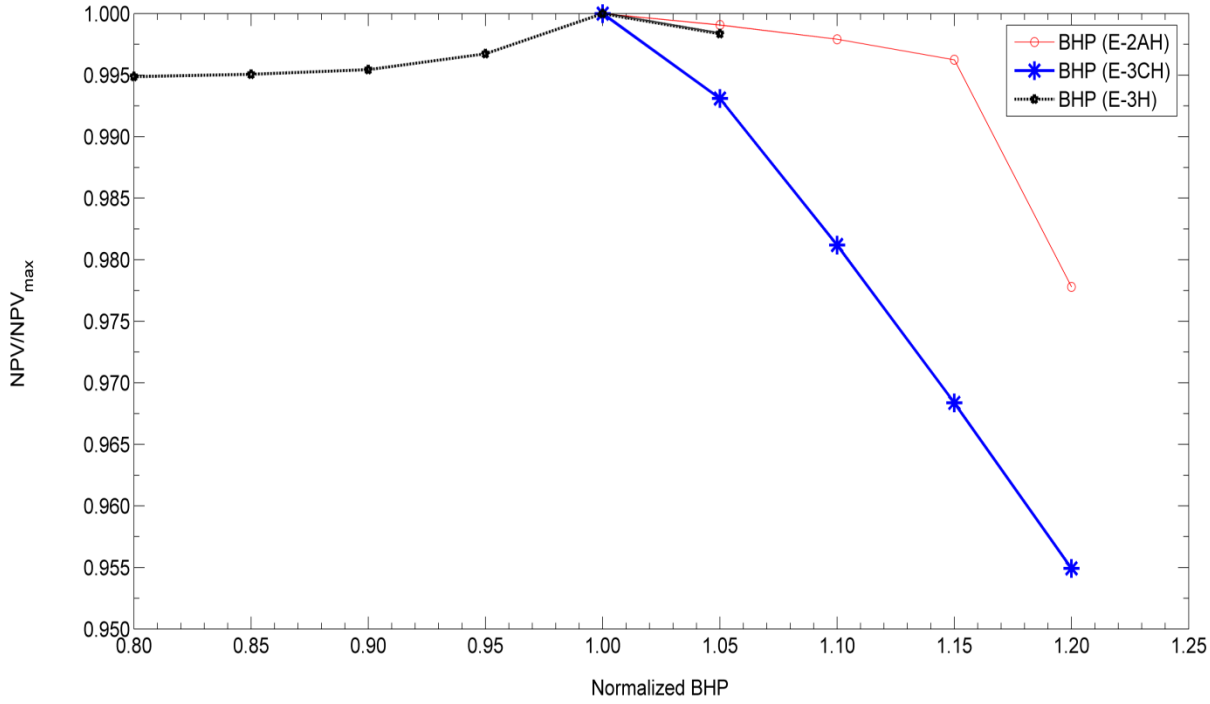

Fig. 4-34: Effect of BHP on NPV

The optimal BHP of well E-3H is about 226.2 bar. The normalized BHP of well E-3H is changed on the interval [0.8, 1.05] in steps of 0.05 for the sensitivity study. Increasing the BHP below the optimal value delays and reduces water production and enhances the NPV, while increasing the BHP above its optimal value causes the oil production to fall below the economic limit. The optimal BHP of wells E-2AH and E-3CH is 150 bar. The normalized BHPs of these two wells are changed on the interval [1.05, 1.2] in steps of 0.05 for the sensitivity analysis. These two wells behave normally in the sense that by increasing the BHP the oil production reduces significantly which affects the NPV. This indicates that well E-3H is the most sensitive well to water production.

Fig. 4-35 presents the effect of cycle ratio on NPV. The optimal cycle ratio is 0.9 which means that in each cycle water is injected for 90% of the time and the rest is allocated to gas injection. It is worth recalling that cycle ratio was changed in steps of 0.05 through the search process of the optimisation. For the sensitivity analysis, this parameter was changed from 0.7 to 1 in steps of 0.05. A cycle ratio of 1 refers to water flood.

As can be seen in Fig. 4-35, for a cycle ratio less than 0.9 (when gas is injected for more than 10% of a cycle), the NPV is lower than the optimum. This implies that increasing the gas injection period above that threshold does not result in enough oil production to make up for the cost of gas injection. When water is injected for more than 90% of a cycle the cost of water handling reduces the NPV below the optimum. The optimal cycle ratio depends strongly on the prices assumed for the NPV calculations.

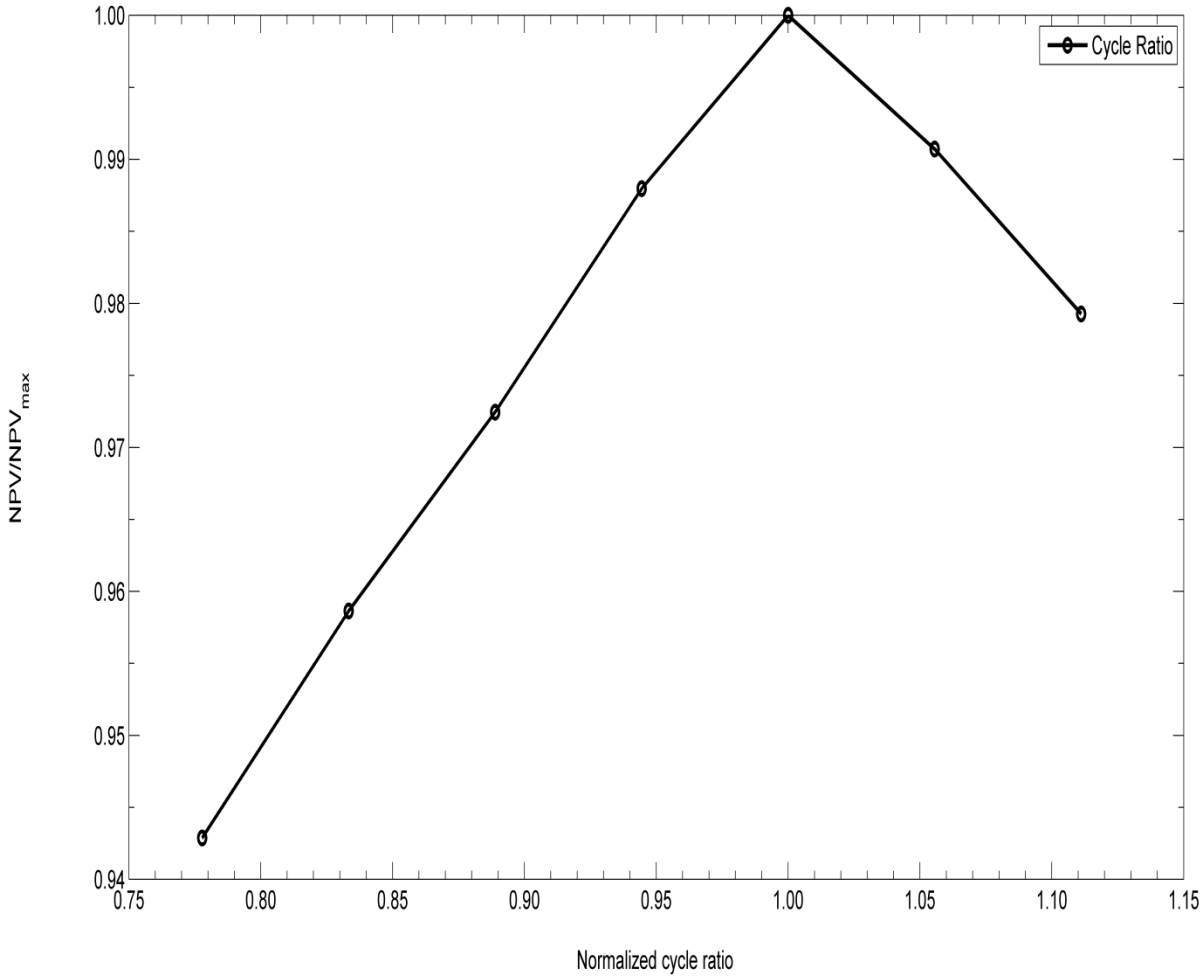

Fig. 4-35: Effect of cycle ratio on NPV

The effect of cycle time on NPV is shown in Fig. 4-36. The cycle time is changed from 2 to 10 months in steps of 1 month to examine its influence on the NPV. 8 months is the optimal cycle time for a 5-year WAG process and cycle times of 7 and 4 months are ranked second and third. This means that the most efficient WAG injection scenario for a period of 5 years is to inject gas for 24 days and then inject water for 216 days (based on the cycle ratio of 0.9) cyclically.

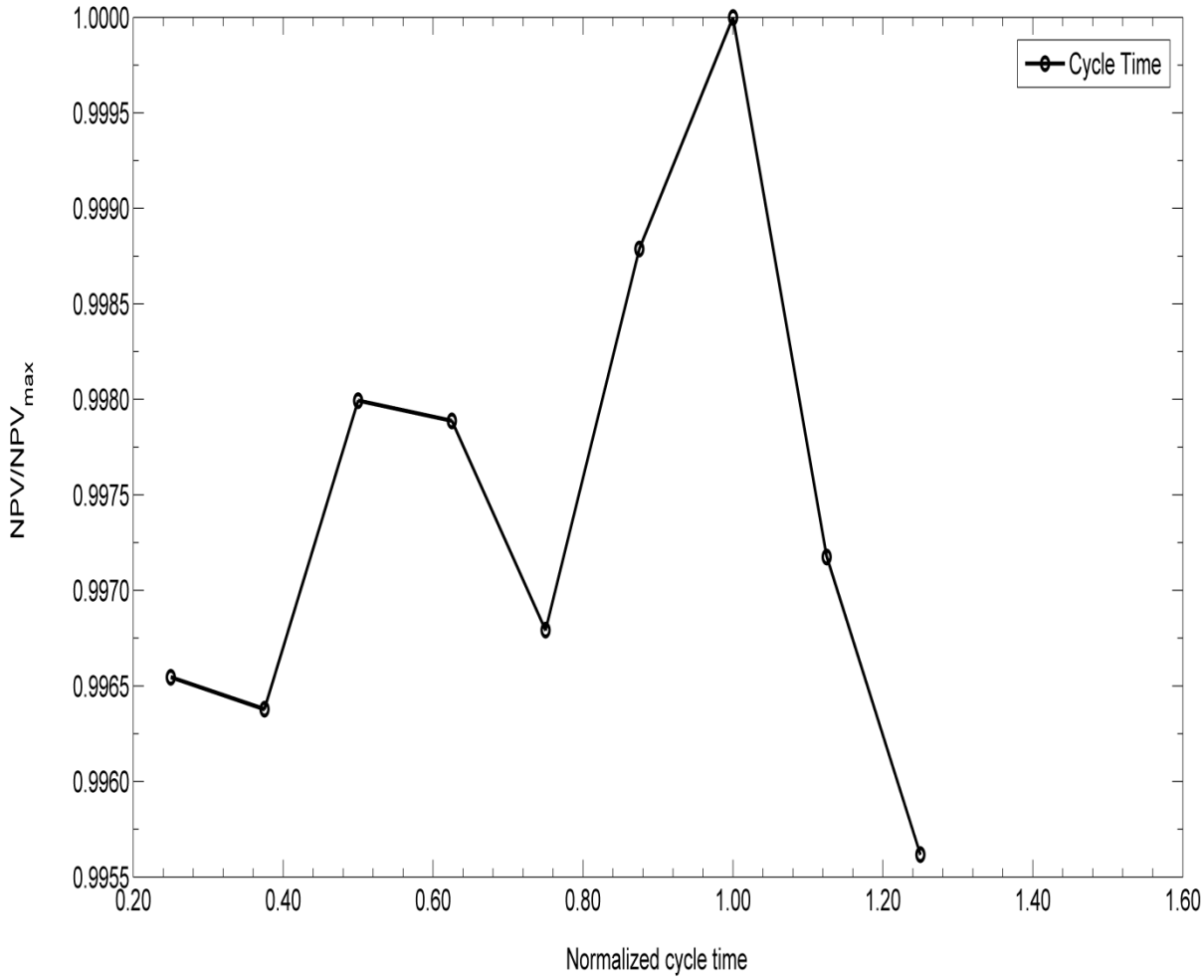

Fig. 4-36: Effect of cycle time on NPV

The effect of the total WAG time is shown in Fig. 4-37. The normalized total time is changed on the interval [0.8, 1.2] in steps of 0.05. As can be seen, the NPV is monotonically increasing versus the total WAG time. This suggests that WAG has the potential of being extended for at least one more year and would still be economical. However, the optimal operational WAG parameters for the 5-year period may not result in the highest NPV for a longer period and the optimal WAG for a longer period would have to be specified in a separate optimisation process.

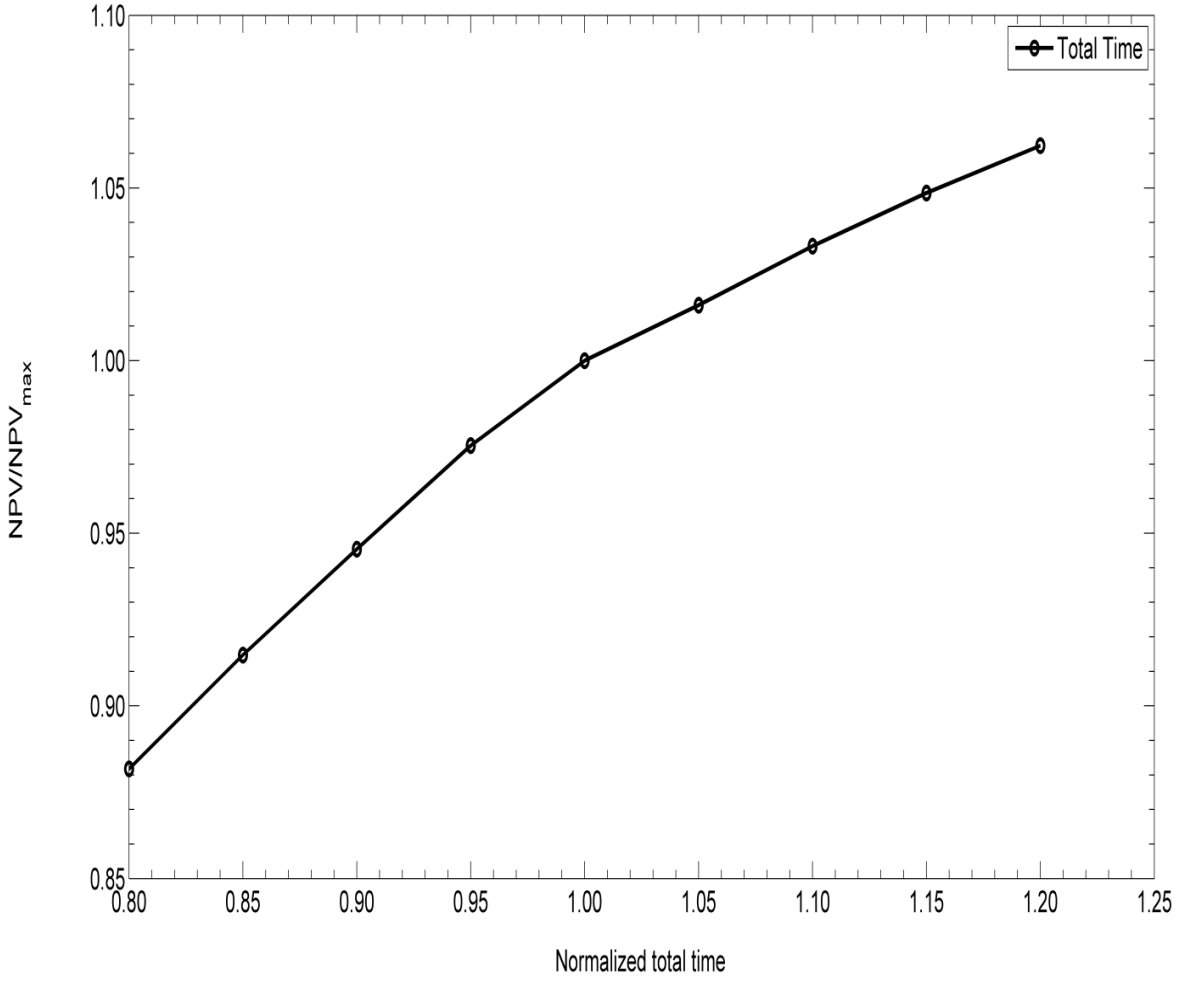

Fig. 4-37: Effect of total WAG time on NPV

And finally, the effect of the amount of enriching components on the NPV is shown in Fig. 4-38. The optimal mole fractions of C_2 to C_4 are 0.2, 0.1 and 0.05, respectively and their normalized values are changed on the interval [0.8, 0.95] in steps of 0.05 for the sensitivity study. The highest change in NPV happens by changing the amount of C_4 in the injection gas as its curve shows the highest slope and the amount of C_2 has the least effect on the NPV. This means that with the prices assumed in this study enriching the injecting gas in such a way that contains more

butane is justified economically and the increase in oil recovery due to a miscible injection is worth the enrichment.

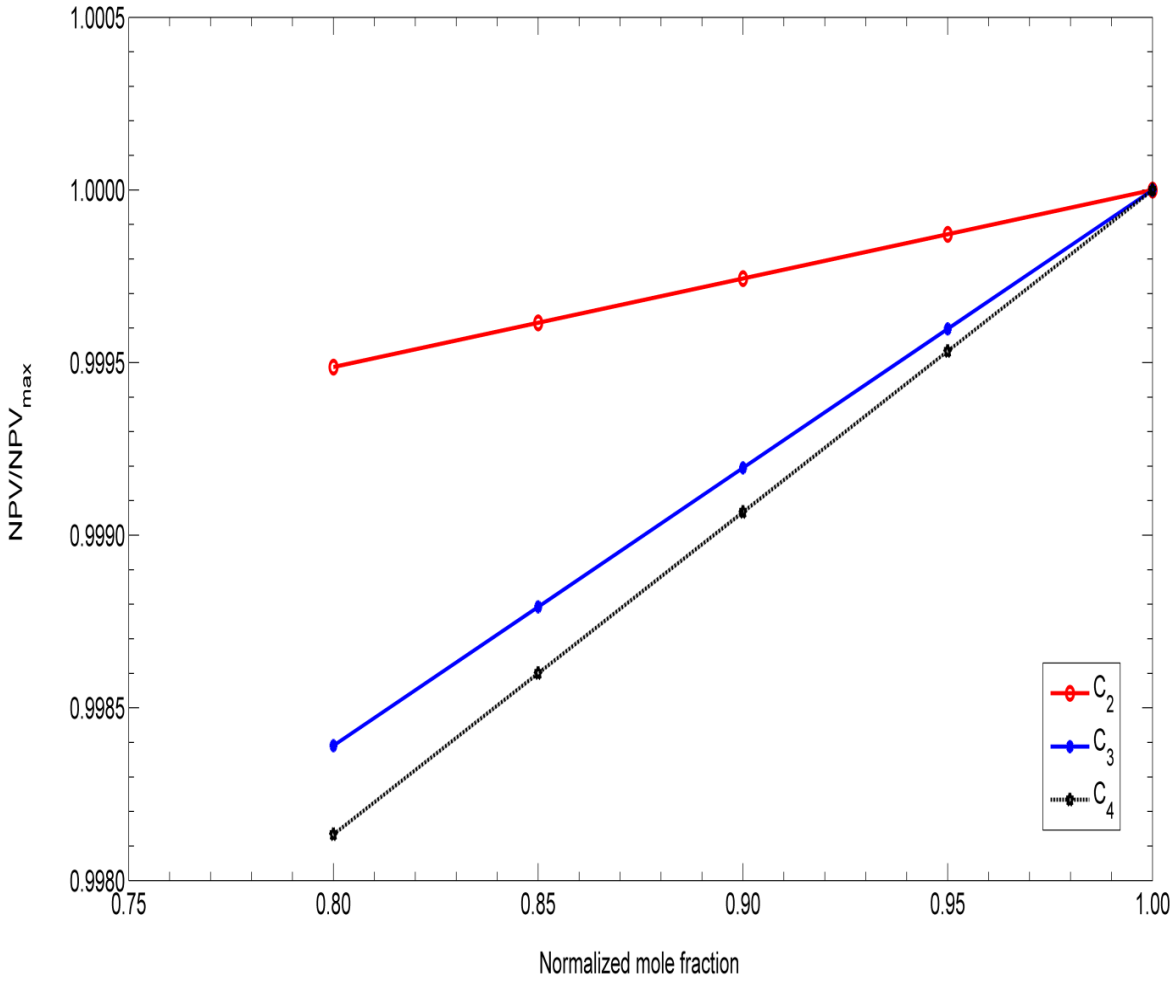

Fig. 4-38: Effect of the amount of enriching components on NPV

4.3.5 Sensitivity Analysis of Economic Parameters

The economic parameters of oil price, gas injection cost, water injection cost and water recycling cost are selected for the sensitivity study to investigate their effect on NPV. When the effect of one economic parameter on NPV is examined, the other parameters are set at the values shown

in Table 3-4. The gas injection cost is \$0.271 / Sm^3 which is the unit price of gas containing 65% C_1, 20% C_2, 10% C_3 and 5% C_4 with the prices assumed for each of the components (see Table 3-4). Fig 4-39 shows the ratio of NPV to the overall maximum NPV of experiment 3 versus the normalized prices (the ratio of each price to its corresponding value in Table 3-4). The normalized oil price is varied on the interval [0.8, 1.2] in steps of 0.05. The other normalized prices are changed on the interval [0, 1.2] to consider the assumption of zero cost for them.

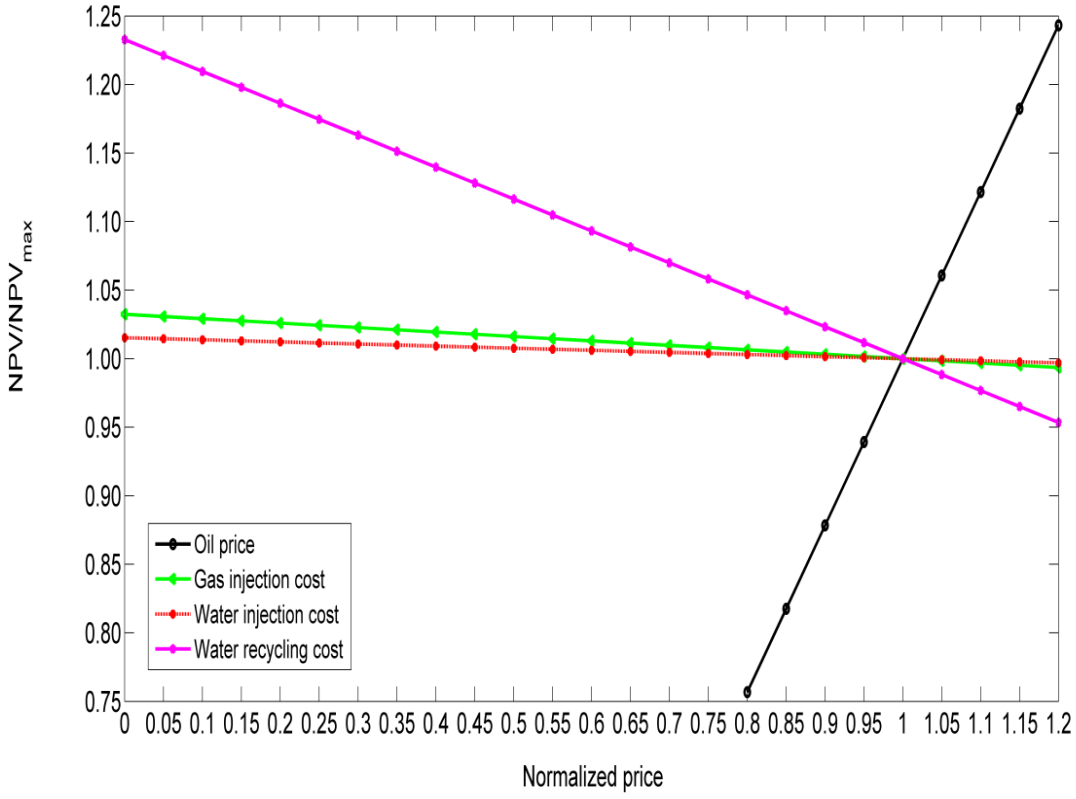

Fig. 4-39: Effect of economic parameters on NPV

As shown in Fig. 4-39, the relative change of NPV versus the relative change of the economic parameters clearly indicates that the NPV of WAG significantly changes as the oil price varies and oil price is the most influential economic parameter on the NPV. Water recycling cost has

the second highest effect on the NPV and gas injection and water injection costs are ranked third and fourth, respectively. The effect of gas and water injection costs are much smaller than that of oil price indicated by much smaller absolute values for their slopes. Evidently, oil price has a positive effect and the costs have negative effects on the NPV as the line slope of oil price is positive and the line slopes of the costs are negative.

4.4 Optimisation of Oil Recovery

In this section, GA and PSO are used to optimise the incremental recovery factor (IRF, see equation (3.7)) or the recovery factor from the start of WAG process on the E-segment of the Norne field. The optimisation variables include two water and two gas injection rates, three BHPs of the oil producers, cycle ratio, cycle time and the mole fractions of C_2, C_3 and C_4 added to the base injection gas. The total WAG time is fixed at 60 months. The top 50 results out of 96 simulation runs from the design of experiments are used as the initial guess matrix for the optimisation techniques and the best of the 50 (the one with maximum oil recovery) is chosen as the reference case for comparison. Three trials of GA and PSO with the same initial guess matrix are run.

4.4.1 Reference Case

The operational point which results in the highest oil recovery among the 96 simulation runs is chosen as the reference case. The variables along with their values and the IRF calculated from the start of the WAG (as time zero) for the reference case of oil recovery optimisation are shown in Table 4-11.

Table 4-11: Variables of the reference case with their values for oil recovery optimisation

Variable	Reference case
Q_w (F-1H) [Sm^3/day]	500
Q_g (F-1H) [Sm^3/day]	10^6
Q_w (F-3H) [Sm^3/day]	500
Q_g (F-3H) [Sm^3/day]	10^6
BHP (E-2AH) [bar]	150
BHP (E-3CH) [bar]	150
BHP (E-3H) [bar]	240
Cycle ratio [-]	0.1
Cycle time [month]	2
Mole fraction of C_2 [-]	0.2
Mole fraction of C_3 [-]	0.1
Mole fraction of C_4 [-]	0.01
IRF [-]	4.45%

4.4.2 Optimisation Results

The maximum IRF of each iteration (among the 50 particles) from the three trials of GA and PSO are plotted versus the iteration index for all the iterations in Fig. 4-40 and Fig. 4-41, respectively. The results of iterations 11 to 40 of PSO are plotted as an inset in Fig. 4-41 for better visualization. The results of all the six trials of GA and PSO are shown in Fig. 4-42.

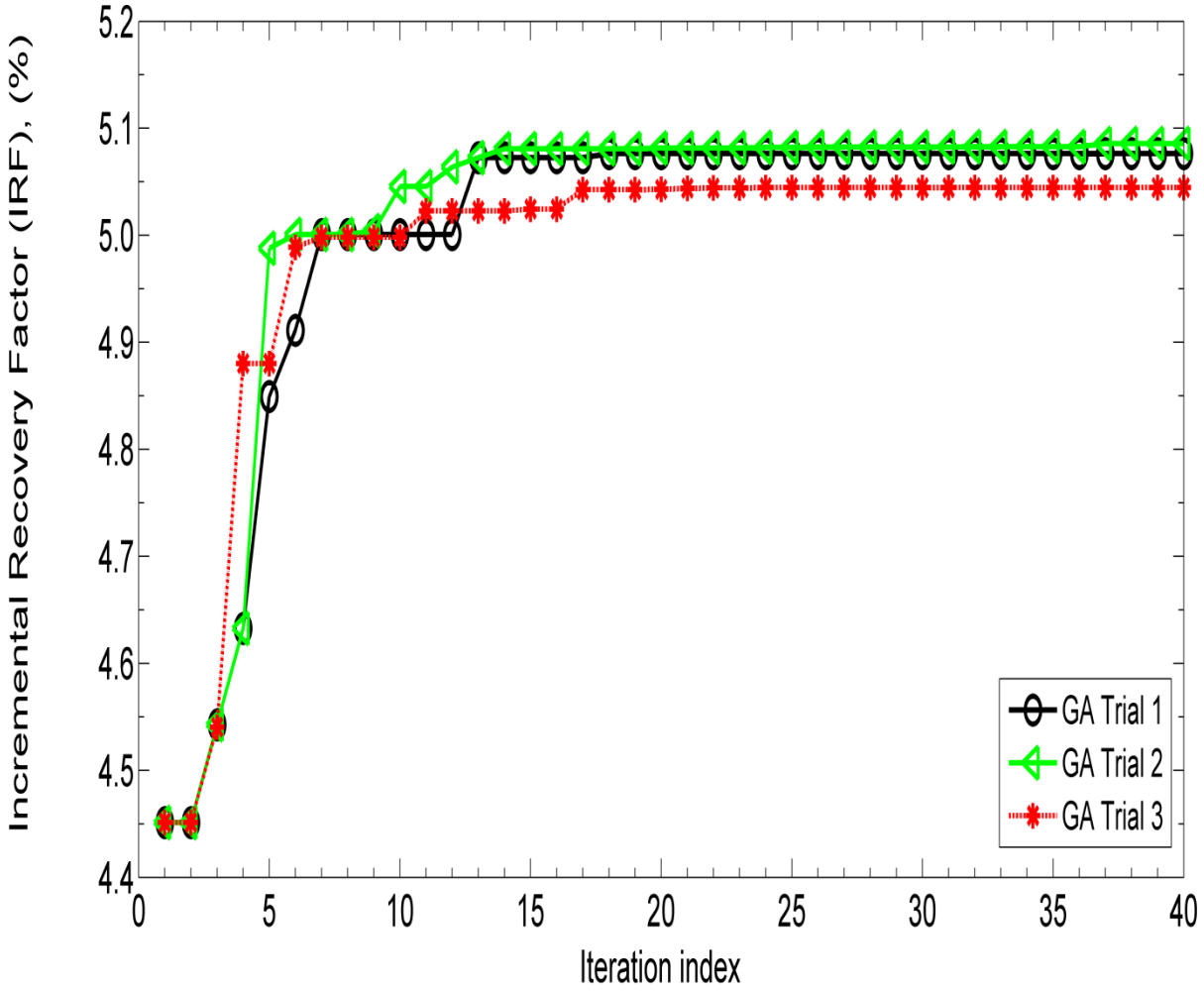

Fig. 4-40: IRF vs. iteration index per trial for GA (oil recovery optimisation)

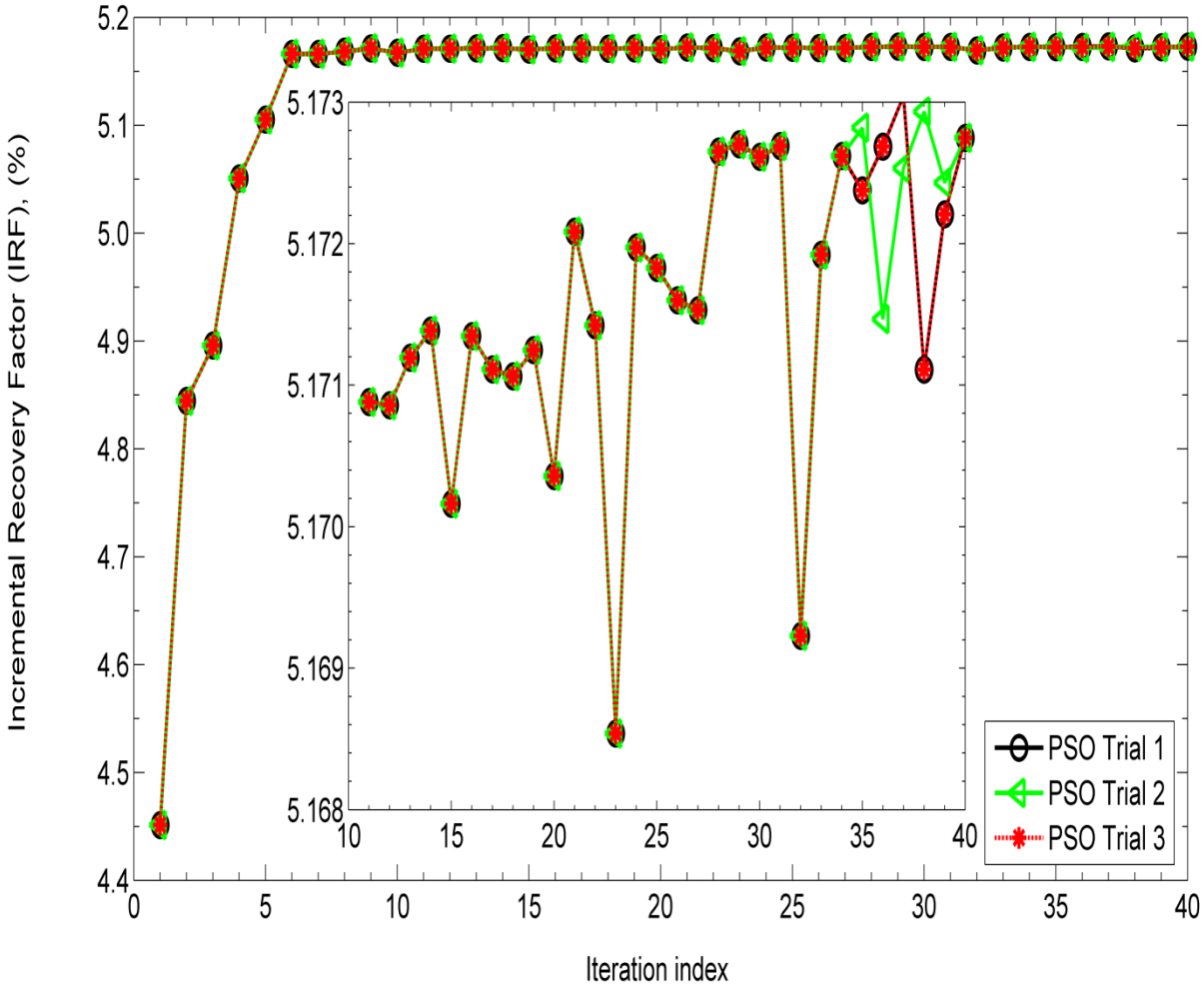

Fig. 4-41: IRF vs. iteration index per trial for PSO (oil recovery optimisation)

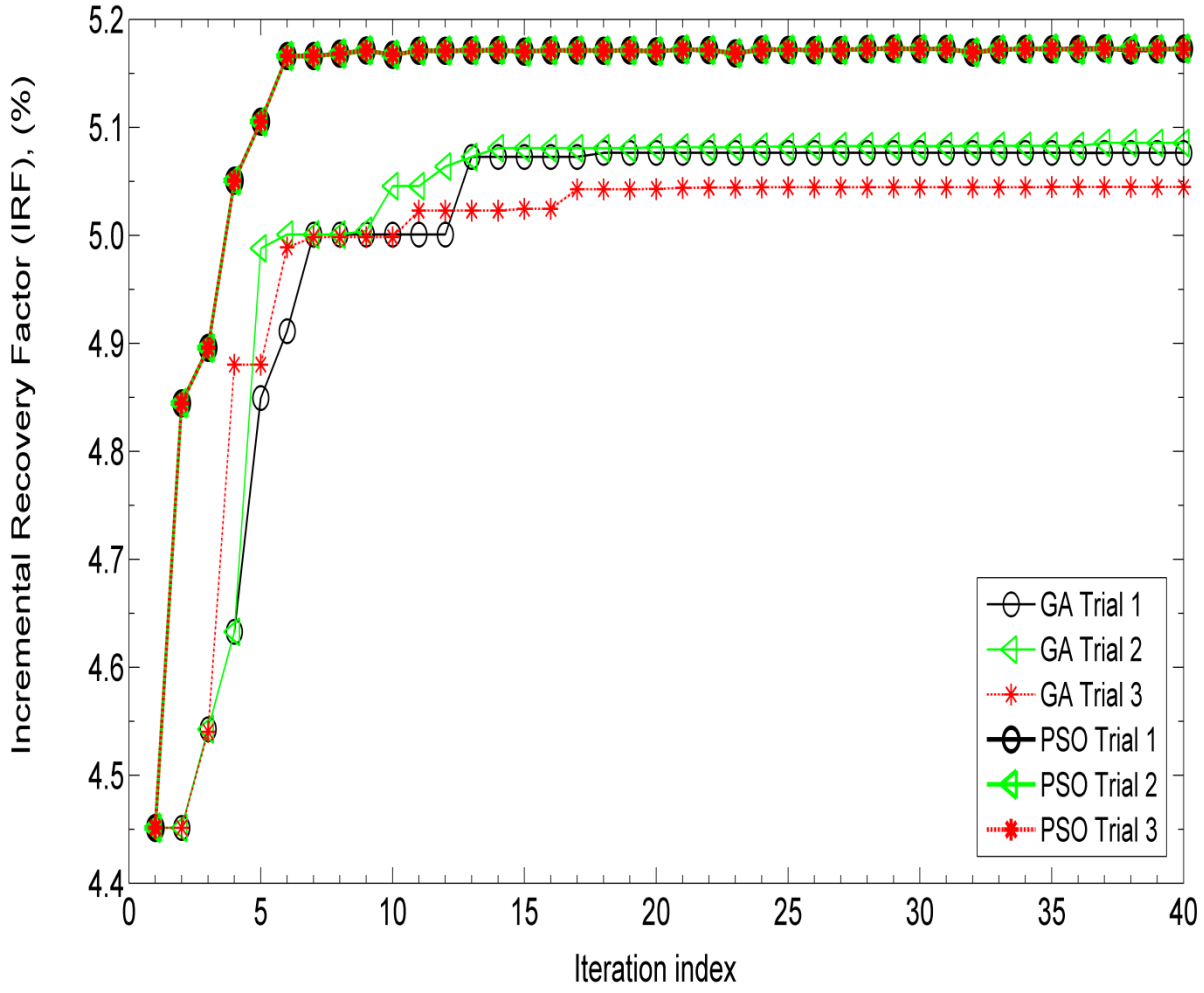

Fig. 4-42 IRF vs. iteration index per trial for GA and PSO (oil recovery optimisation)

Fig. 4-40 shows the convergence of the GA to different solutions and its monotonic increase. Fig. 4-41 shows small fluctuations in the performance of the PSO and its convergence to the same optimal solution in all the three trials. Fig. 4-42 represent the superior performance of PSO compared to GA in all the trials.

The values of the variables for the reference case of oil recovery optimisation along with the optimal solutions and the corresponding IRFs from each of the three trials of GA and PSO are presented in Table 4-12 and 4-13, respectively. The values of the optimised variables which differ from the reference case have been asterisked for each trial.

Table 4-12: The reference case and best operational points of three trials of GA (oil recovery optimisation)

Variable	**Reference case**	**GA Trial 1**	**GA Trial 2**	**GA Trial 3**
Q_w (F-1H) [Sm^3/day]	500	2700*	2700*	2700*
Q_g (F-1H) [Sm^3/day]	10^6	10^6	10^6	10^6
Q_w (F-3H) [Sm^3/day]	500	2700*	2700 *	2700*
Q_g (F-3H) [Sm^3/day]	10^6	10^6	10^6	968781*
BHP (E-2AH) [bar]	150	150	150	167*
BHP (E-3CH) [bar]	150	150	150	158*
BHP (E-3H) [bar]	240	240	237.5*	238*
Cycle ratio [-]	0.1	0.1	0.1	0.1
Cycle time [month]	2	4 *	8*	3*
Mole fraction of C_2 [-]	0.2	0.2	0.2	0.2
Mole fraction of C_3 [-]	0.1	0.1	0.1	0.1
Mole fraction of C_4 [-]	0.01	0.05*	0.05*	0.05*
IRF [-]	4.45%	5.08%	5.08%	5.04%

Table 4-13: The reference case and best operational points of three trials of PSO (oil recovery optimisation)

Variable	Reference case	PSO Trial 1	PSO Trial 2	PSO Trial 3
Q_w (F-1H) [Sm^3/day]	500	2700*	2700*	2700*
Q_g (F-1H) [Sm^3/day]	10^6	10^6	10^6	10^6
Q_w (F-3H) [Sm^3/day]	500	2700*	2700*	2700*
Q_g (F-3H) [Sm^3/day]	10^6	10^6	10^6	10^6
BHP (E-2AH) [bar]	150	150	150	150
BHP (E-3CH) [bar]	150	150	150	150
BHP (E-3H) [bar]	240	209*	209*	209*
Cycle ratio [-]	0.1	0.15*	0.15*	0.15*
Cycle time [month]	2	12*	12*	12*
Mole fraction of C_2 [-]	0.2	0.2	0.2	0.2
Mole fraction of C_3 [-]	0.1	0.1	0.1	0.1
Mole fraction of C_4 [-]	0.01	0.05*	0.05*	0.05*
IRF [-]	4.45%	5.17%	5.17%	5.17%

As Fig. 4-40 to 4-42 and Table 4-12 and 4-13 show, PSO has converged to the same optimal solution in all the three trials. In the optimal solution found by PSO, the values of the variables for the reference case have changed as follows. The water injection rates have increased to their maximum value, the BHP of well E-3H has decreased from 240 bar to 209 bar, the cycle ratio has changed from 0.1 to 0.15, the cycle time has shifted from 2 months to 12 months and the mole fraction of C_4 has increased to 0.05. This has resulted in about 16.2% increase in the IRF compared to the reference case. GA is not able to find the optimal set of BHPs and optimal cycle time found by PSO and reduces one of the gas injection rates to a non-optimal value in one of the trials. GA finds quite different solutions in the three trials, the best of which is about 1.7% lower

than the optimal solution of PSO. As observed in the experiments for NPV optimisation, the global best solutions of PSO fluctuate as a function of the number of iterations, however, those of GA steadily improve.

PSO finds a solution with an IRF in the vicinity of 0.01% of the optimal solution for the first time in iteration 28 of the three trials. GA never finds a solution in the specified range in any of the trials.

The curves of average IRF versus the iteration index for the three trials of GA and the three trials of PSO (150 particles in each iteration of each algorithm) are shown in Fig. 4-43 for both of the algorithms. The error bars present the standard deviations which is a measure of the closeness of the particles of an iteration to their average value. As can be seen, the average IRF for PSO increases monotonically before convergence. GA always shows a lower average value than PSO and in addition to fluctuations, GA does not show convergence in the final iterations. The standard deviation of PSO is steadily decreasing and it is lower than the standard deviation of GA for every iteration. The standard deviation of GA versus the iteration index does not show a monotonic behaviour.

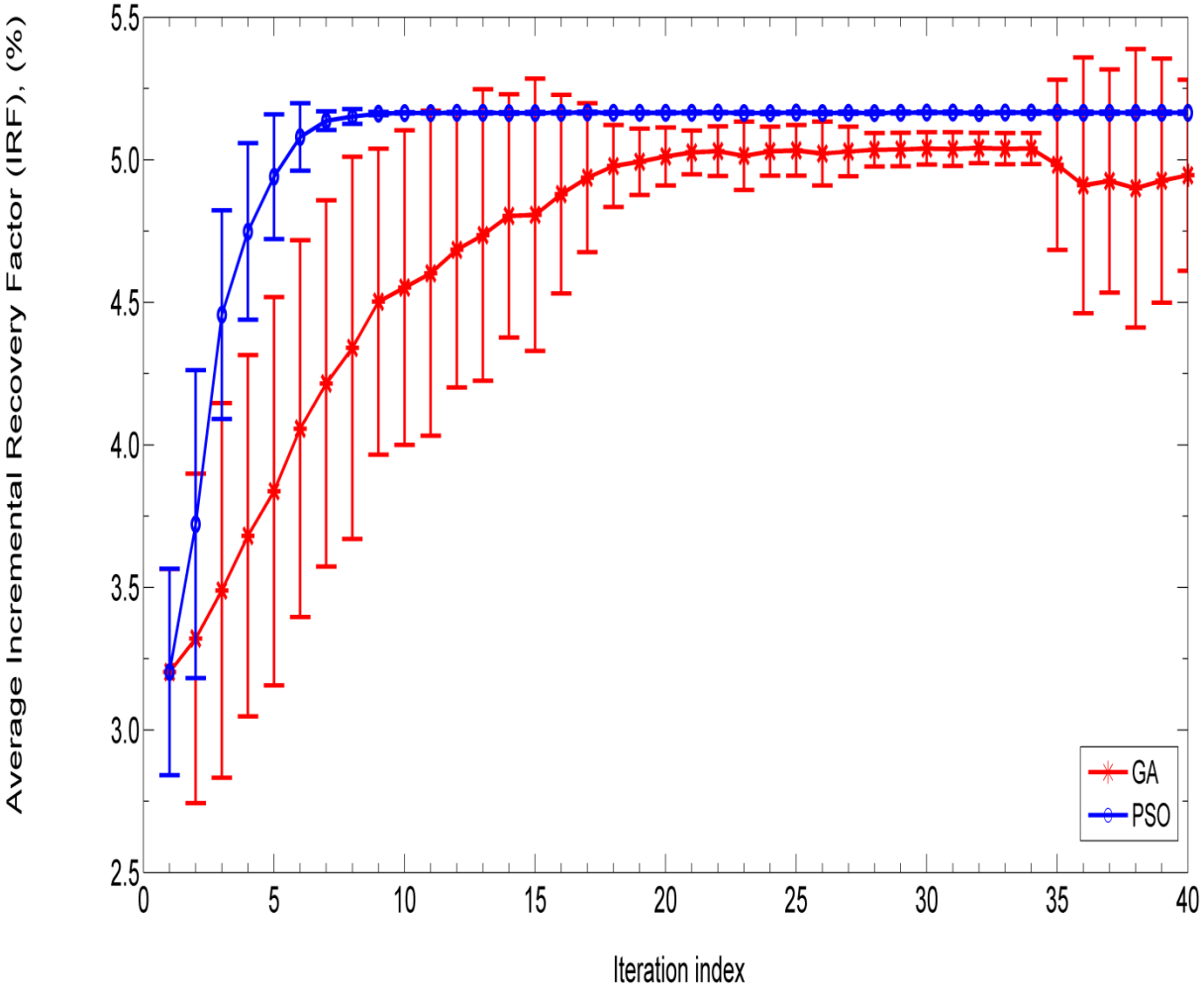

Fig. 4-43: Average performance of GA and PSO for all the three trials (oil recovery optimisation)

Residual IRF is defined in the same way as residual NPV (the relative difference between the maximum overall IRF and the maximum IRF found within the first n iterations). The following bar charts (Fig. 4-44 to Fig. 4-47) show the residual IRF for the first 10, 20, 30 and all 40 iterations for the three trials of GA and PSO.

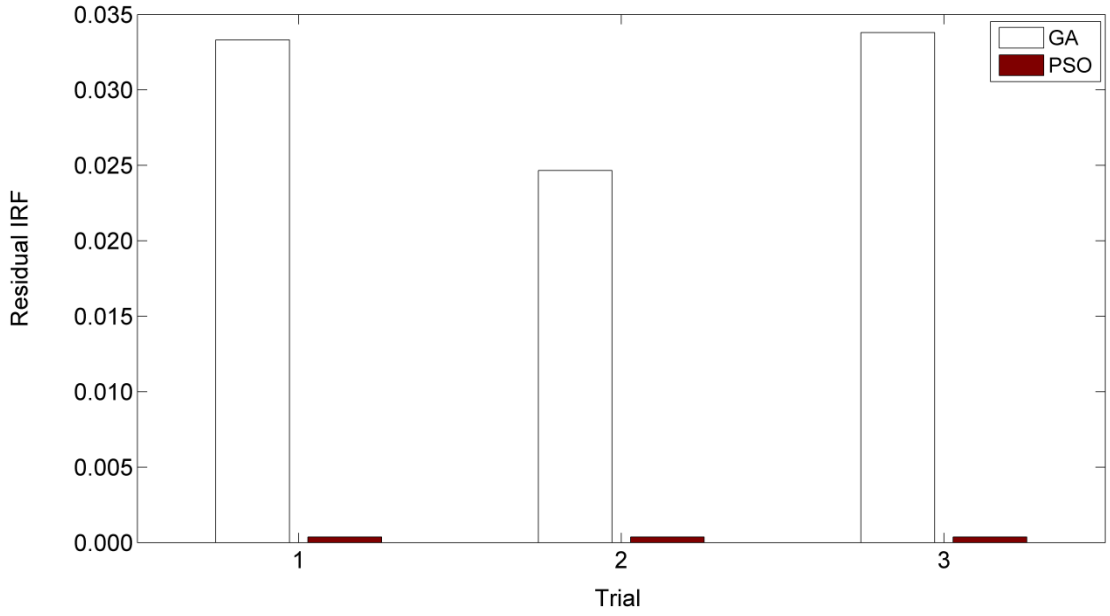

Fig. 4-44: Residual IRF comparisons per trial for iterations 1 to 10 (oil recovery optimisation)

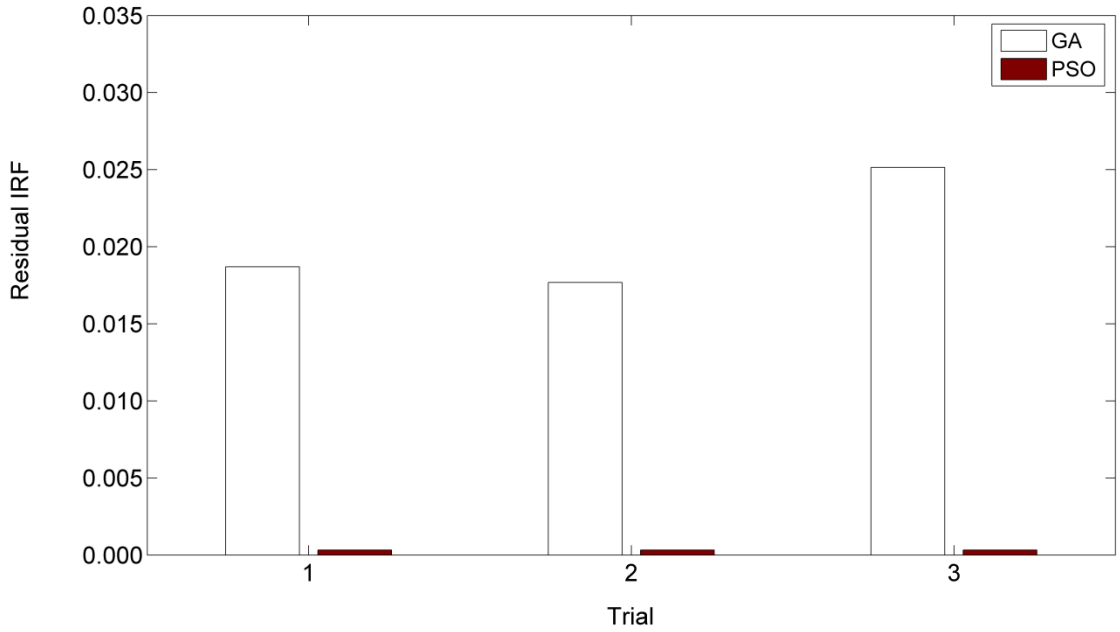

Fig. 4-45: Residual IRF comparisons per trial for iterations 1 to 20 (oil recovery optimisation)

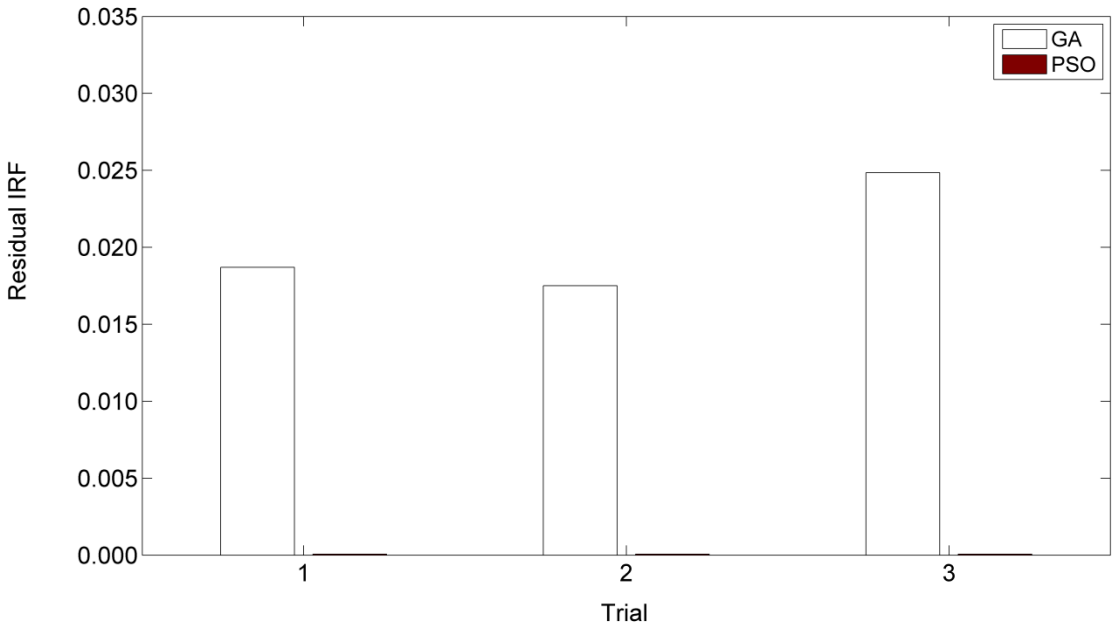

Fig. 4-46: Residual IRF comparisons per trial for iterations 1 to 30 (oil recovery optimisation)

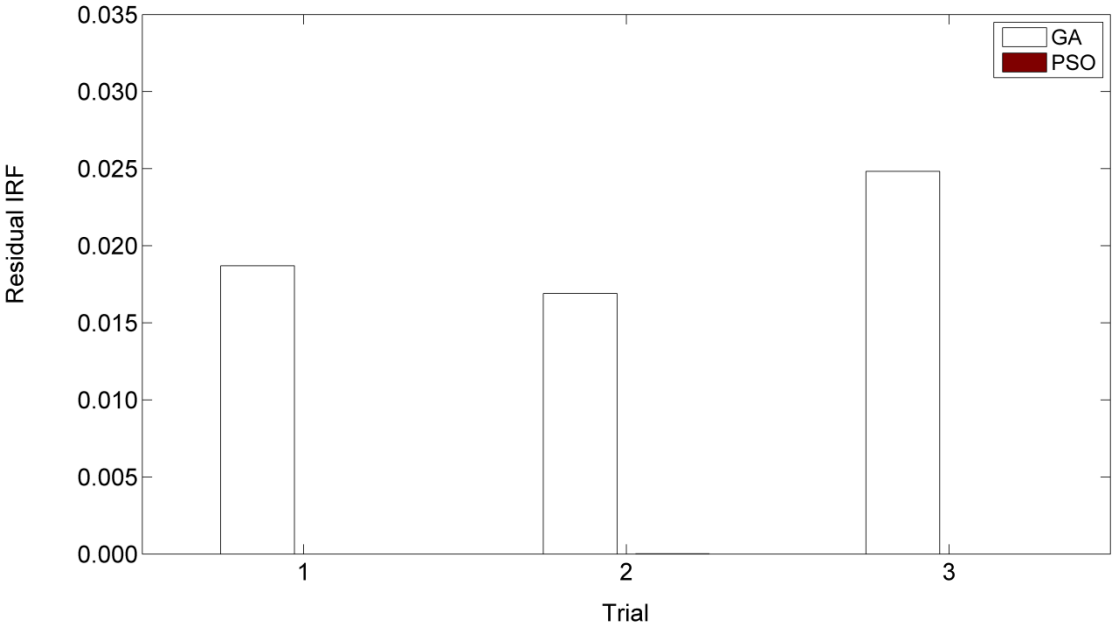

Fig. 4-47: Residual IRF comparisons per trial for iterations 1 to 40 (oil recovery optimisation)

Fig. 4-44 to 4-47 show that the best solution found by PSO is always closer to the optimal solution of the problem than the best answer found by GA regardless of the trial number and the number of iterations included. The curves of the best solutions found by the optimisation algorithms and the average performance versus the iteration index and the bar charts show the general superiority of PSO over GA for the case study of oil recovery optimisation from WAG on the E-segment of the Norne field.

4.4.3 Sensitivity Studies on Oil Recovery

In this section, a sensitivity analysis is conducted to quantify the effect of individual WAG operational parameters on IRF. To investigate the sensitivity of one parameter, all the other variables are kept fixed at their optimal values. The normalized IRF (the ratio of IRF to its maximum value or IRF/IRF_{max}) is plotted versus the normalized variables (the ratio of each variable to its optimal value) and the trend and slope of each curve shows the effect of the corresponding variable on the oil recovery.

In Fig. 4-48, the normalized water and gas injection rates are changed on the interval [0.8, 0.95] in steps of 0.05. As can be seen, at high injection rates of gas and water, the effect of gas injection rate on oil recovery is higher than that of water injection rate. In addition, the injection, whether gas or water, in well F-1H has a greater effect on oil recovery than injection in well F-3H. This indicates that the mobile oil saturation in the zone of the reservoir which is swept by well F-1H is higher than that of well F-3H.

The optimal water injection rates are the same (2700 Sm^3/day) for the experiments of NPV and IRF optimisation, however, the optimal gas injection rates are set at the lower bound (1000 Sm^3/day) for NPV optimisation and at the upper bound (1,000,000 Sm^3/day) for IRF optimisation. When there is no restriction on the injection rates from the point of view of economic benefit (in the case of IRF optimisation), a higher injection rate would probably result in more oil production.

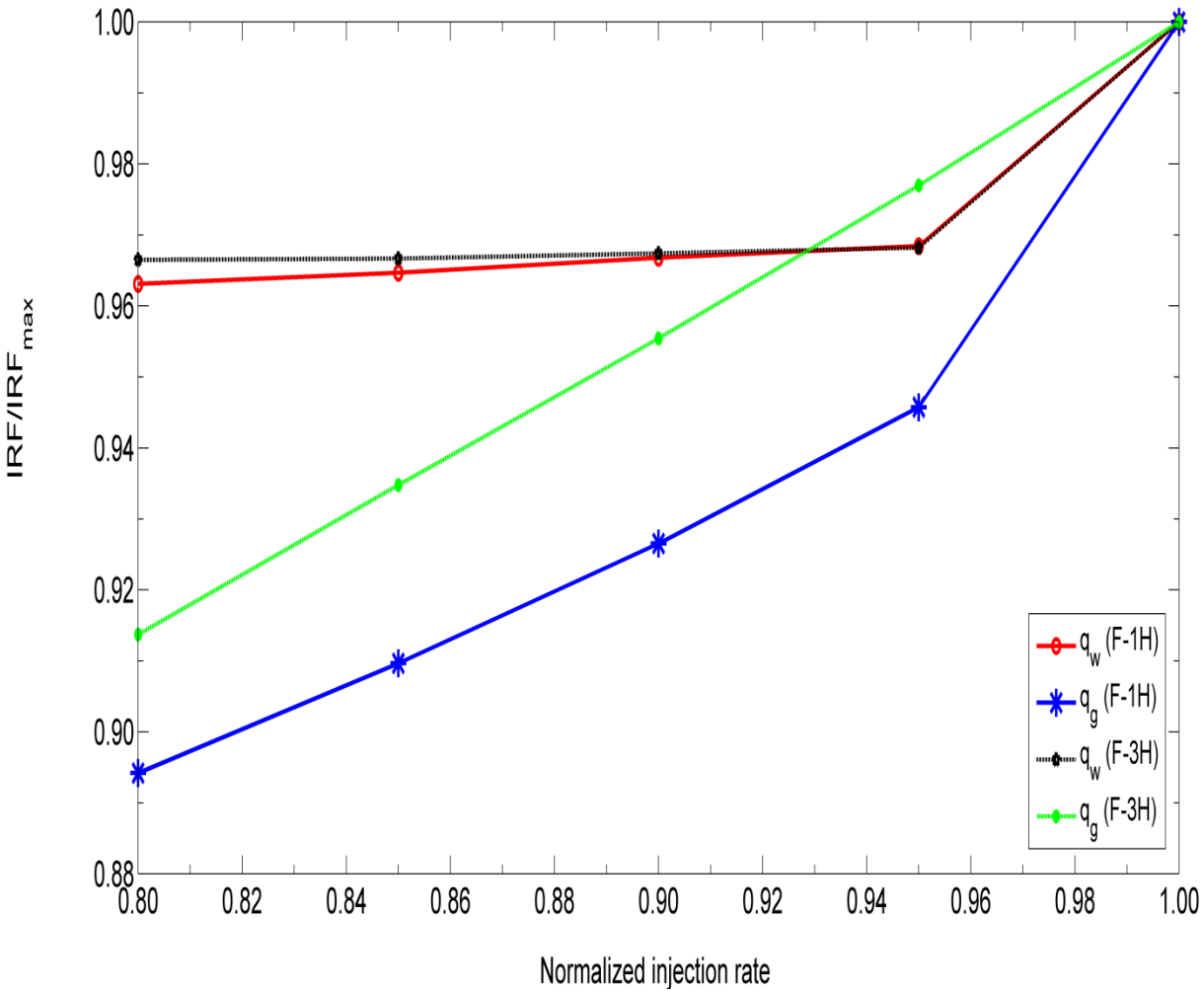

Fig. 4-48: Effect of water and gas injection rates on IRF

The effect of BHPs of the producers on oil recovery is shown in Fig. 4-49.

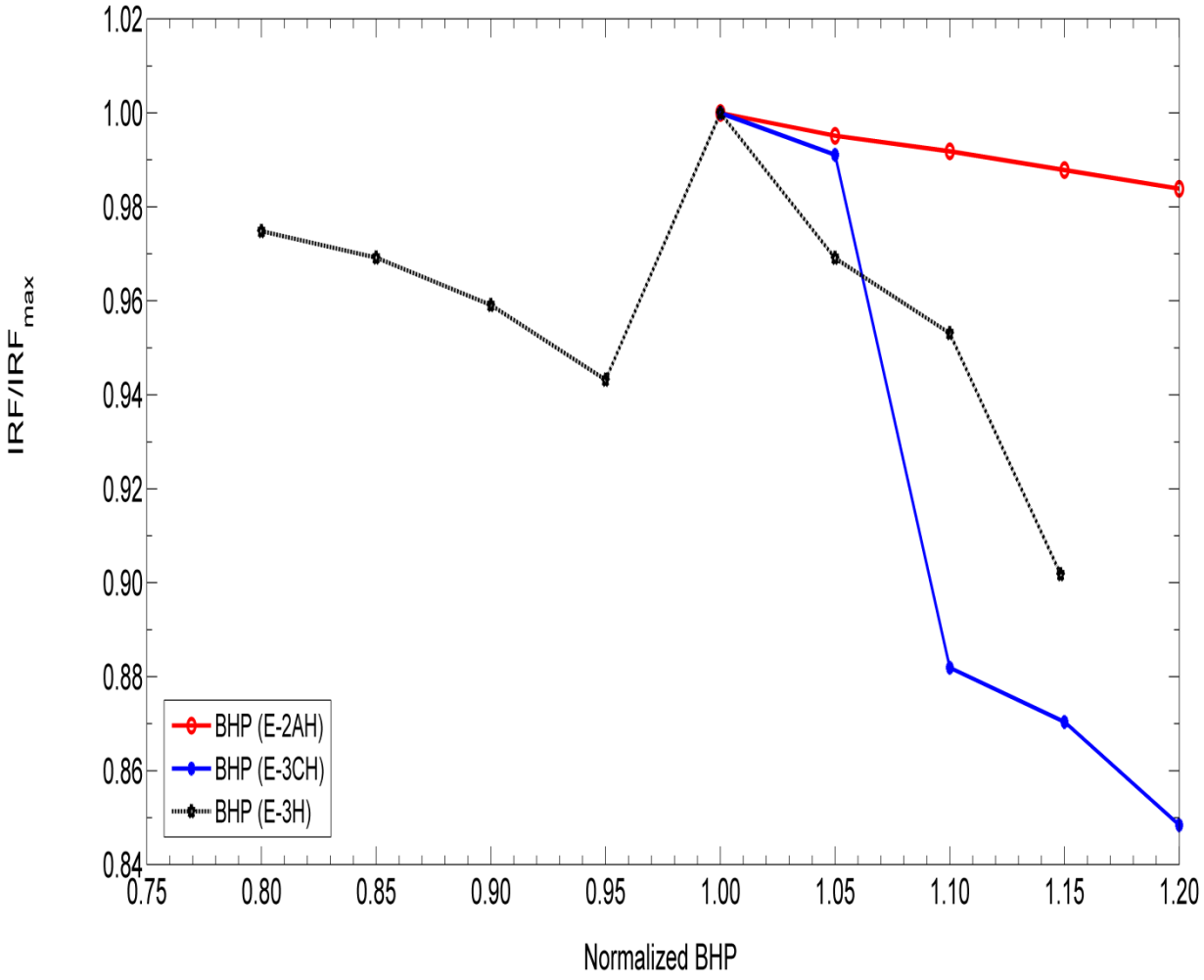

Fig. 4-49: Effect of BHP on IRF

As shown in Fig. 4-49, the optimal BHP for well E-3H is about 209 bar and the other two production wells (E-2AH and E-3CH) would produce the most oil at their lower bounds of BHP (150 bar). For the sensitivity study, the normalized BHP of well E-3H is changed on the interval [0.8, 1.15] in steps of 0.05 and the normalized BHPs of E-2AH and E-3CH are varied on the interval [1.05, 1.2] in steps of 0.05. The oil production of wells E-2AH and E-3CH reduces as their BHP increases and well E-3CH is more sensitive to changes in the BHP. Well E-3H

behaves normally below and above its optimal BHP, in the sense that by increasing the BHP the oil production decreases. As the BHP of well E-3H increases from below the optimal value, water production also decreases and this causes the water cut to reduce and some of the well connections to reopen, so the oil production increases. Although the optimal BHP of well E-3H is a little different for NPV optimisation (226.2 bar) and oil recovery optimisation (209 bar) due to the relative prices of oil and water handling, these results are compatible with the results of NPV optimisation and show the highest sensitivity of well E-3H to water production.

Fig. 4-50 shows the effect of cycle ratio on the IRF. The optimal cycle ratio for the case of oil recovery optimisation is 0.15 which means that in each cycle water is injected for 15% of the time and the rest is allocated to gas injection. It is worth recalling that cycle ratio was changed in steps of 0.05 through the search process of the optimisation. For the sensitivity analysis, this parameter was changed from 0 to 0.3 in steps of 0.05. A cycle ratio of 0 refers to gas flood.

As can be seen in Fig. 4-50, for a cycle ratio less than 0.15 (when gas is injected for more than 85% of a cycle), the oil production reduces because of excessive gas production. When water is injected for more than 15% of a cycle, the longer period of water cannot make up for the shorter period of gas injection from the point of view of oil recovery.

The optimal cycle ratio for the experiments of NPV optimisation is 0.9 which means that longer periods of water injection are more beneficial, however, an optimum of 0.15 for the case of IRF optimisation indicates the greater effect of longer periods of gas injection on the oil recovery.

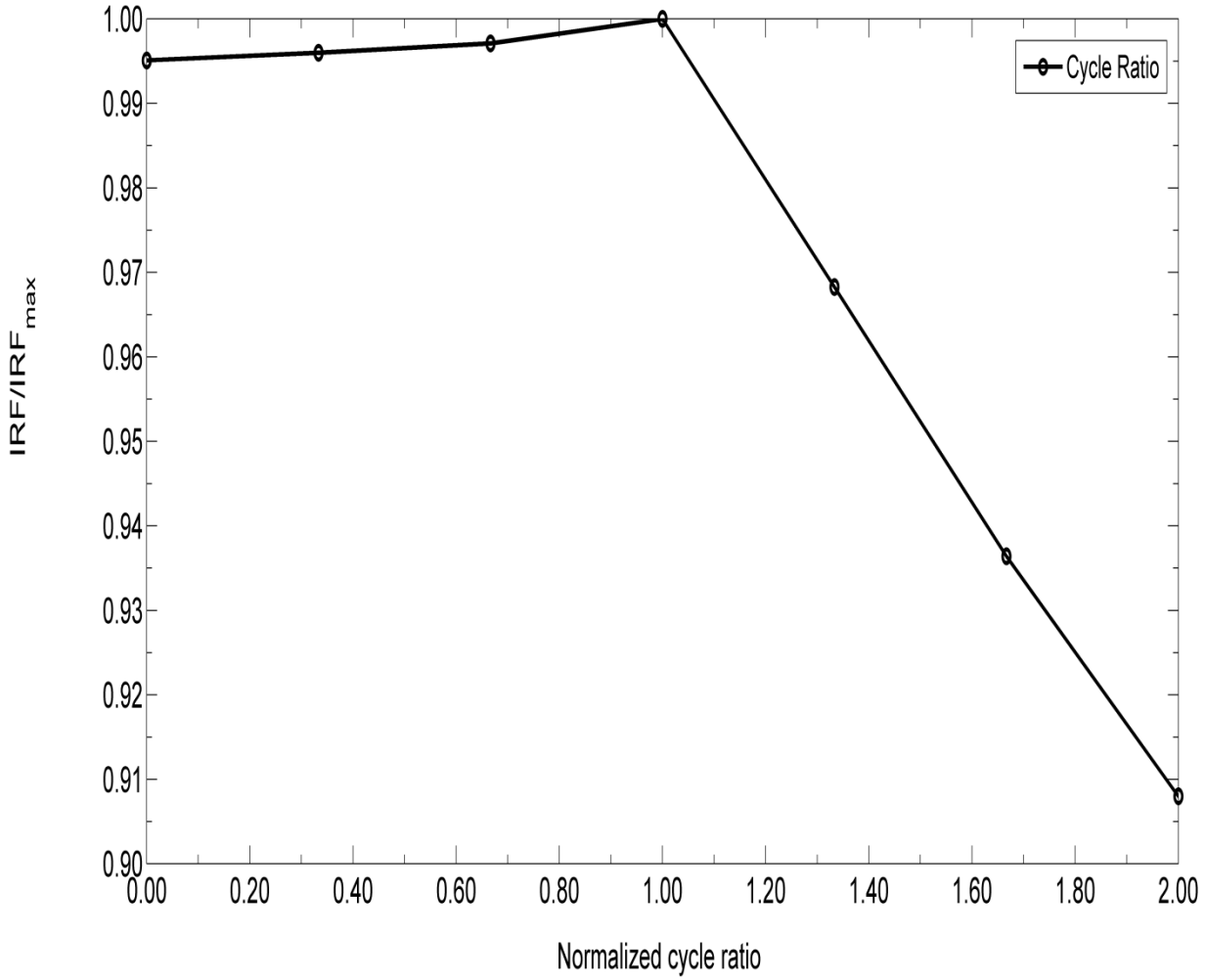

Fig. 4-50: Effect of cycle ratio on IRF

The effect of cycle time on the oil recovery is shown in Fig. 4-51. The cycle time is changed from 2 to 12 months in steps of 1 month to examine its influence on the oil recovery. 12 months yields the highest oil recovery as the optimal cycle time for a 5-year WAG process and cycle times of 10 and 8 months are ranked second and third. This means that the most efficient WAG injection scenario to produce the most oil in a 5-year period is to inject gas for 306 days and then inject water for 24 days (based on the cycle ratio of 0.15) cyclically.

The optimal cycle time for experiment 3 of NPV optimisation is 8 months. This indicates that if more oil recovery is required then less alternation between gas and water injection is necessary.

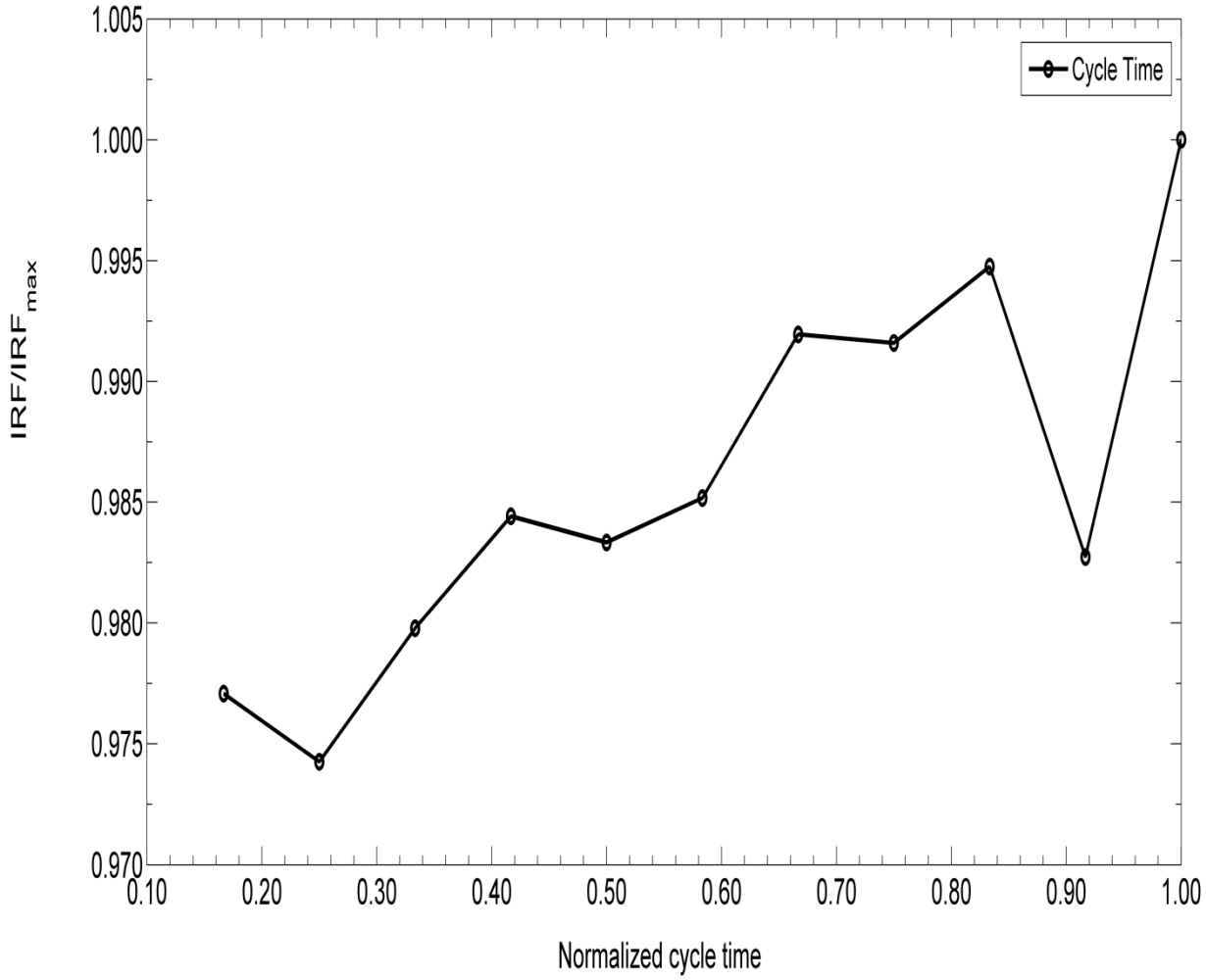

Fig. 4-51: Effect of cycle time on IRF

To investigate the effect of the amount of enriching components on the oil recovery, the mole percentages of C_2, C_3 and C_4 are reduced from 20% to 16% in steps of 1%, from 10% to 8% in steps of 0.5% and from 5% to 4% in steps of 0.25%, respectively. As already mentioned, when each of the mole percentages is altered for the sensitivity study, the rest are kept fixed at their optimal values (20% C_2, 10% C_3 and 5% C_4) and the mole percentage of methane is the free

variable with the obvious constraint of mole fractions sum to unity. Fig. 4-52 and Fig. 4-53 show the effect of the variation in the mole percentages of enriching components on the oil recovery and on the minimum miscibility pressure (MMP) of the Norne oil with the injection gas, respectively. The optimum (minimum) MMP is about 342 bar for the most enriched gas of the optimal solution (65% C_1, 20% C_2, 10% C_3 and 5% C_4). As can be seen, the presence of C_4 in the injection gas has the largest effect on MMP and therefore oil recovery, however, the composition of the injection gas is mainly dictated by the economics and source and availability of the gas.

The richest gas composition is the optimal solution of the experiments of NPV and IRF optimisation. This means that the richest injecting gas yields the most oil recovery as well as the most economic benefit.

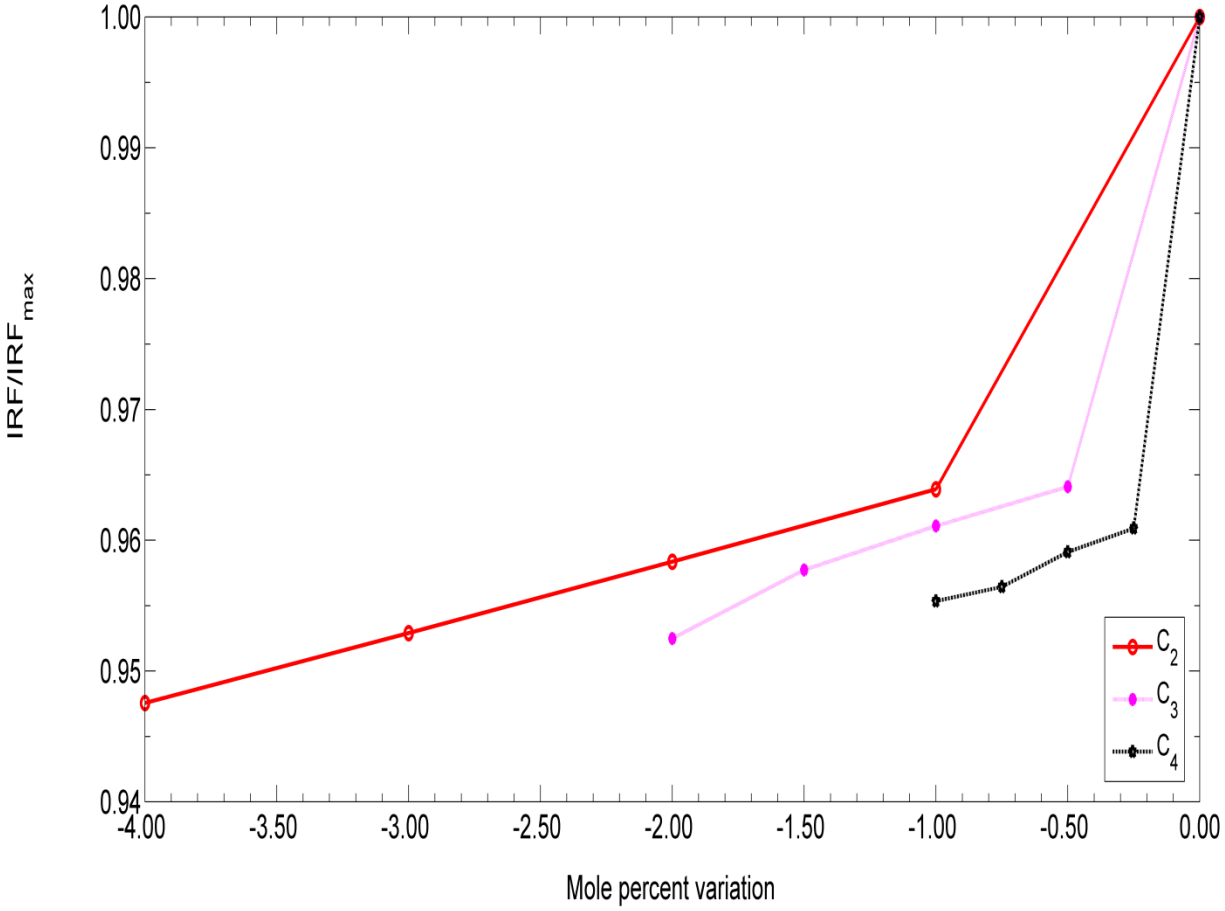

Fig. 4-52: Effect of variation of the amount of enriching components on IRF

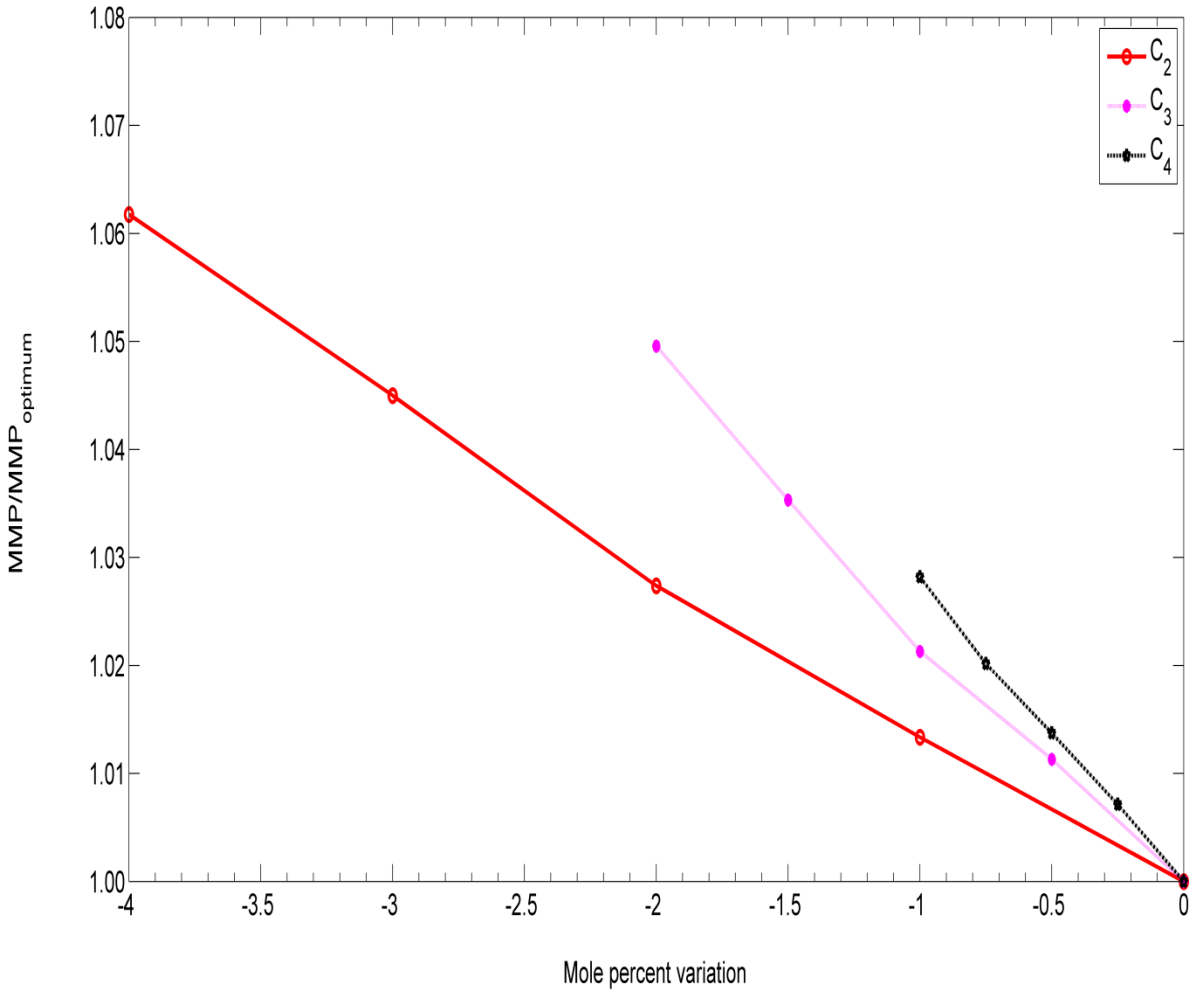

Fig. 4-53: Effect of variation of the amount of enriching components on minimum miscibility pressure

The oil recovery factors from different recovery methods are presented in Fig. 4-54 from the start of the WAG project to the end of 5-year period. The recovery methods under investigation include the optimal WAG (from the point of NPV), water flooding with minimum and maximum injection rates, gas flooding with minimum and maximum injection rates and optimal WAG (from the point of oil recovery). The oil recovery at the start of the project is about 49.15%. The ultimate recoveries from the optimised-recovery WAG, gas flooding with the maximum injection rate (1,000,000 Sm^3/day), the optimised-NPV WAG, water flooding with the maximum injection

rate (2700 Sm^3/day), water flooding with the minimum injection rate (500 Sm^3/day) and gas flooding with the minimum injection rate (1000 Sm^3/day) are 54.31%, 54.04%, 52.57%, 52.17%, 51.53% and 51.22%, respectively. The optimised-NPV WAG process is ranked third after the optimised-recovery WAG and gas flooding with the maximum injection rate. Continuous gas flooding with the minimum injection rate yields the lowest recovery.

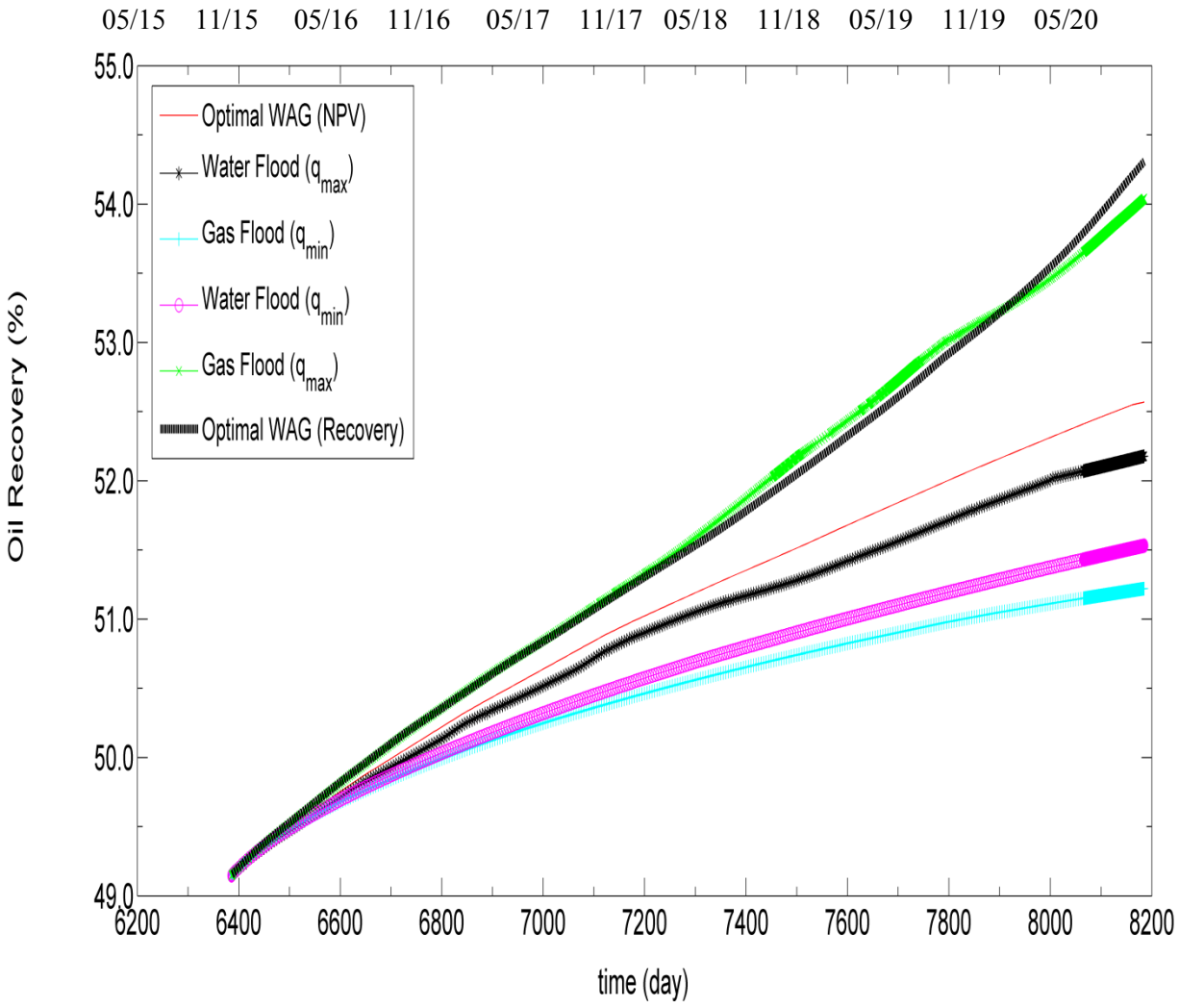

Fig. 4-54: Comparison of the oil recovery among different recovery methods

Chapter 5: Conclusions and Recommendations

5.1 Summary and Conclusions

Two evolutionary algorithms, a genetic algorithm (GA) and particle swarm optimisation (PSO) were employed to develop an optimisation methodology and determine the optimal production-injection parameters in a hydrocarbon WAG process on the Norne E-segment to achieve the highest NPV and highest oil recovery. A compositional simulator, Schlumberger Eclipse E300, was used in this study. The reservoir model was first history matched to reduce the uncertainty in the prediction of the simulations. The full set of optimisation variables consisted of water and gas injection rates, bottom hole pressures of the production wells, cycle ratio, cycle time, total WAG time and composition of the injection gas. Three experiments on the optimisation of NPV with different numbers of controlling variables (9, 12 and 13) and one experiment on the optimisation of oil recovery (with 12 variables and a fixed total WAG time) were defined. A reference case was first obtained for each experiment by means of design of experiments (DOE) and then both GA and PSO were tried four times on each of the NPV optimisation experiments and three times on the experiment of oil recovery optimisation with the same initial guesses for each experiment. A sensitivity analysis was also done to investigate the effect of controlling variables on the objective functions and also the effect of economic parameters on the NPV.

Both of the optimisation techniques were found capable of improving the values of the objective functions (NPV and oil recovery) compared to the reference case and the difference in the values of their optimal solutions was not significant, however, PSO converged to the same optimal

solution in all the trials for each experiment and the optimal solutions found by PSO, except for experiment 1 in which GA converged to the same optimal solution as PSO in only one of the trials, were better than those found by GA. GA usually converged to different solutions in different trials of the same experiment and yielded an inferior solution compared to PSO.

The NPV optimisation for experiment 1 results in optimal NPVs of GA and PSO being 8.2% higher than the NPV of the reference case. In experiment 2, the optimal NPVs of GA and PSO were 12.5% and 12.6% respectively higher than the NPV of the reference case. In the third experiment (including all the 13 variables), the optimal NPVs found by PSO and GA were 14.2% and 13.8% higher than the NPV of the reference case, respectively. The rate of convergence of the optimisation techniques depends on two factors, the problem complexity (the number of decision variables) and the initial guess. It is difficult to isolate the effect of problem complexity on the rate of convergence of optimisation techniques due to the effect of the initial guess. Nevertheless, PSO on average finds a solution in the vicinity of 0.01% of the optimal solution for the first time in iteration 7 of experiment 1, iteration 20 of experiment 2 and iteration 23 of experiment 3. GA finds such an answer only in iteration 9 of one of the trials of experiment 1. In the experiment of oil recovery optimisation, PSO and GA showed an improvement of about 16.2% and 14.2%, respectively, in the value of the incremental recovery factor compared to the reference case.

The conclusions drawn above are based on limited number of trials due to the high computational cost of the reservoir simulations. More trials are required to help us claim the accuracy and reliability of the method, however, the framework was tested successfully and

improvement in the value of the objective functions was observed for the designed WAG experiments.

For the few trials conducted in this study, PSO in general showed better performance than GA from point of overall best solution, best solution found before the termination of the algorithms and the average value of the objective functions in the same iteration of all the trials. However drawing a definite conclusion from the comparison of the performance of stochastic optimisation techniques is problem dependent; PSO would be a better option than GA as a first approach to search for the optimal operational WAG parameters on the field scale in the opinion of the author of this dissertation.

5.2 Recommendations for Future Research

The optimisation process in this study was based on a fixed well pattern. The optimisation of well placement can be further investigated for a WAG process by placing new injection or production wells, shut-in or doing new completions in the existing wells. Further improvement in the production performance is expected via the integrated optimisation of well control and well placement.

The reservoir model was history matched and then water flooded up to a specific point in time. The time to initiate WAG could be added to the optimisation variables. However WAG is usually performed as a tertiary recovery method, the time to start WAG is a matter of discussion and can be included as a parameter to investigate for WAG optimisation.

The use of proxy models or surrogates for reservoir simulator is another field of research which has been fairly well investigated in literature. The surrogates are expected to mimic the performance of the reservoir simulator and yield acceptable results after being trained and tested, however they are computationally cheaper, so a greater number of function evaluations can be included in the search process of optimisation techniques and the chance of finding better results would be improved.

History matching could be investigated more thoroughly to reduce the uncertainty of the simulation predictions. Other parameters including fault transmissibilities, flow capacity and the ratio of vertical to horizontal permeability, etc. could be added to the tuning parameters to obtain a better match. The effect of geological uncertainty can also be investigated by using multiple realizations of the reservoir.

A better compositional PVT model could be achieved by means of laboratory test data on fluid properties.

More realistic economic parameters, especially for gas and water injection costs could be assumed. This of course depends on the time of study, the field location and availability of the injection materials. Financial uncertainty could be considered in a future work.

Only four trials for each experiment of NPV optimisation and three trials for IRF optimisation were conducted in this study due to the computational limitations. This might reduce the

reliability of the optimisation results. Running more trials is recommended to help draw statistically sound conclusions.

And last but not least, other optimisation techniques, especially those of stochastic nature which do not need access to the simulator code and gradient information, can also be tested on the same problem. In this study, we selected GA and PSO off the shelf to optimise over all the variables simultaneously. Differential Evolution (DE) and Covariance Matrix Adaptation Evolution Strategy (CMA-ES), to name a few, are in the category of stochastic optimisation techniques which have been used in the optimisation of well control and placement [184, 185]. In addition, the application of deterministic optimisation approaches such as generalized pattern search (GPS) and Hooke-Jeeves directed search can be evaluated. Trying a sequential approach to optimise variables sequentially and in a decoupled manner due to the different nature of the input variables (continuous versus discrete) may also be of interest.

References

1. Lake, L.W., *Enhanced oil recovery.* 1989.
2. Archer, J.S. and C.G. Wall, *Petroleum engineering: principles and practice*. 2012: Springer Science & Business Media.
3. Speight, J.G., *Enhanced recovery methods for heavy oil and tar sands*. 2013: Elsevier.
4. Kulkarni, M.M. and D.N. Rao, *Experimental investigation of miscible and immiscible Water-Alternating-Gas (WAG) process performance.* Journal of Petroleum Science and Engineering, 2005. **48**(1): p. 1-20.
5. Yadav, G., F. Dullien, I. Chatzis, and I. Macdonald, *Microscopic distribution of wetting and nonwetting phases in sandstones during immiscible displacements.* SPE Reservoir Engineering, 1987. **2**(02): p. 137-147.
6. Christensen, J.R., E.H. Stenby, and A. Skauge, *Review of WAG field experience.* SPE Reservoir Evaluation & Engineering, 2001. **4**(02): p. 97-106.
7. Righi, E.F., J. Royo, P. Gentil, R. Castelo, A. Del Monte, and S. Bosco. *Experimental study of tertiary immiscible WAG injection*. *SPE/DOE Symposium on Improved Oil Recovery*. 2004. Society of Petroleum Engineers.
8. Tzimas, E., A. Georgakaki, C. Garcia-Cortes, and S. Peteves, *Enhanced oil recovery using carbon dioxide in the European energy system*. 2005: Publications Office.
9. Rao, S., *Engineering optimisation: theory and practice*. 2009: John Wiley & Sons.
10. Statoil, *PL128 Norne Field Reservoir Management Plan.*
11. Center–NTNU, I., *Norne Field (E-segment) Case Description.* 2008.
12. Nangacovié, H.L.M., *Application of WAG and SWAG injection Techniques in Norne E-Segment.* 2012.
13. OJG editors. 2013; Available from: http://www.ogj.com/articles/2013/09/statoil-makes-oil-discovery-near-norne-field-in-norwegian-sea.html.
14. Stalkup Jr, F.I., *Status of miscible displacement.* Journal of Petroleum Technology, 1983. **35**(04): p. 815-826.
15. Benham, A., W. Dowden, and W. Kunzman, *Miscible Fluid Displacement-Prediction of Miscibility.* Trans., AIME, 1960. **219**: p. 229-37.
16. Dong, M., J. Foraie, S. Huang, and I. Chatzis, *Analysis of immiscible water-alternating-gas (WAG) injection using micromodel tests.* Journal of Canadian Petroleum Technology, 2005. **44**(2): p. 17-25.
17. Green, D.W. and G.P. Willhite, *Enhanced Oil Recovery, Henry L. Doherty Memorial Fund of AIME.* Society of Petroleum Engineers: Richardson, TX, 1998.
18. Al-Wahaibi, Y.M., *First-Contact-Miscible and Multicontact-Miscible Gas Injection within a Channeling Heterogeneity System.* Energy & Fuels, 2010. **24**(3): p. 1813-1821.
19. Stalkup, F. *Displacement behavior of the condensing/vaporizing gas drive process*. *SPE Annual Technical Conference and Exhibition*. 1987.
20. Johns, R., B. Dindoruk, and F. Orr Jr, *Analytical theory of combined condensing/vaporizing gas drives.* SPE Advanced Technology Series, 1993. **1**(02): p. 7-16.

21. Shokrollahi, A., M. Arabloo, F. Gharagheizi, and A.H. Mohammadi, *Intelligent model for prediction of CO_2 – Reservoir oil minimum miscibility pressure.* Fuel, 2013. **112**(0): p. 375-384.
22. Zolghadr, A., M. Riazi, M. Escrochi, and S. Ayatollahi, *Investigating the Effects of Temperature, Pressure, and Paraffin Groups on the N_2 Miscibility in Hydrocarbon Liquids using Interfacial Tension Measurement Method.* Industrial & Engineering Chemistry Research, 2013. **52**: p. 9851-9857.
23. Ayirala, S. and D. Rao. *Comparative evaluation of a new MMP determination technique*. *SPE/DOE Symposium on Improved Oil Recovery*. 2006.
24. Danesh, A., *PVT and phase behaviour of petroleum reservoir fluids*. Vol. 47. 1998: Elsevier.
25. Christiansen, R.L. and H.K. Haines, *Rapid measurement of minimum miscibility pressure with the rising-bubble apparatus.* SPE Reservoir Engineering, 1987. **2**(04): p. 523-527.
26. Rao, D.N., *A new technique of vanishing interfacial tension for miscibility determination.* Fluid phase equilibria, 1997. **139**(1): p. 311-324.
27. Elsharkawy, A.M., F.H. Poettmann, and R.L. Christiansen, *Measuring CO_2 minimum miscibility pressures: Slim-tube or rising-bubble method?* Energy & fuels, 1996. **10**(2): p. 443-449.
28. Rao, D. and J. Lee. *Miscibility Evaluation for Terra Nova Offshore Field*. in *Canadian International Petroleum Conference*. 2000. Petroleum Society of Canada.
29. Quijada, M.G., *Optimisation of A CO_2 Flood Design Wasson Field-West Texas*, 2005, Texas A&M University.
30. Ma, J., *Design of an Effective Water-alternating-gas (WAG) Injection Process Using Artificial Expert Systems*, 2010, The Pennsylvania State University.
31. Chen, S., H. Li, D. Yang, and P. Tontiwachwuthikul, *Optimal Parametric Design for Water-Alternating-Gas (WAG) Process in a CO_2-Miscible Flooding Reservoir.*
32. Rogers, J.D. and R.B. Grigg, *A literature analysis of the WAG injectivity abnormalities in the CO_2 process.* SPE Reservoir Evaluation & Engineering, 2001. **4**(05): p. 375-386.
33. Mollaei, A. and M. Delshad, *A Novel Forecasting Tool for Water Alternating Gas (WAG) Floods*, Society of Petroleum Engineers.
34. Song, Z., Z. Li, M. Wei, F. Lai, and B. Bai, *Sensitivity analysis of water-alternating-CO_2 flooding for enhanced oil recovery in high water cut oil reservoirs.* Computers & Fluids, 2014. **99**: p. 93-103.
35. Sanchez, N.L. *Management of water alternating gas (WAG) injection projects*. *Latin American and Caribbean Petroleum Engineering Conference*. 1999. Society of Petroleum Engineers.
36. Touray, S., M. Subject, and N.S. Halifax, *EFFECT OF WATER ALTERNATING GAS INJECTION ON ULTIMATE OIL RECOVERY*. 2013.
37. Donaldson, E.C., G.V. Chilingarian, and T.F. Yen, *Enhanced oil recovery, II: Processes and operations*. Vol. 2. 1989: Access Online via Elsevier.
38. Kulkarni, M. and D. Rao. *Experimental investigation of various methods of tertiary gas injection*. *SPE Annual Technical Conference and Exhibition*. 2004. Society of Petroleum Engineers.
39. Bunge, A. and C. Radke, *CO_2 flooding strategy in a communicating layered reservoir.* Journal of Petroleum Technology, 1982. **34**(12): p. 2,746-2,756.

40. Jafari, M., *LABORATORY STUDY FOR WATER, GAS AND WAG INJECTION IN LAB SCALE AND CORE CONDITION.* Petroleum & Coal, 2014. **56**(2): p. 175-181.
41. Tiab, D. and E.C. Donaldson, *Petrophysics: theory and practice of measuring reservoir rock and fluid transport properties*. 2011: Gulf professional publishing.
42. Al-Anazi, A. and I. Gates, *A support vector machine algorithm to classify lithofacies and model permeability in heterogeneous reservoirs.* Engineering Geology, 2010. **114**(3): p. 267-277.
43. Ahmed, T., *Reservoir engineering handbook*. 2006: Gulf Professional Publishing.
44. Donaldson, E.C. and W. Alam, *Wettability*. 2013: Elsevier.
45. Amyx, J.W., D.M. Bass, and R.L. Whiting, *Petroleum reservoir engineering: physical properties*. Vol. 1. 1960: McGraw-Hill College.
46. Vizika, O. and J. Lombard, *Wettability and spreading: two key parameters in oil recovery with three-phase gravity drainage.* SPE Reservoir Engineering, 1996. **11**(01): p. 54-60.
47. Jackson, D., G. Andrews, and E. Claridge. *Optimum WAG ratio vs. Rock wettability in CO_2 flooding*. *SPE Annual Technical Conference and Exhibition*. 1985. Society of Petroleum Engineers.
48. Kulkarni, M.M., *Immiscible and miscible gas-oil displacements in porous media*, 2003, Citeseer.
49. Hemmati-Sarapardeh, A., M. Khishvand, A. Naseri, and A.H. Mohammadi, *Toward reservoir oil viscosity correlation.* Chemical Engineering Science, 2013. **90**: p. 53-68.
50. Hemmati-Sarapardeh, A., S.-M.-J. Majidi, B. Mahmoudi, S.A. Ahmad Ramazani, and A. Mohammadi, *Experimental measurement and modeling of saturated reservoir oil viscosity.* Korean Journal of Chemical Engineering, 2014. **31**(7): p. 1253-1264.
51. Hemmati-Sarapardeh, A., A. Shokrollahi, A. Tatar, F. Gharagheizi, A.H. Mohammadi, and A. Naseri, *Reservoir Oil Viscosity Determination Using a Rigorous Approach.* Fuel, 2014. **116**(1): p. 39-48.
52. Jarrell, P.M., *Practical aspects of CO_2 flooding*. 2002: Richardson, Tex.: Henry L. Doherty Memorial Fund of AIME, Society of Petroleum Engineers.
53. Awan, A.R., R. Teigland, and J. Kleppe, *A survey of North Sea enhanced-oil-recovery projects initiated during the years 1975 to 2005.* SPE Reservoir Evaluation & Engineering, 2008. **11**(03): p. 497-512.
54. Chen, S., H. Li, D. Yang, and P. Tontiwachwuthikul, *Optimal parametric design for water-alternating-gas (WAG) process in a CO_2-miscible flooding reservoir.* Journal of Canadian Petroleum Technology, 2010. **49**(10): p. 75-82.
55. Jethwa, D., B. Rothkopf, and C. Paulson. *Successful Miscible Gas Injection in a Mature UK North Sea Field*. *SPE Annual Technical Conference and Exhibition*. 2000. Society of Petroleum Engineers.
56. Chaussumier, D. and S. Sakthikumar. *Alwyn North IOR Gas Injection Potential-A Case Study*. *Middle East Oil Show and Conference*. 1997. Society of Petroleum Engineers.
57. Gharbi, R.B. *Integrated Reservoir Simulation Studies to Optimise Recovery from a Carbonate Reservoir*. *SPE Asia Pacific Oil and Gas Conference and Exhibition*. 2003. Society of Petroleum Engineers.
58. Al Shalabi, E.W., *Modeling the effect of injecting low salinity water on oil recovery from carbonate reservoirs*. 2014.
59. Caudle, B. and A. Dyes, *Improving miscible displacement by gas-water injection.* 1958.

60. Lien, S., S. Lie, H. Fjellbirkeland, and S. Larsen. *Brage Field, lessons learned after 5 years of production*. *European Petroleum Conference*. 1998. Society of Petroleum Engineers.
61. Baojun, F., D. Xingjia, and Y. Cai, *Pilot Test of Water Alternating Gas Injection in Heterogeneous Thick Reservoir of Positive Rhythm Sedimentation of Daqing Oil Field.* SPE Advanced Technology Series, 1997. **5**(01): p. 41-48.
62. Slotte, P., H. Stenmark, and T. Aurdal, *Snorre WAG pilot.* RUTH Program Summary, 1992. **1995**.
63. Crogh, N.A., K. Eide, and S.E. Morterud. *WAG injection at the Statfjord Field, a success story*. *European Petroleum Conference*. 2002. Society of Petroleum Engineers.
64. Dalen, V., R. Instefjord, and R. Kristensen, *A WAG injection pilot in the Lower Brent Formation at the Gullfaks Field.* Geological Society, London, Special Publications, 1995. **84**(1): p. 143-152.
65. Instefjord, R. and A.C. Todnem. *10 years of WAG injection in Lower Brent at the Gullfaks Field*. *European Petroleum Conference*. 2002. Society of Petroleum Engineers.
66. Stenmark, H. and P. Andfossen. *Snorre WAG Pilot-A Case Study*. *8th European Symposium on Improved Oil Recovery*. 1995.
67. Skauge, A. and E. Berg. *Immiscible WAG injection in the Fensfjord formation of the Brage Oil field*. *9th European Symposium on Improved Oil Recovery*. 1997.
68. Wu, X., D. Ogbe, T. Zhu, and S. Khataniar. *Critical Design Factors and Evaluation of Recovery Performance of Miscible Displacement and WAG Process*. *Canadian International Petroleum Conference*. 2004. Petroleum Society of Canada.
69. Taber, J.J., F. Martin, and R. Seright, *EOR screening criteria revisited-Part 1: Introduction to screening criteria and enhanced recovery field projects.* SPE Reservoir Engineering, 1997. **12**(03): p. 189-198.
70. Taber, J., F. Martin, and R. Seright, *EOR screening criteria revisited—Part 2: Applications and impact of oil prices.* SPE Reservoir Engineering, 1997. **12**(03): p. 199-206.
71. Diaz, D., Z. Bassiouni, W. Kimbrell, and J. Wolcott. *Screening criteria for application of carbon dioxide miscible displacement in waterflooded reservoirs containing light oil*. *SPE/DOE Improved Oil Recovery Symposium*. 1996. Society of Petroleum Engineers.
72. Manrique, E., G. Calderon, L. Mayo, and M. Stirpe. *Water-alternating-gas flooding in Venezuela: Selection of candidates based on screening criteria of international field experiences*. *European Petroleum Conference*. 1998. Society of Petroleum Engineers.
73. Atabay, S., O.M. Dronen, F. Hvidsten, J. Magne, and A.R. Fawke. *Developing a Toolbox for Evaluating of Water Injection Performance on the Norne Field*. *SPE Europec/EAGE Annual Conference*. 2012. Society of Petroleum Engineers.
74. Greenwalt, W.A., S. Vela, L. Christian, and J. Shirer, *A field test of nitrogen WAG injectivity.* Journal of Petroleum Technology, 1982. **34**(02): p. 266-272.
75. Browrhe, M. and L. Sugg, *East Vacuum Grayburg-San Andres Unit C02 Injection Project: Development and Results to Date.* 1987.
76. Kleinstelber, S.W., *The Wertz Tensleep CO_2 Flood: Design and Initial Performance.* Journal of Petroleum Technology, 1990. **42**(05): p. 630-636.
77. Omoregie, Z. and G. Jackson, *Early performance of a large hydrocarbon miscible flood at the Mitsue field, Alberta.* paper SPE, 1987. **16718**: p. 27-30.

78. Kord, S. and S. Ayatollahi, *Asphaltene precipitation in live crude oil during natural depletion: Experimental investigation and modeling.* Fluid Phase Equilibria, 2012. **336**(0): p. 63-70.
79. Hemmati-Sarapardeh, A., R. Alipour-Yeganeh-Marand, A. Naseri, A. Safiabadi, F. Gharagheizi, P. Ilani-Kashkouli, and A.H. Mohammadi, *Asphaltene precipitation due to natural depletion of reservoir: Determination using a SARA fraction based intelligent model.* Fluid Phase Equilibria, 2013. **354**(0): p. 177-184.
80. Kamari, A., A. Safiri, and A.H. Mohammadi, *A Compositional Model for Estimating Asphaltene Precipitation Conditions in Live Reservoir Oil Systems.* Journal of Dispersion Science and Technology, 2014(just-accepted): p. 301-309.
81. Hermansen, H., L. Thomas, J. Sylte, and B. Aasboe. *Twenty five years of Ekofisk reservoir management*. *SPE Annual Technical Conference and Exhibition*. 1997. Society of Petroleum Engineers.
82. Tanner, C., P. Baxley, and W. Miller, *Production performance of the Wasson Denver Unit CO_2 flood.* 1992.
83. Peaceman, D.W., *Fundamentals of numerical reservoir simulation*. Vol. 6. 2000: Elsevier.
84. Satter, A. and G.C. Thakur, *Integrated petroleum reservoir management: a team approach*. 1994: PennWell Books.
85. Wang, P., *Development and applications of production optimisation techniques for petroleum fields*, 2003, Stanford University.
86. Khor, C.S. and A. Elkamel, *Production systems optimisation methods for petroleum fields.* 2008.
87. Carroll, J. and R.N. Horne, *Multivariate optimisation of production systems.* JPT Journal of petroleum technology, 1992. **44**(7): p. 782-789.
88. Dantzig, G.B., *Linear programming and extensions*. 1998: Princeton university press.
89. Klee, V. and G.J. Minty, *How good is the simplex algorithm*, 1970, DTIC Document.
90. Karmarkar, N. *A new polynomial-time algorithm for linear programming*. *Proceedings of the sixteenth annual ACM symposium on Theory of computing*. 1984. ACM.
91. Gomory, R.E., *Outline of an algorithm for integer solutions to linear programs.* Bulletin of the American Mathematical Society, 1958. **64**(5): p. 275-278.
92. Land, A.H. and A.G. Doig, *An automatic method for solving discrete programming problems*, *50 Years of Integer Programming 1958-2008*. 2010, Springer. p. 105-132.
93. Rao, S.S. and S. Rao, *Engineering optimisation: theory and practice*. 2009: John Wiley & Sons.
94. Fujii, H. and R. Horne, *Multivariate optimisation of networked production systems.* SPE Production & Facilities, 1995. **10**(03): p. 165-171.
95. Ciaurri, D.E., T. Mukerji, and L.J. Durlofsky, *Derivative-free optimisation for oil field operations*, *Computational Optimisation and Applications in Engineering and Industry*. 2011, Springer. p. 19-55.
96. Humphries, T.D., R.D. Haynes, and L.A. James, *Simultaneous and sequential approaches to joint optimisation of well placement and control.* Computational Geosciences, 2013: p. 1-16.
97. Mofarrah, M. and A. NahanMoghadam, *Application of Artificial Intelligence in EOR.* World Academy of Science, Engineering and Technology, 2014. **1**: p. 193.

98. Holland, J.H., *Adaptation in natural and artificial systems: An introductory analysis with applications to biology, control, and artificial intelligence*. 1975: U Michigan Press.
99. Michalewicz, Z., *Genetic algorithms+ data structures= evolution programs*. 1996: springer.
100. Chen, G., K. Fu, Z. Liang, T. Sema, C. Li, P. Tontiwachwuthikul, and R. Idem, *The genetic algorithm based back propagation neural network for MMP prediction in CO_2-EOR process.* Fuel, 2014. **126**(0): p. 202-212.
101. Tabassum, M. and K. Mathew, *A genetic algorithm analysis towards optimisation solutions.* International Journal of Digital Information and Wireless Communications (IJDIWC), 2014. **4**(1): p. 124-142.
102. Liao, Y.-H. and C.-T. Sun, *An educational genetic algorithms learning tool.* IEEE Trans. Education, 2001. **44**(2): p. 20.
103. Bush, M. and J. Carter, *Application of a modified genetic algorithm to parameter estimation in the petroleum industry.* Intelligent Engineering Systems through Artificial Neural Networks, 1996. **6**: p. 397-402.
104. Soleng, H.H. *Oil reservoir production forecasting with uncertainty estimation using genetic algorithms*. *Evolutionary Computation, 1999. CEC 99. Proceedings of the 1999 Congress on*. 1999. IEEE.
105. Romero, C., J. Carter, A. Gringarten, and R. Zimmerman. *A modified genetic algorithm for reservoir characterisation*. *International Oil and Gas Conference and Exhibition in China*. 2000. Society of Petroleum Engineers.
106. Rahman, M., M. Rahman, and S. Rahman, *An integrated model for multiobjective design optimisation of hydraulic fracturing.* Journal of Petroleum Science and Engineering, 2001. **31**(1): p. 41-62.
107. Túpac, Y.J., M.M.B. Vellasco, and M.A.C. Pacheco, *Selection of alternatives for oil field development by genetic algorithms.* Revista de Engenharia Térmica, 2002. **1**(2).
108. Yu, T., D. Wilkinson, and D. Xie, *A hybrid GP-fuzzy approach for resevoir characterization*, *Genetic Programming Theory and Practice*. 2003, Springer. p. 271-289.
109. Emera, M.K. and H.K. Sarma, *Use of genetic algorithm to estimate CO_2-oil minimum miscibility pressure—a key parameter in design of CO_2 miscible flood.* Journal of petroleum science and engineering, 2005. **46**(1): p. 37-52.
110. Saemi, M., M. Ahmadi, and A.Y. Varjani, *Design of neural networks using genetic algorithm for the permeability estimation of the reservoir.* Journal of Petroleum Science and Engineering, 2007. **59**(1): p. 97-105.
111. Dehghani, S., M.V. Sefti, A. Ameri, and N.S. Kaveh, *Minimum miscibility pressure prediction based on a hybrid neural genetic algorithm.* Chemical Engineering Research and Design, 2008. **86**(2): p. 173-185.
112. AlQuraishi, A.A., *Determination of crude oil saturation pressure using linear genetic programming.* Energy & Fuels, 2009. **23**(2): p. 884-887.
113. Salmachi, A., M. Sayyafzadeh, and M. Haghighi, *Infill well placement optimisation in coal bed methane reservoirs using genetic algorithm.* Fuel, 2013. **111**: p. 248-258.
114. Ahmadi, M.A., S. Zendehboudi, A. Bahadori, L. James, A. Lohi, A. Elkamel, and I. Chatzis, *Recovery Rate of Vapor Extraction in Heavy Oil Reservoirs Experimental, Statistical, and Modeling Studies.* Industrial & Engineering Chemistry Research, 2014. **53**(41): p. 16091-16106.

115. Xu, S., M. Zhang, F. Zeng, and C. Chan, *Application of Genetic Algorithm (GA) in History Matching of the Vapour Extraction (VAPEX) Heavy Oil Recovery Process.* Natural Resources Research, 2015. **24**(2): p. 221-237.
116. Eberhart, R.C. and J. Kennedy. *A new optimiser using particle swarm theory*. *Proceedings of the sixth international symposium on micro machine and human science*. 1995. New York, NY.
117. Sayyad, H., A.K. Manshad, and H. Rostami, *Application of hybrid neural particle swarm optimisation algorithm for prediction of MMP.* Fuel, 2014. **116**: p. 625-633.
118. Shi, Y. and R. Eberhart. *A modified particle swarm optimiser*. *Evolutionary Computation Proceedings, 1998. IEEE World Congress on Computational Intelligence., The 1998 IEEE International Conference on*. 1998. IEEE.
119. El-Hawary, M.E., *Electrical power systems: design and analysis*. Vol. 2. 1995: John Wiley & Sons.
120. Ahmadi, M.A. and S.R. Shadizadeh, *New approach for prediction of asphaltene precipitation due to natural depletion by using evolutionary algorithm concept.* Fuel, 2012. **102**: p. 716-723.
121. Millonas, M.M. *Swarms, phase transitions, and collective intelligence*. *SANTA FE INSTITUTE STUDIES IN THE SCIENCES OF COMPLEXITY-PROCEEDINGS VOLUME-*. 1994. ADDISON-WESLEY PUBLISHING CO.
122. Wang, X., W. Wan, X. Zhang, and X. Yu, *Annealed particle filter based on particle swarm optimisation for articulated three-dimensional human motion tracking.* Optical Engineering, 2010. **49**(1): p. 017204-017204-11.
123. Aote, S.S., M. Raghuwanshi, and L. Malik, *A brief review on particle swarm optimisation: limitations & future directions.* International Journal of Computer Science Engineering (IJCSE), 2013.
124. Onwunalu, J.E. and L.J. Durlofsky, *Application of a particle swarm optimisation algorithm for determining optimum well location and type.* Computational Geosciences, 2010. **14**(1): p. 183-198.
125. Assareh, E., M. Behrang, M. Assari, and A. Ghanbarzadeh, *Application of PSO (particle swarm optimisation) and GA (genetic algorithm) techniques on demand estimation of oil in Iran.* Energy, 2010. **35**(12): p. 5223-5229.
126. Zendehboudi, S., M.A. Ahmadi, L. James, and I. Chatzis, *Prediction of condensate-to-gas ratio for retrograde gas condensate reservoirs using artificial neural network with particle swarm optimisation.* Energy & Fuels, 2012. **26**(6): p. 3432-3447.
127. Wang, X. and X. Qiu, *Application of particle swarm optimisation for enhanced cyclic steam stimulation in a offshore heavy oil reservoir.* arXiv preprint arXiv:1306.4092, 2013.
128. Zendehboudi, S., A.R. Rajabzadeh, A. Bahadori, I. Chatzis, M.B. Dusseault, A. Elkamel, A. Lohi, and M. Fowler, *Connectionist Model to Estimate Performance of Steam-Assisted Gravity Drainage in Fractured and Unfractured Petroleum Reservoirs: Enhanced Oil Recovery Implications.* Industrial & Engineering Chemistry Research, 2014. **53**(4): p. 1645-1662.
129. Jesmani, M., M.C. Bellout, R. Hanea, and B. Foss. *Particle Swarm Optimisation Algorithm for Optimum Well Placement Subject to Realistic Field Development Constraints*. *SPE Reservoir Characterisation and Simulation Conference and Exhibition*. 2015. Society of Petroleum Engineers.

130. Pontryagin, L.S., *Mathematical theory of optimal processes*. 1987: CRC Press.
131. Bellman, R., *Introduction to the mathematical theory of control processes*. Vol. 2. 1971: IMA.
132. Ross, I.M., *A primer on pontryagin's principle in optimal control*. 2009: Collegiate Publ.
133. Bellman, R., *On the theory of dynamic programming.* Proceedings of the National Academy of Sciences of the United States of America, 1952. **38**(8): p. 716.
134. Utgoff, P.E., *Incremental induction of decision trees.* Machine learning, 1989. **4**(2): p. 161-186.
135. Jackson, P., *Introduction to expert systems.* 1986.
136. Russell, S. and P. Norvig, *Artificial intelligence: a modern approach.* 1995.
137. Nwigbo Stella, N. and A.O. Chuks, *Expert System: A Catalyst in Educational Development in Nigeria.* 2011.
138. Montgomery, D.C., *Design and analysis of experiments*. Vol. 7. 1984: Wiley New York.
139. Box, G.E. and K. Wilson, *On the experimental attainment of optimum conditions.* Journal of the Royal Statistical Society. Series B (Methodological), 1951. **13**(1): p. 1-45.
140. Fedorov, V.V., *Theory of optimal experiments*. 1972: Elsevier.
141. Box, G.E., J.S. Hunter, and W.G. Hunter, *Statistics for experimenters: design, innovation, and discovery.* AMC, 2005. **10**: p. 12.
142. Kroese, D.P., T. Brereton, T. Taimre, and Z.I. Botev, *Why the Monte Carlo method is so important today.* Wiley Interdisciplinary Reviews: Computational Statistics, 2014. **6**(6): p. 386-392.
143. Hastings, W.K., *Monte Carlo sampling methods using Markov chains and their applications.* Biometrika, 1970. **57**(1): p. 97-109.
144. Murtha, J.A., *Monte Carlo simulation: its status and future.* Journal of Petroleum Technology, 1997. **49**(04): p. 361-373.
145. Murtha, J.A., *Incorporating Historical Data Into Monte Carlo Simulation.* SPE Computer Applications, 1994. **6**(02): p. 11-17.
146. Kalman, R.E., *A new approach to linear filtering and prediction problems.* Journal of Fluids Engineering, 1960. **82**(1): p. 35-45.
147. Houtekamer, P.L. and H.L. Mitchell, *Data assimilation using an ensemble Kalman filter technique.* Monthly Weather Review, 1998. **126**(3): p. 796-811.
148. Lorentzen, R.J., K.K. Fjelde, J. Frøyen, A.C. Lage, G. Nævdal, and E.H. Vefring. *Underbalanced drilling: Real time data interpretation and decision support*. *SPE/IADC drilling conference*. 2001. Society of Petroleum Engineers.
149. Nævdal, G., T. Mannseth, and E.H. Vefring. *Near-well reservoir monitoring through ensemble Kalman filter*. *SPE/DOE Improved Oil Recovery Symposium*. 2002.
150. Kirkpatrick, S., C.D. Gelatt, and M.P. Vecchi, *Optimisation by simulated annealing.* science, 1983. **220**(4598): p. 671-680.
151. Glover, F., *Tabu search fundamentals and uses*. 1995: Citeseer.
152. Mehos, G.J. and W.F. Ramirez, *Use of optimal control theory to optimise carbon dioxide miscible-flooding enhanced oil recovery.* Journal of Petroleum Science and Engineering, 1989. **2**(4): p. 247-260.
153. Wackowski, R., C. Stevens, L. Masoner, V. Attanucci, J. Larson, and K. Aslesen. *Applying Rigorous Decision Analysis Methodology to Optimisation of a Tertiary Recovery Project: Rangely Weber Sand Unit Colorado*. *Oil and Gas Economics Finance and Management Conference*. 1992. Society of Petroleum Engineers.

154. Bedrikovetsky, P., G. Andrade, L. Ferreira, and G. Menezes. *Optimisation of tertiary water-alternate-CO_2 injection*. *SPE Latin America/Caribbean Petroleum Engineering Conference*. 1996. Society of Petroleum Engineers.
155. Guo, X., Z. Du, L. Sun, W. Huang, and C. Zhang. *Optimisation of tertiary water-alternate-CO_2 flood in Jilin oil field of China: Laboratory and simulation studies*. *SPE/DOE Symposium on Improved Oil Recovery*. 2006. Society of Petroleum Engineers.
156. Attanucci, V., K. Aslesen, K. Hejl, and C. Wright. *WAG Process Optimisation in the Rangely CO_2 Miscible Flood*. *SPE Annual Technical Conference and Exhibition*. 1993. Society of Petroleum Engineers.
157. Pritchard, D. and R. Nieman. *Improving oil recovery through WAG cycle optimisation in a gravity-overide-dominated miscible flood*. *SPE/DOE Enhanced Oil Recovery Symposium*. 1992. Society of Petroleum Engineers.
158. Hallam, R.J., T.D. Ma, and E.W. Reinbold, *Performance evaluation and optimisation of the Kuparuk hydrocarbon miscible water-alternating-gas flood.* Geological Society, London, Special Publications, 1995. **84**(1): p. 153-164.
159. Johns, R.T., L. Bermudez, and H. Parakh. *WAG Optimisation for Gas Floods Above the MME*. *SPE Annual Technical Conference and Exhibition*. 2003. Society of Petroleum Engineers.
160. Gharbi, R., *Application of an expert system to optimise reservoir performance.* Journal of Petroleum Science and Engineering, 2005. **49**(3): p. 261-273.
161. Esmaiel, T.E. and J.C. Heeremans. *Optimisation of the WAG process under Uncertainty in a Smart Wells Environment: Utility Theory Approach*. *Intelligent Energy Conference and Exhibition*. 2006. Society of Petroleum Engineers.
162. Ghomian, Y., G.A. Pope, and K. Sepehrnoori. *Hysteresis and field-scale optimisation of WAG injection for coupled CO_2-EOR and sequestration*. *SPE Symposium on Improved Oil Recovery*. 2008. Society of Petroleum Engineers.
163. Ghaderi, S.M., C.R. Clarkson, and Y. Chen. *Optimisation of WAG Process for Coupled CO_2 EOR-Storage in Tight Oil Formations: An Experimental Design Approach*. *SPE Canadian Unconventional Resources Conference*. 2012. Society of Petroleum Engineers.
164. Odi, U. and A. Gupta. *Optimisation and Design of Carbon Dioxide Flooding*. *Abu Dhabi International Petroleum Exhibition and Conference*. 2010. Society of Petroleum Engineers.
165. Jahangiri, H.R., *Optimisation of coupled CO_2 sequestration and enhanced oil recovery*. 2012: University of Southern California.
166. Rahmawati, S.D., C.H. Whitson, and B. Foss, *A mixed-integer non-linear problem formulation for miscible WAG injection.* Journal of Petroleum Science and Engineering, 2013. **109**: p. 164-176.
167. Yang, D., Q. Zhang, H. Cui, H. Feng, and L. Li, *Optimisation of Multivariate Production-Injection System for Water-Alternating-Gas Miscible Flooding in Pubei Oil Field*, 2000, Society of Petroleum Engineers.
168. Yang, D., Q. Zhang, and Y. Gu, *Integrated optimisation and control of the production-injection operation systems for hydrocarbon reservoirs.* Journal of petroleum science and Engineering, 2003. **37**(1): p. 69-81.
169. Verlo, S.B. and M. Hetland, *Development of a field case with real production and 4D data from the Norne Field as a benchmark case for future reservoir simulation model testing.* Master's degree, NTNU, 2008.

170. Statoil, 2015; Available from: *http://www.statoil.com/en/OurOperations/Crudeoil/Crudeoilassays/Pages/Norne.aspx*
171. Manual, P.U., *Calsep A*, 2005, S.
172. Holm, L. and V. Josendal, *Mechanisms of oil displacement by carbon dioxide.* Journal of petroleum Technology, 1974. **26**(12): p. 1,427-1,438.
173. Ertekin, T., J.H. Abou-Kassem, and G.R. King, *Basic applied reservoir simulation*. 2001: Society of Petroleum Engineers Richardson, TX.
174. ECLIPSE, S., *ECLIPSE Reference Manual 2004A*. 2004.
175. Sharma, G. and K. Sharma Mahendra, *Particle technology and surface phenomena in minerals and petroleum*. 1991: Springer.
176. Corey, A.T., *The interrelation between gas and oil relative permeabilities.* Producers monthly, 1954. **19**(1): p. 38-41.
177. Corey, A., *Hydraulic properties of porous media.* Colorade State University, Hydraulic Papers, (3).
178. Powell, J.C., *Analysis of the NGL Supply & Utilization Strategies*. 2011.
179. Vazquez, M., A. Suarez, H. Aponte, L. Ocanto, and J. Fernandes. *Global Optimisation of Oil Production Systems A Unified Operational View*. *SPE Annual Technical Conference and Exhibition*. 2001. Society of Petroleum Engineers.
180. Svedeman, S., *Criteria for sizing multiphase flowlines for erosive/corrosive service.* SPE Production & Facilities, 1994. **9**(01): p. 74-80.
181. Cai, X., J. Zeng, Y. Tan, and Z. Cui, *Individual parameter selection strategy for particle swarm optimisation*. 2009: INTECH Open Access Publisher.
182. Bansal, J., P. Singh, M. Saraswat, A. Verma, S.S. Jadon, and A. Abraham. *Inertia weight strategies in particle swarm optimisation*. *Nature and Biologically Inspired Computing (NaBIC), 2011 Third World Congress on*. 2011. IEEE.
183. Czitrom, V., *One-factor-at-a-time versus designed experiments.* The American Statistician, 1999. **53**(2): p. 126-131.
184. Wang, X., R.D. Haynes, and Q. Feng, *Well Control Optimisation using Derivative-Free Algorithms and a Multiscale Approach.* arXiv preprint arXiv:1509.04693, 2015.
185. Carosio, G.L.C., T.D. Humphries, R.D. Haynes, and C.G. Farquharson. *A closer look at differential evolution for the optimal well placement problem*. in *Proceedings of the 2015 on Genetic and Evolutionary Computation Conference*. 2015. ACM.

Appendix A

Example: If the total volumes of produced oil, gas and water and the total volumes of injected gas and water for two years of WAG injection are as shown in Table A-1, the NPV using equation (3.6) with the prices assumed in Table 3-4 for the most enriched injection gas is calculated as follows

Table A-1: The total volumes of injected and produced fluids for a two-year WAG process

Year number	Q_o^{prod} [Sm^3]	Q_g^{prod} [Sm^3]	Q_w^{prod} [Sm^3]	Q_g^{inj} [Sm^3]	Q_w^{inj} [Sm^3]
1	2.2217×10^5	2.5998×10^7	1.1315×10^6	1.02×10^5	1.6659×10^6
2	1.7662×10^5	2.1667×10^7	1.1284×10^6	4.9×10^4	1.8117×10^6

$$NPV=\left\{Q_o^{prod}(1)c_o-\left[Q_g^{inj}(1)\right]c_g-\left[Q_w^{inj}(1)\right]c_w\right\}(1+r)^{-1}+\ldots$$
$$\left\{Q_o^{prod}(2)c_o-\left[Q_g^{inj}(2)-Q_g^{prod}(1)\right]c_g-Q_g^{prod}(1)c_g^{'}-\left[Q_w^{inj}(2)-Q_w^{prod}(1)\right]c_w-Q_w^{prod}(1)c_w^{'}\right\}(1+r)^{-2}+\ldots$$
$$[Q_g^{prod}(2)(c_g-c_g^{'})+Q_w^{prod}(2)(c_w-c_w^{'})](1+r)^{-2}$$

$$NPV=\left\{2.2217\times10^5\times377-\left[1.02\times10^5\right]0.271-\left[1.6659\times10^6\right]6\right\}1.05^{-1}+\ldots$$
$$\{1.7662\times10^5\times377-\left[4.9\times10^4-2.5998\times10^7\right]0.271-2.5998\times10^7\times0.271\times0.7-\ldots$$
$$\left[1.8117\times10^6-1.1315\times10^6\right]6-1.1315\times10^6\times38\}1.05^{-2}+\ldots$$
$$\left[2.1667\times10^7(0.271-0.271\times0.7)+1.1284\times10^6(6-38)\right]1.05^{-2}=\$58.7\text{ million}$$